

**KONINKLIJK NEDERLANDS
METEOROLOGISCH INSTITUUT**

WETENSCHAPPELIJK RAPPORT
SCIENTIFIC REPORT

W.R. 82 - 2

J.D. Opsteegh

On the origin and variability of the
stationary waves in the atmosphere



De Bilt, 1982

Publikatienummer: K.N.M.I. W.R. 82 - 2 (DM)

Koninklijk Nederlands Meteorologisch Instituut,
Dynamisch Meteorologisch onderzoek,
Postbus 201,
3730 AE De Bilt,
Nederland.

U.D.C.: 551.513.7 :
551.511.3 :
551.509.313 :
551.509.333

CONTENTS

	Page
VOORWOORD	1
SAMENVATTING	3
I. GENERAL INTRODUCTION	9
1.1. Atmospheric predictability	9
1.2. History on LRWP in the Netherlands	15
1.3. Overview of work presented in this thesis	17
1.4. Plans for the near future	21
1.5. References	24
II. A DIAGNOSTIC STUDY OF THE TIME-MEAN ATMOSPHERE OVER NORTHWESTERN EUROPE DURING WINTER	31
2.1. Introduction	34
2.2. Formulation of the problem for the time-mean atmosphere	36
2.3. Data and analysis	39
2.4. Reliability of the eddy statistics	42
2.5. Mean state of the atmosphere over Northwestern Europe during the winter of 1976/1977.	44
2.6. Second-order eddy statistics over Northwestern Europe	51
2.7. Estimates of the terms in the equations for mean momentum and temperature	57
2.8. Third-order eddy statistics	61
2.9. Estimates of the terms in the horizon- tal eddy flux equations	66
2.10. Discussion and concluding remarks	75
2.11. References	78
III. SEASONAL DIFFERENCES IN THE STATIONARY RESPONSE OF A LINEARIZED PRIMITIVE EQUATION MODEL: PROSPECTS FOR LONG RANGE WEATHER FORECASTING?	81
3.1. Introduction	83
3.2. Derivation of the model equations	86

3.3.	Behavior of the model in the zonal wavenumber domain	90	
3.4.	The influence of heating in the tropics on the standing waves in middle latitudes	98	
3.5.	The influence of different zonally-symmetric states in different seasons	105	
3.6.	Discussion	112	
3.7.	References	115	
3.8.	Appendix A	118	
3.9.	Appendix B	120	
IV.	ON THE IMPORTANCE OF THE HADLEY AND FERREL CIRCULATION FOR TELECONNECTIONS FORCED BY LOW-LATITUDE HEAT SOURCES		123
4.1.	Introduction	125	
4.2.	Description of the model	127	
4.3.	Description of the zonally averaged mean state	130	
4.4.	Experiments with the hemispheric model	130	
4.5.	Cross equatorial propagation	142	
4.6.	Some simple arguments and concluding remarks	145	
4.7.	References	150	
V.	A SIMULATION OF THE JANUARY STANDING WAVE PATTERN INCLUDING THE EFFECTS OF TRANSIENT EDDIES		151
5.1.	Introduction	154	
5.2.	The model	155	
5.3.	The forcing functions	160	
5.4.	Results	166	
5.5.	Conclusions and discussion	181	
5.6.	References	185	
VI.	APPENDIX		189
6.1.	A note on the boundary conditions	190	
6.2.	References	192	
	CURRICULUM VITAE		193

Voorwoord

Het onderzoek waarvan de resultaten in dit proefschrift worden beschreven, werd gestart in 1977. Doel van het onderzoek was om te komen tot een beter begrip van de processen die een rol spelen bij klimaatvariaties op termijnen van een maand tot een jaar, in de hoop dat dit zal leiden tot bruikbare lange termijn verwachtingen. Met dit proefschrift is slechts een klein stukje op een lange (en wellicht doodlopende) weg afgelegd. Niettemin hebben de resultaten mij sterk gestimuleerd om op de ingeslagen weg verder te gaan.

In de beginfase van dit onderzoek werden lange en vaak heftige discussies gevoerd met Huug van den Dool, Hans Reiff en Hans Oerlemans. Ik heb van hen veel geleerd en denk vaak met weemoed terug aan deze periode.

Een groot deel van het onderzoek werd gedaan samen met Huug van den Dool. Deze samenwerking is van grote betekenis geweest voor de kwaliteit van dit proefschrift. Bovendien is Huug een vriend voor mij geworden.

Met Anandu Vernekar heb ik het onderzoek verricht, dat heeft geleid tot het vierde artikel. Hij heeft het mogelijk gemaakt dat ik gedurende een jaar in de Verenigde Staten heb kunnen werken.

Henk Tennekes heeft op het KNMI de ruimte gecreëerd waardoor dit onderzoek mogelijk werd. Hij heeft mij sterk gestimuleerd in het ontplooiën van eigen creatieve vermogens. Ik heb dankbaar geprofiteerd van zijn enorme ervaring in het schrijven van artikelen.

Fons Baede heeft het werk steeds aangemoedigd en het voor de buitenwacht gemotiveerd en verdedigd.

Met mijn promotor Cor Schuurmans heb ik het afgelopen jaar vele ochtenden doorgebracht om het werk in al zijn details te bespreken. Dit was niet alleen plezierig, maar Cor heeft mij ook nieuwe impulsen gegeven.

Dit proefschrift had nooit tot stand kunnen komen zonder Marlie Collet, die het heeft getypt, en Co Wittebol, die het heeft gedrukt. Vele figuren werden getekend door Rob Meijer.

Naast de mensen, die ik veel dank verschuldigd ben voor hun bijdrage aan de totstandkoming van dit proefschrift, wil ik iedereen bedanken die heeft bijgedragen aan de vriendschappelijke sfeer waarin ik de afgelopen jaren mijn werk heb kunnen doen.

SAMENVATTING

Dit proefschrift bestaat uit vier afzonderlijke studies. Het gemeenschappelijke aspect in deze studies is dat ze allen te maken hebben met lange termijn voorspelbaarheid van het weer. Het uiteindelijke doel is om te komen tot een antwoord op de vraag of klimaatvariatiaties, op tijdschalen van een maand tot een seizoen vooruit, geheel of gedeeltelijk voorspelbaar zijn.

Voorspelbaarheid op lange termijn is een ander probleem dan de voorspelling van het weer op een termijn van een tot enkele dagen vooruit. Voor de korte termijn verwachting is de atmosferische drukverdeling aan het begin van de verwachtingsperiode van groot belang. Het korte termijn voorspelprobleem is dus een beginvoorwaarde probleem, d.w.z. vanuit een gegeven verdeling van de hoge en lage drukgebieden over de aarde kan een verwachting van de atmosferische drukverdeling enkele dagen vooruit worden gemaakt. De voorspelling van de ontwikkeling van de circulatie komt tot stand met behulp van modellen. Voor de zeer korte termijn (korter dan 24 uur vooruit) is de modelvoorstelling zo eenvoudig dat zonder hulp van computers een verwachting kan worden gemaakt. Voor iets langere termijnen moet de hulp van computers worden ingeroepen. De computer modellen zijn gebaseerd op de natuurkundige wetten voor stromende media. Deze wetten kunnen worden geformuleerd in wiskundige vergelijkingen. Door integratie in de tijd van deze vergelijkingen wordt de verandering in de atmosferische drukverdeling beschreven.

In principe is het mogelijk om de drukverdeling een maand of zelfs een jaar vooruit te berekenen. Echter de betrouwbaarheid van de voorspelling neemt sterk af met toenemende voorspelperiode. Tot vijf dagen vooruit kan zinvolle informatie over het te verwachten weer worden gegeven. Voor langere perioden is de fout in de ligging en intensiteit van voorspelde hoge en lage druk systemen zo groot geworden, dat de voorspelling niet langer als zinvol wordt ervaren. Het toenemen van de fouten met de voorspelperiode kan voor een gedeelte worden verklaard door het feit dat de atmosferische modellen geen exacte copiën zijn van de werkelijke atmosfeer. Een van de belangrijkste verschillen is dat de toestand van de model atmosfeer wordt gerepresenteerd in een eindig aantal punten (roosterpunten), die regelmatig verdeeld over de aarde verspreid liggen. Hierdoor treden fouten op in de beschrijving van de

dynamische processen van grote schaal druksystemen, zoals depressies. Bovendien worden processen, die zich afspelen op een ruimteschaal kleiner dan de afstand tussen de roosterpunten, verwaarloosd, of hun invloed op de grotere schaal druksystemen wordt slechts op gebrekkige wijze geparameteriseerd.

Afgezien van modelgebreken bestaat er een fundamentele beperking aan de voorspelbaarheid van het weer. Deze beperking houdt verband met het niet-lineaire karakter van de atmosfeer, d.w.z. dat processen die zich tegelijkertijd op verschillende ruimteschalen afspelen elkaar kunnen beïnvloeden. Een bui met een afmeting van enkele honderden meters en een levensduur van een uur heeft invloed op de ontwikkeling van een depressie, die een afmeting van enkele duizenden kilometers en een levensduur van enkele dagen heeft. Het niet-lineaire karakter van de atmosfeer heeft tot gevolg dat willekeurig kleine fouten in de beschrijving van de begintoestand uiteindelijk leiden tot een wezenlijke aantasting van de nauwkeurigheid in de voorspelling van grote schaal druksystemen. Dit leidt tot een maximum in de voorspelbaarheid van de hoge en lage drukgebieden, die in belangrijke mate het weer bepalen. Dit maximum is niet precies aan te geven, maar ligt in de orde van een week. Een verwachting van de z.g. "weersystemen" een maand of langer vooruit is dus zinloos. Als we op deze termijn iets willen voorspellen zullen we onszelf beperkingen moeten opleggen.

Bij nader onderzoek van het spectrum aan atmosferische golven blijkt dat naast de weersystemen, die voor de korte termijn verwachting zo belangrijk zijn, ook zeer lange, bijna stationaire, golven voorkomen. Deze stationaire golven hebben een golflengte in de orde van tienduizend kilometer. In tegenstelling tot de weersystemen hebben de stationaire golven een zeer lange levensduur. Op maand of seizoengemiddelde kaarten van de atmosferische circulatie kunnen zij zonder uitzondering worden terug gevonden. De stationaire golven zijn niet de dragers van het weer, maar vervullen een sturende rol, d.w.z. zij bepalen welke baan de depressies zullen volgen. Indien het mogelijk is de persistente stationaire golven te voorspellen kan iets over het gemiddelde weer over een periode van bijvoorbeeld een maand worden gezegd.

In tegenstelling tot de weersystemen, waarvan de ontwikkeling bijna volledig wordt bepaald door de begincondities, worden de stationaire golven gedomineerd door de randvoorwaarden. De condities aan het aard-

oppervlak, zoals de ligging van gebergten en de verdeling van continenten en oceanen, zijn van groot belang voor de fase en amplitude van stationaire golven. Veranderingen in de condities aan het aardoppervlak, zoals een anormale temperatuurverdeling aan het oppervlak van de oceanen, leiden tot veranderingen in het stationaire golfpatroon. Het zijn de veranderingen in de stationaire golven, opgewekt door anomalieën (afwijkingen van normaal) in de condities aan het aardoppervlak, die lange termijn verwachters in de toekomst hopen te voorspellen.

Naast de condities aan het aardoppervlak oefenen, door het niet lineaire karakter van de atmosfeer, de weersystemen eveneens invloed uit op de stationaire golven. Algemeen wordt aangenomen dat deze invloed onvoorspelbaar is, tenzij het gemiddelde effect van de weersystemen kan worden uitgedrukt in voorspelbare parameters. Dit laatste moet nog niet uitgesloten worden geacht. Zolang de parameterisatie van de invloed van weersystemen niet lukt is het van belang het relatieve effect te onderzoeken van het aardoppervlak t.o.v. de invloed van de weersystemen. Dit wordt wel de signaal-ruis verhouding genoemd en als een maat beschouwd voor de voorspelbaarheid van de stationaire golven. Statistische studies van de signaal-ruis verhouding geven een pessimistisch beeld van de voorspelbaarheid. In deze studies worden echter aannamen gedaan die de conclusies op zijn minst onzeker maken.

Wiskundige vergelijkingen voor de stationaire golven kunnen worden opgesteld door de vergelijkingen voor de atmosferische stroming te middelen over bijvoorbeeld een maand of een seizoen. Op deze manier worden de hoogfrequente weersystemen weggefilterd. Ze manifesteren zich als extra kracht en verwarming in de vergelijkingen die nu zijn uitgedrukt in de variabelen van de stationaire golven. De weersystemen worden als grote schaal turbulentie opgevat. Het verschil met echte turbulentie is dat de grote schaal turbulentie zich in het geheel niet met een diffusie benadering laat beschrijven.

In het eerste artikel worden de vergelijkingen voor de seizoensgemiddelde stroming onderzocht m.b.v. metingen van de atmosferische circulatie boven west Europa. Alle belangrijke termen in de vergelijkingen worden bepaald uit waarnemingen, zodat kan worden afgeschat welke termen in de vergelijkingen moeten worden gehandhaafd bij de

opzet van een model voor de stationaire golven. Vastgesteld wordt dat de invloed van de weersystemen zich manifesteert als een van de dominante termen in de vergelijkingen. Door wiskundige manipulaties kunnen aparte vergelijkingen worden opgesteld voor de ontwikkeling van de grote schaal turbulentie. Ook deze vergelijkingen worden met behulp van waarnemingen bestudeerd. Getracht wordt om eenvoudige relaties te vinden voor de grote schaal turbulentie, die in de vergelijkingen voor de stationaire golven kunnen worden gebruikt. Dit is niet gelukt.

In het tweede artikel wordt een model ontwikkeld voor de stationaire golven. Ze worden opgevat als lineaire perturbaties van een gemiddelde stroming. Het effect dat ze op elkaar uitoefenen wordt verwaarloosd. Hiermee zien we af van de beschrijving van potentieel interessant gedrag, zoals het bestaan van meerdere atmosferische configuraties voor één bepaalde toestand van het aardoppervlak. Echter uit waarnemingsstudies en ook met modelsimulaties is aangetoond, dat de stationaire golven zich ongeveer lineair gedragen.

Met het model is onderzocht wat de invloed is van een locale atmosferische warmtebron. Deze verwarming kan bijvoorbeeld het gevolg zijn van plaatselijk hoge oceaan temperaturen. Uit de experimenten blijkt dat anomalieën in de oppervlakte condities van de tropische en subtropische gebieden heel gemakkelijk stationaire golven opwekken die zich uitstrekken tot onze geografische breedte. De energie van de golven plant zich voort langs een grootcirkel. De amplitude van de golf neemt toe met toenemende breedte. Ligt de warmtebron volledig in de tropische oostenwind gordel dan worden slechts golven opgewekt die zich beperken tot de tropen. Uit dit experiment kan worden geconcludeerd dat anomalieën in de oppervlakte temperatuur van de tropische oceanen van groot belang zijn voor de verklaring en eventueel voorspelling van anomalieën in de stationaire golven. Recente waarnemingsstudies en modelsimulaties bevestigen elkaar op dit punt.

De invloed van een constante anomale warmtebron is gesimuleerd voor de vier seizoenen, zowel voor een warmtebron op gematigde breedte als in de tropen. De model respons blijkt sterk af te hangen van het seizoen voor een warmte bron op gematigde breedte. De seizoensafhankelijkheid is zwakker voor een tropische warmtebron, behalve in het zomer seizoen. In de zomer zijn de tropische oostenwinden zover naar het noorden opge-

schoven, dat de warmtebron volledig in de oostenwind zone ligt. Als gevolg hiervan treden slechts tropische circulaties op en wordt geen golfpatroon op gematigde breedte opgewekt. Uit deze experimenten blijkt, dat zelfs bij zeer persistente anomale condities aan het aardoppervlak, er toch veranderingen kunnen optreden in de atmosferische respons. Dit wordt veroorzaakt door veranderingen in de "normale" circulatie, zoals het zwakker worden van de westenwinden en het noordwaarts opschuiven van de oostenwinden van winter naar zomer.

In het derde artikel wordt onderzocht wat het effect is van de tropische Hadley circulatie voor de opgewekte anomale stationaire golven, speciaal met betrekking tot het vermogen van die golven om energie door de oostenwind gordel van het ene halfrond naar het andere te transporteren. De Hadley circulatie is een directe thermische circulatie in de tropen. Wanneer de Hadley circulatie wordt verwaarloosd (zoals in het tweede artikel werd gedaan) blijft de respons beperkt tot het halfrond waar de warmtebron ligt. Ligt die warmtebron in de oostenwinden dan is er geen respons op de gematigde breedte. De reden is dat zonder Hadley circulatie de stationaire golven, waar we in zijn geïnteresseerd (Rossby golven), niet kunnen bestaan als perturbaties van een gemiddelde oostenwind. Wanneer de Hadley cel wordt meegenomen kunnen stationaire Rossby golven wel bestaan in de oostenwind zone.

Het vermogen om golfenergie door de oostenwind gordel heen te transporteren is afhankelijk van de sterkte van de wind. Naarmate de oostenwinden krachtiger worden neemt dit vermogen af en wel sterker naarmate de golflengte langs de equator kleiner is. De energie van de golven wordt getransporteerd met de groepsnelheid. Deze blijkt hetzelfde te hebben als de noord-zuid gerichte wind (meridionale wind) van de Hadley circulatie. Waait de wind in de Hadley cel naar het noorden dan kan golfenergie van het zuidelijk naar het noordelijk halfrond worden getransporteerd, maar niet andersom. In de winter is de meridionale wind van de Hadley cel in de bovenste helft van de atmosfeer naar het noorden gericht en onderin naar het zuiden. Onderin kan dus energie naar het zuidelijk halfrond worden getransporteerd en bovenin naar het noordelijk halfrond. Echter op geringe hoogte zijn de oostenwinden veel sterker dan op grote hoogte, zodat het transport van golfenergie van

het zuidelijk naar het noordelijk halfrond veel makkelijker verloopt dan andersom. Dit betekent dat in de winter het zuidelijk halfrond meegenomen dient te worden om het effect van anomalieën in de oppervlakte condities te berekenen. In de zomer, als de Hadley cel van teken omdraait, is de invloed van het zuidelijk halfrond geringer.

In het vierde artikel wordt de relatieve invloed van interne forcering door de weersystemen op de stationaire golven onderzocht. Dit is gedaan door de stationaire golven te simuleren voor normale condities aan het aardoppervlak en voor normale interne forcering. Normaal wordt gedefinieerd als een langjarig gemiddelde van de condities in de maand januari. De interne forcering door de weersystemen wordt als kracht en verwarming voorgeschreven in de vergelijkingen, en is bepaald uit metingen over lange tijd. De invloed van het aardoppervlak wordt beschreven door de bergen en de ligging van continenten en oceanen. Uit de simulatie experimenten blijkt dat de invloed van het aardoppervlak vooral wordt veroorzaakt door de bergen. De effecten van de interne forcering door de weersystemen is vergelijkbaar in grootte met het bergeffect. Dit is uit een oogpunt van signaalruis verhouding ontmoedigend, aangezien het waarschijnlijk is dat de interne forcering relatief nog belangrijker wordt voor de afwijkingen van normale condities, die we zo graag willen voorspellen. De resultaten suggereren echter het bestaan van een eenvoudige fase relatie tussen de golven opgewekt door bergen, en de intern geforceerde golven. Als deze fase relatie ook opgaat voor anomale stationaire golven, kan wellicht het anomale effect van interne forcering worden geparаметeriseerd in termen van anomale condities aan het aardoppervlak.

I. GENERAL INTRODUCTION

This thesis consists of four studies on certain aspects of the general circulation of the atmosphere, which are related to the problem of long range weather prediction (LRWP). The main topic of the papers is to formulate and test a set of equations appropriate to describe the dynamics of the monthly or seasonal mean atmosphere without dealing directly with the dynamics of the daily weather systems. Such models of the atmosphere are usually called "Statistical-Dynamical" models, that is, they describe the dynamics of the low frequency part of atmospheric waves, whereas the statistical effect of higher frequencies is parameterized.

In the first paper nearly all terms in the equations for the time mean flow are computed from upper air observations over Western Europe in order to find the dominant terms. An attempt to close this system of equations was made by scaling the equations for the horizontal eddy fluxes of temperature and momentum with the same data. In the second and third papers a dynamical model for the time-mean flow is developed and a number of experiments are performed to show the general characteristics of the model. In the fourth paper the model is tested against observations by simulating the normal standing eddies for January. I will come back to the results and conclusions of the various papers later in this chapter, but first atmospheric predictability will be discussed and an overview will be presented of work on LRWP that has been done in the Netherlands.

1.1. Atmospheric predictability

From the second half of the nineteenth century scientists from all over the world have shown great interest in the problem of LRWP. Excellent reviews of the enormous quantity of papers on this problem have been given by Namias (1968) and recently by Nicholls (1980). Together these two papers cover the history of LRWP up to 1979. Since 1968 a great number of papers was published dealing with LRWP problems (Nicholls, 1980). In order to get an impression of the progress that has been made since then it is interesting to read both Namias' and Nicholls' vision on future developments in the field of LRWP. In spite of the fact that Namias realises the complexity of the problem very well, his view is much more optimistic than Nicholls' view twelve

years later. Apparently the papers published since 1968 illustrate the enormous difficulties one faces in this particular field.

What is so difficult in predicting the weather beyond a few days? Why is it not possible to integrate our present atmospheric models in time to give an accurate prediction of the position and strength of all large-scale pressure systems a month or a season ahead? In spite of the complexity of the models they still suffer from serious deficiencies. Errors are introduced permanently during the integration because the continuous fluid is represented in a limited number of points and because the parameterization of processes that take place on scales smaller than the resolvable scales is inaccurate. However, apart from these model shortcomings, which may be partly overcome in the future, there is a much more fundamental problem in predicting weather systems on longer time scales. Even if the laws governing atmospheric evolution are strictly deterministic, perfectly known and perfectly modelled on a computer, we will always have to accept that the initial state of the model atmosphere contains small errors. This imperfect knowledge of the initial state is the reason that predictability of large-scale weather systems is limited. Because of the nonlinear nature of atmospheric flow, inaccuracies in small systems will propagate into larger scales, finally affecting synoptic and planetary scales. Predictability is thus dependant on how rapidly two atmospheres which have slightly different initial conditions but are otherwise identical will diverge. Lorenz (1969) estimated the doubling times for errors in all scales. He found that this error growth is related to the lifetime of the eddies. Small eddies with a short lifetime have a short error doubling time. In synoptic eddies with a lifetime of several days the errors double in a few days. On the basis of these results Lorenz (1969) indicated an absolute maximum range of predictability of individual synoptic-scale cyclones and anticyclones, which is considerably shorter than a month.

Does this mean that monthly or seasonal forecasts are impossible? It certainly means that we will never be able to predict the weather for a particular day a month or so in advance. However, instead of predicting individual weather-systems we can turn to climate and try to predict the average weather over a certain period. The prediction of climate variables has long been recognized as a useful approach to LRWP.

Considering the prediction problem, von Neumann (1955) made a distinction between atmospheric motions on very short time scales, for which prediction is almost completely determined by the initial state and motions on very long time scales which are independent of the initial conditions. An example of the latter motion is the wave-pattern that shows up on multi-year average maps of the monthly or seasonal-mean circulation. Climate variables on very long time scales are, for a given chemical composition of the atmosphere, determined by solar forcing and properties of the underlying surface of the earth. Von Neumann (1955) also distinguished an intermediate time scale for which the initial conditions as well as the boundary conditions are important. He expected that the limit cases (i.e. very short and very long time scales) are probably easiest to deal with. This has proven to be true. Both on the very short and on the very long time scales considerable progress has been made. On the very short time scale it is possible now to predict the position and strength of individual large scale cyclones and anti-cyclones four to five days in advance (Hollingsworth et al, 1980). On very long time scales most features of the general circulation have been reproduced, at least qualitatively, by integrating detailed general circulation models (GCM's) in time using appropriate boundary conditions (see e.g. Smagorinsky 1963, Arakawa et al 1969, Somerville et al 1974, Manabe and Terpstra 1974). These models have to be integrated sufficiently long to exclude influences of the initial state on the statistical or climate properties of the flow. Experiments with GCM's are therefore expensive. Models dealing directly with the dynamics of the very long time scales are less expensive and sometimes more informative. This type of models is usually called "Statistical-Dynamical" models (SD models). For the simulation of the zonally-symmetric component of the general circulation SD models have been used in a number of papers (Kurihara 1970, Saltzman and Vernekar 1971). The statistical effect of all individual transient and standing eddies is parameterized in terms of zonally-symmetric climate variables. For the zonally-asymmetric component of the general circulation (standing eddies) the effect of transients is less easy to parameterize. In simulation studies of the standing waves this internal forcing mechanism is generally neglected. Only external forcing effects caused by inhomogeneities in the underlying surface of the earth are taken into account (Smagorinsky

1953, Egger 1976, Ashe 1979, Hoskins and Karoly 1981).

In contrast with the limit cases little progress has been made in predicting intermediate time scales such as interannual variations in monthly or seasonal mean circulation. Both variations in boundary conditions as well as variations of internal forcing by transient eddies are important for this problem. The use of GCM's in LRWP has been considerably less successful than in the limit cases (Spar, 1977, Spar and Lutz 1979, Gilchrist 1977). In a number of sensitivity studies with GCM's the existence of relations between anomalous (deviating from normal) conditions at the earth's surface and anomalies in the circulation is shown. For instance Rowntree (1972, 1976) showed the importance of sea surface temperature anomalies (STA's) in the tropics and Mintz (1981) studied the impact of soil moisture. The simulation with a GCM of the effects of anomalous boundary conditions may have some predictive prospects if externally forced waves (signal) can be distinguished from variations due to the natural variability of the model (noise). If the signal is small compared to the noise this will not be an easy task.

Only few SD models have been used for the prediction of the anomalies in monthly or seasonal mean circulation. Adem (1964) uses only the thermodynamic equation to simulate the effects of anomalous boundary forcing. Internal forcing is treated as diffusion but this can hardly be justified. Egger (1977) investigated the influence of mid-latitude and tropical STA's with a linear steady-state model. Internal forcing is neglected. In contrast with GCM's this type of models do not generate any noise and the results may be directly applied for prediction purposes. An advantage of Egger's model over a GCM is that the equations are formulated in anomalous perturbations so there is no need to reproduce features of the "normal" circulation.

If we assume that anomalous internal forcing by transient eddies is an unpredictable factor in LRWP a key question determining the rate of success of LRWP models is: how important are the external forcing factors for the anomalies in monthly or seasonal mean circulation? If we look at the variability of those mean maps and compare this with the high degree of persistence in the conditions at the earth's surface we have some reason to be pessimistic about a strong connection between surface conditions and anomalous atmospheric waves. This impression is

confirmed by several statistical studies (see e.g. Madden 1976) on the predictability of short term climate. The results of Madden's studies suggest that the variance of time mean quantities in middle latitudes can almost be explained as a result of day to day variations of the weather. In the tropics the situation seems to be somewhat better. In those regions a clear signal can potentially be distinguished from the noise. However, these pessimistic results are dependent on certain assumptions regarding the contribution of daily weather variations to the observed frequency spectrum. For instance in Madden (1976) it is assumed that external forcing factors do not contribute to frequencies with periods smaller than a season. Clearly this assumption is rather arbitrary. Hence we should not regard these results as the final answer to our question but rather as an indication that the maximum skill in predicting mean weather will not be very high. Another weakness of these predictability studies is that they deal with a general level of predictability and do not consider the possibility that the climate variables on some occasions might have a high level of predictability or that certain aspects are more predictable than others.

The results of observational studies and model simulations dealing directly with the relation between anomalous external forcing and climate anomalies suggest that this relation indeed exists but the effects are always weak and/or local compared to the observed variability of atmospheric flow. The weakness of the effects may be partly due to improper sampling of the observational data, because the underlying physical mechanisms often are not understood well. An example is the effect of positive STA's in the tropical Mid-Pacific during certain phases of Southern Oscillation cycles. A signal due to this tropical forcing in the yearly mean circulation is almost nonexistent in mid-latitudes. However, if we stratify our data seasonally a strong signal in the mean winter circulation at middle latitudes shows up, even if we simply compute a composite pattern of all winters with warm equatorial Pacific STA's (see e.g. Horel and Wallace 1980). From numerical simulations of this phenomenon it is clear now that the exact location of the tropical easterlies is important (Opsteegh and van den Dool 1980, Hoskins and Karoly 1981). In summer the transition of easterlies to westerlies shifts to the north and in that case the atmospheric response

is restricted to the tropics. However, if only a part of the forcing takes place in regions where the wind is westerly a stationary Rossby wave is generated and wave energy propagates to higher latitudes approximately along a great circle route.

This example illustrates that we may have some hope to improve existing LRWP methods. This hope is based on the indication that on occasion a strong relation exists between external forcing and atmospheric flow but that this relation is not clear yet because atmospheric responses may depend critically on subtle changes in some internal parameters. One reason for such behavior is the existence of resonance. For resonance to occur it is necessary that wave energy is internally trapped (Tung and Lindzen 1979). If forced tropospheric waves propagate their energy vertically into the middle and high atmosphere the energy is radiated away. However, if the waves are reflected back into the troposphere amplification may occur. Solar heating might play a role in slightly changing the refractive index in the stratosphere thereby influencing the resonance properties of the troposphere. Matters are even more complicated because of the nonlinear nature of the flow. It has been shown that simple nonlinear forced atmospheres have more than one stable equilibrium solution (Charney and Devore 1979). This may also be the case for the statistical or climate properties of the atmosphere. Dependent on relatively small excitations, the climate system may jump from one stable state to the other. This behavior is called almost intransitive (Lorenz 1968).

In order to show strong relations between anomalies in the surface conditions and interannual variations in climate, it is thus important to understand the crucial internal parameters that determine the response of the climate system to external forces. Knowledge of the parameters for which the response is sensitive probably will make it easier to show the relation with boundary conditions. This can be done by sampling observational data with regards to these parameters or with model simulations for which the crucial parameters are controlled.

If we are able to properly simulate the response to surface forcing, the problem of predicting mean weather is a problem of predicting surface conditions. This is not a trivial problem because the surface and the atmosphere are highly interactive. Nevertheless surface conditions in

general have a much higher persistence than atmospheric conditions, which makes prediction hopefully somewhat easier. In order to fully account for the interaction between atmosphere and surface conditions, models coupling the atmosphere and the surface must be developed. Especially the evolution of the mixed layer in the oceans, covering a large part of the globe, must be predicted simultaneously, thereby accounting for the energy exchange between air and water.

1.2. History on LRWP in the Netherlands

Nearly all work on LRWP in the Netherlands has been inspired by developments in other countries. In 1908 Braak started to work on long range prediction of monsoonal rainfall for the Netherlands East Indies (now Indonesia). His work was based on findings of a tropical wave phenomenon by Hildebrandsson (1897). Hildebrandsson discovered the existence of a phase relationship between surface pressure anomalies at Sydney and Buenos Aires.

Walker described the year-to-year fluctuations in sea level pressure, surface air temperature and precipitation of this global scale phenomenon (Walker 1928, Walker and Bliss 1937). He named it the Southern Oscillation. Braak (1910, 1912, 1919) and later Berlage (1934, 1957), de Boer (1947a, 1947b) and Euwe (1949) made use of the features of the Southern Oscillation to predict anomalies in surface pressure and rainfall for Indonesia during the dry and wet monsoon. Although the monsoon predictions were not very reliable, a significant contribution was made to the analysis of planetary-scale tropical waves. Berlage (1966) pointed at the important connection between the Southern Oscillation and El Niño.

In the Netherlands Gallé (1917) started to work on long-range weather predictions during the first world war. He assumed that the trade winds are the driving forces for the Gulf Stream. On the basis of this assumption he correlated the strength of the easterlies with temperatures in Europe a few months later. A limited data set indeed indicated a positive correlation but when the computations in 1930 were repeated with a more extensive data set the correlation almost disappeared.

In 1933 Braak produced the first official forecasts for the Netherlands based on the sunspot cycle. Later Visser (1946) and van der Bijl (1952)

approached the problem with statistical methods. They searched for periodicities, correlations, and regression equations. Van der Bijl (1954) has written a very readable book in Dutch on how throughout history people have been involved in predicting weather a season or a whole year in advance. He also gives a description of scientific methods developed in various countries in the twentieth century. In his thesis Schuurmans (1969) showed some influence of solar flares on the tropospheric circulation, but was not able to use the relations in LRWP.

In 1968 Schuurmans started to produce monthly mean weather forecasts based on analogous situations (Schuurmans 1973). From historical daily surface pressure maps (1881-present) years were selected that showed some resemblance in the development of the circulation for a certain period of time. The years found to have analogous circulations were used to predict monthly mean temperature, the number of dry days and sunshine. The use of analogues is based on the assumption of the existence of unspecified but persistent forces acting the same way in years with similar circulation patterns. Van den Dool (1975) had a more physical but less direct approach to the prediction problem. In two observational studies he investigated the spectral structure of the atmosphere in the time domain for large scale low frequencies as well as for small scale high frequency waves. In a third study he estimated the terms in the equation for eddy kinetic energy and tried to close this equation with a diffusion approximation for the third order terms.

Van den Dool (1976) also developed transition rules for the Netherlands, which give the chances for a warm, cold or normal month as a function of mean temperature in the past month. These rules were determined from the observed records at de Bilt. In most cases they express the tendency for a surface temperature anomaly to persist in the next month. Van den Dool and Nap (1980) speculated that the persistence in temperature is a local boundary layer effect caused by the presence of the North Sea. The influence of this heat reservoir decreases sharply landward, so that transition rules are of practical value only in a small zone along the coast.

Baede en Reiff (1977) developed a barotropic model for time mean flow. Starting from initial conditions of five day mean flow they integrated the model in time to produce forecasts for the mean circulation in the next week. They assumed that medium range predictability of low frequency

waves could be improved by neglecting the interaction with synoptic, and subsynoptic scale waves. Their efforts were not unsuccessful but the foundation of the European Centre For Medium Range Weather Forecasts made further research on time scales of a week redundant.

Oerlemans (1975, 1977a) investigated the relation between STA's in the mid-latitude part of the Atlantic and prevailing circulation types over Western Europe and between STA's and monthly mean air temperatures in de Bilt. In both papers he found significant relations. With a linear steady-state barotropic model in a β channel he simulated the influence of STA's on the mean circulation (Oerlemans 1977b). Both phase and amplitude of the waves appeared to be strongly dependent on the strength of the zonal mean flow, indicating that the atmospheric response to persistent surface forcing will be different in different seasons.

The skill of the analogue method, transition rules, sea temperature rules and persistence, as well as the official monthly forecasts issued by the weather services in the United States, England and Germany (all applied to the Netherlands or nearby locations) was computed by Nap et al (1981) for the period 1970 to 1979. The main conclusion of the paper is that some skill is present only for the prediction of mean temperature but without exception it is disappointingly low. Simple statistical methods, such as transition rules and sea temperature rules, perform at least as well as more sophisticated and time consuming methods.

1.3. Overview of the work presented in this thesis

In 1978 it was decided that the development of methods leading directly to a prediction of climate anomalies on terms of a month to a year is useless without a better knowledge of the underlying physical factors determining the state of the climate system. It was decided to give up the idea of developing methods leading directly to LRWP. Opsteegh and van den Dool (1979) investigated the properties of the seasonal mean atmosphere. We took radiosonde observations over Western Europe for the winter of 1976/77. Nearly all terms in the prediction equations for the time mean quantities \bar{u} , \bar{v} and \bar{T} were estimated. It was found that the tendency terms are negligible and that the internal eddy forces are comparable in magnitude to the advective part of the acceleration. We

tried to find closure relations for the eddy forces in the equations for the time-mean flow by scaling the prediction equations for the horizontal second order eddy statistics $\overline{u'^2}$, $\overline{v'^2}$, $\overline{u'v'}$, $\overline{u'T'}$, $\overline{v'T'}$. It was also found that the equations for the fluxes are essentially maintenance equations. The second-order ageostrophic and the third-order terms are difficult to compute from observations and are probably inaccurate. However, we think that the estimate of the order of magnitude of both classes of terms is correct. The results indicate that they play a significant role in the balance of the equations for the fluxes. Parameterization of these unknowns is probably even more difficult than the direct parameterization of second-order fluxes in terms of the time mean flow.

On the basis of these observational results we decided to develop a numerical model (Opsteegh and van den Dool 1980). The model is based on the assumption that anomalies in monthly or seasonal-mean atmosphere can be regarded as forced stationary planetary waves. The assumption was first made by Egger (1977) in his simulation of the effects of STA's on the mean circulation. As the observed normal standing waves in the atmosphere are mainly linear (Lau 1979), we decided to apply the assumption of linearity also for anomalous standing eddies. The equations are linearized around a zonally symmetric state which depends on latitude and height according to observations. The model is formulated in the primitive equations on a sphere. The tendency terms have been neglected, so the equations are directly solved for forced stationary waves. The model has two levels in the vertical with boundaries at the earth's surface and at 200 mb. At 200 mb a rigid lid condition is applied. In the zonal direction the variables are represented by Fourier series, while in the meridional direction a gridpoint representation is used. The equations are solved on the Northern Hemisphere with symmetric boundary conditions at the equator.

We have studied the amplitude and phase relations of the model response as a function of latitude for a very simple heating, which is sinusoidal in zonal direction with zonal wavenumber m ($m = 1, \dots, 10$) and constant in meridional direction. For the zonal symmetric state we used February mean conditions.

The response of the model to tropical forcing indicates that heat sources in the tropics can have a substantial influence on the middle and high latitudes, provided that part of the heating is in the westerlies. We have compared the model response for such a heating with similar experiments with a general circulation model and with teleconnection patterns derived from observations for Northern Hemisphere winters with a warm equatorial Pacific. In all cases we find strong similarities of hemispheric wave patterns. Apparently surface conditions in the tropics not only generate tropical wave phenomena such as the Southern Oscillation, influencing climate anomalies in the tropics, but on some occasions may also be the cause of a mid-latitude wave pattern. Our search for possibilities of long-range predictions for the Netherlands finally leads to the same tropical sources as Berlage studied so many years ago in order to make monsoonal predictions for Indonesia.

We have tested the sensitivity of the model to changing conditions in the zonally symmetric state by computing the response to a fixed heating for zonally symmetric conditions in all seasons. This was done for a heat source in the tropics as well as in the middle latitudes. Both in amplitude and phase the response to exactly the same heating can change substantially from one season to the next. In summer the mid-latitude response to a tropical heat source is negligible because the heating is located in the easterlies. In the other seasons a pronounced mid-latitude wave pattern results from tropical forcing. The sensitivity of the response to changes in the zonally symmetric state may be an indication that small changes in the zonally symmetric state of the atmosphere affect atmospheric responses to persistent zonally asymmetric forcing considerably. Therefore a meaningful connection between persistent surface conditions and variable climate anomalies is not unlikely. On the other hand, in order to predict the climate response we must know these subtle changes in the internal state of the atmosphere such as the strength of the zonally symmetric westerly winds, the location of the zero wind line, changes in refractive index in the stratosphere and so on. It remains to be seen whether this will be possible. Changes in the zonally symmetric state may in itself be somehow related to the same external forcing or may be generated internally by climate noise.

As mentioned earlier we assume in this thesis that planetary waves are linear perturbations of the zonally symmetric state. So far the zonally symmetric state is defined by the zonal mean zonal wind and the zonal mean temperature distribution. Zonally symmetric meridional circulations were neglected. In the third paper (Opsteegh 1982) the Hadley and Ferrel circulations are included in the prescribed zonally symmetric state. The sensitivity of the model response to this rather weak meridional circulation is tested, especially for forcing in the tropics. The results indicate that the existence of a meridional circulation in the easterlies may have large consequences. From the linear barotropic vorticity equation it is derived that Rossby wave solutions exist in an easterly mean flow with a weak meridional component. The structure of these waves is such that they transport energy in only one direction, which is given by the direction of the meridional wind in the Hadley cell. As a consequence a heat source located in the tropical easterlies or in the subtropics of the southern hemisphere (summer hemisphere) gives a remote response at middle and high latitudes of the northern hemisphere. Energy transport in opposite direction is negligible.

So far we have only studied the effects of local anomalies in surface conditions on the anomalies in the circulation. The same linear model can also be applied to simulate the normal standing eddies resulting from normal external forcing by the earth's surface and internal forcing by transient eddies. In the fourth paper (Opsteegh van Vernekar 1981) we have simulated the normal January standing wave pattern. The surface forcing consists of mountain forcing and thermal forcing resulting from the contrast between continents and oceans. Mountain effects are incorporated by introducing vertical velocities at the surface boundary. The diabatic heating is calculated using parameterized forms of the heating processes. The transient eddy effects are derived from observations by computing the gradients of the observed eddy fluxes $\overline{u'^2}$, $\overline{u'v'}$, $\overline{v'^2}$, $\overline{u'T'}$ and $\overline{v'T'}$. These internal forces are then prescribed in the model. Separate and combined responses to all three forcing components have been computed.

When all the effects are incorporated the results at middle and lower latitudes show good agreement with observations. However, at higher latitudes, where the zonal mean winds are very weak, the

assumption of linearity does not hold. Here we find unrealistic responses to internal forcing by transient eddies.

The effects of mountains are stronger than the effects of thermal forcing. The response to the combined surface effects shows only some agreement with the observed standing eddy pattern. The effects of transient eddies are comparable in magnitude to the mountain effects. The results suggest the existence of a phase relationship between externally and internally forced waves. A likely explanation for this relation is that the phase of the planetary waves forced by the surface determines the areas where cyclogenetic activity can take place. It is this organization of cyclogenetic activity which determines the phase of the internally forced waves.

Earlier results with two-dimensional β plane models suggest that the normal standing waves can almost be explained from direct surface forcing alone. In these models an assumption on the meridional scale of the waves has to be made. Derome and Wiin Nielsen (1971) show that their results are highly dependent on the particular choice of this parameter. Later simulations with more realistic three-dimensional models (Egger 1976, Ashe 1979, Hoskins and Karoly 1981) show the same level of agreement with observations as found in this study when only surface forcing is incorporated: some areas compare very well, in other areas there are serious phase errors.

The fact that internal forcing by transient eddies seems to play a significant role for the explanation of the observed normal standing eddy pattern is disappointing from the point of view of a long range forecaster, because it is likely that variations in internal forcing are even more important for the anomalous standing eddies. However, we have also found a slight indication of some kind of organization of internal eddy forcing by externally forced planetary waves. If such a relation holds not only for the normal situation but also for the anomalies in particular months, we have a possibility of parameterizing the effects of transient eddies in terms of anomalous conditions at the earth's surface.

1.4. Plans for the near future

From the experiments described in this thesis we may conclude that the dynamical framework of the model is adequate to realistically

simulate mean atmospheric responses to persistent forcing at middle and low latitudes. Nevertheless, the model has some serious drawbacks. First, a realistic vertical distribution of anomalous diabatic heating can not be prescribed. Therefore the parameterization of the effect of surface anomalies such as STA's has to be extremely simple. In such a scheme we would like to distinguish between conditions for which a surface anomaly only results in shallow diabatic heating close to the earth's surface and conditions for which the diabatic heating extends to the middle and upper troposphere. Second, in the present model we apply a rigid lid condition at the top of the troposphere, which means that the energy of all waves is reflected back. However, in reality the very long waves propagate their energy vertically into the stratosphere (Charney and Drazin 1961). We can therefore expect that in the two-level model the responses are too often dominated by resonant wavenumbers. In order to solve both problems we are developing a high-resolution version of the two-level model.

In most of the experiments described in this thesis we have simply prescribed a diabatic heat source. As we are concerned with the effects of anomalous boundary forcing we are developing a parameterization scheme to translate these effects in terms of anomalous diabatic heating.

With a high resolution version of the steady-state model in which the parameterization scheme is included we are planning to do simulation studies to explain observed atmospheric anomalies. With a hemispheric observational data set of surface conditions (STA's, anomalous snow and ice cover) and internal forcing by transient eddies we will try to simulate observed anomalies in monthly and seasonal mean circulation for many cases. As we have found that responses are sensitive to anomalies in the zonally-symmetric state we will use the observed zonal mean state rather than the climatological mean as was done in this thesis. Mountain effects caused by anomalies in the zonally-symmetric zonal wind will be taken into account. From the results of this experiment we hope that we will be able to answer the question on the importance of forcing by the earth's surface for observed anomalies in monthly and seasonal-mean circulation.

In order to ever predict anomalies in the zonally-asymmetric component of the circulation with a type of model described in this thesis, both anomalies in surface conditions and anomalies in the zonally-symmetric circulation will have to be predicted. A model for the zonally-symmetric circulation is presently developed. We have no idea how to predict anomalies in this component of the circulation, but we plan to do simulation studies with anomalous forcing derived from observations, in order to get some idea which processes are important.

We plan to start the prediction of surface conditions with prediction of STA's. For this purpose we are developing a model for the mixed layer of the ocean. The main driving force for this model will be the monthly mean surface wind distribution. This model will be coupled with the steady-state model by assuming that the mixed layer is very slow compared to the atmosphere. In that case forced waves in the atmosphere are approximately in equilibrium with STA's but not vice versa. The idea is to compute a steady-state atmospheric response to some observed distribution of STA's and next drive the model for the mixed layer with the computed surface winds. This driving force gives rise to a change of temperatures in the mixed layer which can be predicted. We think of a time step of the order of several days to a week. After one time step with the mixed layer model the steady-state atmospheric response to the new STA distribution is computed and so on.

Concerning the influence of internal forcing by transients for LRWP we will investigate with simulation experiments whether part of the anomalies in this forcing component is related to anomalous externally forces waves in a way as described by Opsteegh and Vernekar (1982) or that variations in internal forcing must be regarded as unpredictable sampling fluctuations.

So far we have neglected the nonlinear part in the dynamics of the planetary waves. It might be possible that nonlinear aspects are essential for the explanation of the occurrence of so called "regimes" in the circulation. Experiments with simple forced nonlinear systems (Egger, 1978, Charney and Devore 1979) point in this direction. It is not clear what the implication of such potential nonlinear behavior is for the problem of LRWP. In fact only one thing is clear in this field: it will take a long time (if ever) before interannual variations in climate can be predicted with a skill that is of some practical value.

1.5. References

- Adem, J., 1964: On the physical basis for the numerical prediction of monthly and seasonal temperatures in the troposphere-ocean-continent system. *Mon. Wea. Rev.*, 92, 91-103.
- Arakawa, A., A. Katayama and Y. Mintz, 1969: Numerical simulation of the general circulation of the atmosphere. Proceedings of the WMO/IUGG Symposium on Numerical Weather Prediction, Tokyo, Meteorological Society of Japan, Tokyo.
- Ashe, S., 1979: A nonlinear model of the time-average axially asymmetric flow induced by topography and diabatic heating. *J. Atm. Sci.*, 36, 109-126.
- Baede, A.P.M., and J. Reiff, 1977: Resultaten van een experiment betreffende de voorspelbaarheid van de golven $n = 3-10$ in een 5-daags gemiddeld barotroop model. Scientific Report of the Royal Netherlands Meteorological Institute. W.R. 77-4.
- Berlage, H.P., 1934: Further researches into the possibility of long-range forecasting in Netherlands India. K.M.M.O. Batavia, Verhandelingen, 26.
- Berlage, H.P., 1957: Fluctuations of the general atmospheric circulation of more than one year, their nature and prognostic value. Royal Netherlands Meteorological Institute, Mededelingen en Verhandelingen, 69.
- Berlage, H.P., 1966: The southern oscillation and world weather. Royal Netherlands Meteorological Institute, Mededelingen en Verhandelingen, 88.
- Boer, H.J. de, 1947a: Further researches into the physical reality of some long periodic cycles on the barometric pressure of Batavia. K.M.M.O. Batavia, Verhandelingen, 30.
- Boer, H.J. de, 1947b: On forecasting the beginning and the end of the dry monsoon in Java and Madura. K.M.M.O. Batavia, Verhandelingen, 32.

- Braak, C., 1910: Periodische Klimaschwankungen. *Met. Z.*, 27, 121.
- Braak, C., 1912: A long range weather forecast for the eastmonsoon on Java. *Proc. Roy. Acad. Amsterdam*, 21 I, 929.
- Braak, C., 1919: Atmospheric variations of short and long duration in the Malay Archipelago and neighbouring regions and the possibility to forecast them. *K.M.M.O. Batavia, Verhandelingen*, 5.
- Bijl, W. van der, 1952: Toepassing van statistische methoden in de klimatologie. Thesis Utrecht; *K.N.M.I. Mededelingen en Verhandelingen*, 58.
- Bijl, W. van der, 1954: Weersverwachtingen op lange termijn. *K.N.M.I. verspreide opstellen*, 1.
- Charney, J.G., and A. Eliassen, 1949: A numerical method for predicting the perturbations of the middle latitude westerlies. *Tellus*, 1, 38-55.
- Charney, J.G., and P.G. Drazin, 1961: Propagation of planetary-scale disturbances from the lower into the upper atmosphere. *J. Geophys. Res.*, 66, 83-109.
- Charney, J.G., and J.G. Devore, 1979: Multiple flow equilibria in the atmospheric and blocking. *J. Atmos. Sci.*, 36, 1205-1216.
- Derome, J., and A. Wiinr.Nielsen, 1971: Response of a middle latitude model atmosphere to forcing by topography and stationary heat sources. *Mon. Wea. Rev.*, 99, 564-576.
- Dool, H.M. van den, 1975: Three studies on spectral structures of the horizontal atmospheric motion in the time domain. Thesis Utrecht.
- Dool, H.M. van den, 1976: Verwachtingen van de maandgemiddelde temperatuur m.b.v. overgangsregels. Scientific Report of the Royal Netherlands Meteorological Institute. W.R. 76-14.
- Dool, H.M. van den, and J.L. Nap, 1981: An explanation of persistence in monthly mean temperatures in the Netherlands. *Tellus*, 33, 123-131.

- Egger, J., 1976: On the theory of steady perturbations in the troposphere. *Tellus*, 28, 381-389.
- Egger, J., 1977: On the linear theory of the atmospheric response to sea surface temperature anomalies. *J. Atmos. Sci.*, 34, 603-614.
- Egger, J., 1978: Dynamics of blocking highs. *J. Atmos. Sci.*, 35, 1788-1801.
- Euwe, W., 1949: Forecasting rainfall in the period Dec-Jan-Feb for Java and Madoura. K.M.M.O. Batavia, Verhandelingen, 39.
- Gallé, P.H., 1917: Over het verband tussen schommelingen en de sterkte van den Noordoostpassaat van den Atlantischen Oceaan en schommelingen en verschijnselen op hydrografisch en meteorologisch gebied. *Ts. K.N.A.G. 2e S.*, 34, 192-210.
- Gilchrist, A., 1977: An experiment on extended range prediction using a general circulation model and including the influence of sea surface temperature anomalies. *Beitr. zur Phys. der Atm.*, 25-40.
- Hildebrandsson, H.H., 1897: Quelques recherches sur les centres d'action de l'atmosphère. *Kon. Svenska Vetens.-Adkad. Handl.*, 29.
- Hollingsworth, A., K. Arpe, M. Tiedtke, M. Capaldo and H. Savijärvi, 1980: The performance of a medium range forecast model in winter. Impact of physical parameterization. *Mon. Wea. Rev.*, 108, 1736-1773.
- Horel, J.D., and J.M. Wallace, 1981: Planetary scale atmospheric phenomena associated with the Southern Oscillation. *Mon. Wea. Rev.*, 109, 813-829.
- Hoskins, B.J., and D.J. Karoly, 1981: The steady linear response of a spherical atmosphere to thermal and orographic forcing. *J. Atmos. Sci.*, 38, 1179-1196.
- Kurihara, Y., 1970: A statistical-dynamical model of the general circulation of the atmosphere. *J. Atmos. Sci.*, 27, 847-870.
- Lau, N.C.L., 1979: The observed structure of tropospheric stationary waves and the local balances of vorticity and heat. *J. Atm. Sci.*, 36, 996-1016.

- Lorenz, E.N., 1968: Climate determinism. Meteor. Monographs, Vol. 8, No. 30, pp. 1-3.
- Lorenz, E.N., 1969: Three approaches to atmospheric predictability. Bull. Amer. Meteor. Soc., 50, 345-349.
- Madden, R.A., 1976: Estimates of the natural variability of time-averaged sea level pressure. Mon. Wea. Rev., 104, 942-952.
- Manabe, S., and T.B. Terpstra, 1974: The effects of mountains on the general circulation of the atmosphere as identified by numerical experiments. J. Atmos. Sci., 31, 3-42.
- Mintz, Y., 1981: The sensitivity of numerically simulated climate to land surface conditions. Proceedings of the study conference on land surface processes in atmospheric general circulation models, Greenbelt, Maryland, 5-10 January, 1981.
- Namias, J., 1968: Long range weather forecasting history, current status and outlook. Bull. Amer. Meteor. Soc., 49, 438-470.
- Nap, J.L., H.M. van den Dool and J. Oerlemans, 1981: A verification of monthly weather forecasts in the seventies. Mon. Wea. Rev., 109, 306-312.
- Neumann, J. von, 1955: Some remarks on the problem of forecasting climatic fluctuations. Dynamics of Climate. pp. 9-11. The proceedings of a conference on the application of numerical integration techniques to the problem of the general circulation (R.L. Pfeffer, Ed.), Pergamon Press, London.
- Nicholls, N., 1980: Long-range weather forecasting: value, status and prospects. Rev. Geophys. Space Phys., 18, 771-788.
- Oerlemans, J., 1975: On the occurrence of "Grosswetterlagen" in winter related to anomalies in North Atlantic sea temperature. Meteor. Rdsch., 28, 83-88.
- Oerlemans, J., 1977: Het verband tussen anomalieën in de temperatuur van de Noordatlantische Oceaan en de maandgemiddelde temperatuur in De Bilt en de bruikbaarheid hiervan voor de maandverwachting. Scientific Report of the Royal Netherlands Meteorological Institute. W.R. 77-11.

- Oerlemans, J., 1977: The influence of stationary heating on time-mean atmospheric flow forced to be equivalent-barotropic. Beitr. Phys. Atmos., 50, 247-252.
- Opsteegh, J.D., and H.M. van den Dool, 1979: A diagnostic study of time-mean atmosphere over Northwestern Europe during winter. J. Atm. Sci., 36, 1862-1879.
- Opsteegh, J.D., and H.M. van den Dool, 1980: Seasonal differences in the stationary response of a linearized primitive equation model. Prospects for long range weather forecasting? J. Atmos. Sci., 37, 2169-2185.
- Opsteegh, J.D., 1982: On the importance of the Hadley and Ferrel circulation for teleconnections forced by low-latitude heat sources. To be published.
- Opsteegh, J.D., and A.D. Vernekar, 1982: A simulation of the January standing wave pattern including the effects of transient eddies. Accepted for publication in J. Atmos. Sci..
- Rowntree, P.R., 1972: The influence of tropical east Pacific Ocean temperature on the atmosphere. Quart. J. Roy. Meteor. Soc., 98, 290-231.
- Rowntree, P.R., 1976: Response of the atmosphere to a tropical Atlantic Ocean temperature anomaly. Quart. J. Roy. Meteor. Soc., 102, 607-625.
- Saltzman, B. and A.D. Vernekar, 1971: An equilibrium solution for the axially-symmetric component of the earth's macroclimate. J. Geophys. Res., 76, 1498-1524.
- Schuurmans, C.J.E., 1969: The influence of solar flares on the tropospheric circulation. Thesis Utrecht. K.N.M.I. Mededelingen en Verhandelingen, 92.
- Schuurmans, C.J.E., 1973: A 4 year experiment in long-range weather forecasting using circulation analogues. Meteor. Rdsch. 26, 2-4.

- Smagorinsky, J., 1953: The dynamical influence of large-scale heat sources and sinks on the quasi-stationary mean motions in the atmosphere. *Quart. J. Roy. Meteor. Soc.*, 100, 342-366.
- Smagorinsky, J., 1963: General circulation experiments with the primitive equations: I. The basic experiment. *Mon. Wea. Rev.*, 91, 99-164.
- Somerville, R.C.J., P.H. Stone, M. Halem, J.E. Hanssen, J.S. Hogan, J.S. Druryan, L.M. Russell, A.A. Lacis, W.J. Quirk and J. Tenenbaum, 1974: The GISS model of the global atmosphere. *J. Atmos. Sci.*, 31, 84-117.
- Spar, J., 1977: Monthly mean forecast experiments with the GISS model. *Mon. Wea. Rev.*, 105, 535-539.
- Spar, J., and R. Lutz, 1979: Simulations of the monthly mean atmosphere for February 1976 with the GISS model. *Mon. Wea. Rev.*, 107, 181-192.
- Tung, K.K., and R.S. Lindzen, 1979: A theory of stationary long waves: Part II: Resonant Rossby waves in the presence of realistic vertical shear. *Mon. Wea. Rev.*, 107, 735-750.
- Visser, S.W., 1946: Long-range weather forecasts in the Netherlands. *K.N.M.I. Mededelingen en Verhandelingen*, 51.
- Walker, G.T., 1928: World Weather II. *Mem. Roy. Meteor. Soc.*, II, no. 17, 97-106.
- Walker, G.T., and E.W. Bliss, 1937: World weather VI. *Mem. Roy. Meteor. Soc.*, 4, 119-139.

- II. A Diagnostic Study of the Time-Mean Atmosphere over
Northwestern Europe during Winter.[†]

J.D. Opsteegh and H.M. van den Dool.

[†]Published in J. Atmos. Sci., 1979, 36, 1862-1879.

Abstract

A diagnostic study has been performed to investigate the prospects for developing a time-averaged statistical-dynamical model for the purpose of long-range weather-forecasts. Estimates are made of nearly all terms in the equations describing the evolution of the time-mean quantities \bar{u} , \bar{v} , \bar{T} , $\bar{\omega}$ and the horizontal second-order eddy statistics $\overline{u'^2}$, $\overline{v'^2}$, $\overline{u'v'}$, $\overline{u'T'}$, $\overline{v'T'}$. These calculations were performed over Northwestern Europe, using radiosonde observations of wind, temperature and height for the winter of 1976/1977. Geostrophic winds were estimated from objective analyses, while vertical velocities were determined with a quasi-geostrophic baroclinic model. For each equation approximate balances are presented on the basis of these estimates.

In the equations for the mean quantities the time derivatives are more than one order of magnitude smaller than the unknown second-order eddy statistics. The same holds for the time derivatives of second-order eddy statistics compared with the unknown third-order and ageostrophic terms in the equations for these eddy fluxes. Therefore we state that the system of time-averaged equations has no ability to describe the evolution of one specific mean state of the atmosphere to a mean state in the future, because for this purpose a closure of the system or a parameterization of second-order or third-order terms has to be extremely accurate. But even in the case that only the stationary waves of the mean flow are treated, a higher order closure scheme does not seem to be feasible because third-order terms and ageostrophic second-order terms are probably large and very difficult to parameterize. This implies that a preferable approach is to explore in greater depth the possibility of parameterizing the second-order statistics directly.

Notation and definition

x, y	= curvilinear coordinates pointing east and north
λ, ϕ	= geographical longitude and latitude
dx	= $a \cos \phi d\lambda$
dy	= $a d\phi$
p	= pressure, vertical coordinate
t	= time
$u = dx/dt$	= zonal wind component
$v = dy/dt$	= meridional wind component
$\omega = dp/dt$	= vertical wind component
$u_g = -\frac{\alpha}{f} \frac{\partial p}{\partial y}$	= geostrophic zonal wind component
$u_{ag} = u - u_g$	= ageostrophic zonal wind component
$v_g = \frac{\alpha}{f} \frac{\partial p}{\partial x}$	= geostrophic meridional wind component
$v_{ag} = v - v_g$	= ageostrophic meridional wind component
T	= temperature
z	= height above sea level
$\phi = gz$	= geopotential
α	= specific volume
a	= average radius of the earth
c_p	= specific heat at constant pressure
$f = 2\Omega \sin \phi$	= Coriolis parameter
g	= acceleration of gravity
R	= gas constant
F_x, F_y	= components of horizontal friction
Q	= diabatic heating
Ω	= angular velocity of the earth
\overline{F}	= time average of F
$F' = F - \overline{F}$	= departure of time average of F
$\sigma = \frac{RT}{pc_p} - \frac{\partial T}{\partial p}$	= static stability

2.1. Introduction

In order to predict the changes in the large-scale atmospheric circulation pattern we have to integrate the equations that describe the dynamical processes which are involved in these changes. The way in which we are allowed to modify the equations strongly depends on the integration time. If we integrate only one day ahead we can look at the atmosphere as a quasi-geostrophic system. On a time-scale of several days, say 3-14, we have to integrate deterministic equations that include diabatic heating as a very important driving mechanism. Finally, on the time-scales of climate fluctuations dynamical processes have to be parameterized. For the purpose of long-range weather forecasts we are interested in anomalies in the time-mean circulation (about one month). But until now we hardly know which processes are responsible for such anomalies and to what extent.

Of course we can try to make long-range weather forecasts with a general circulation model (GCM) in which all forcing functions are taken into account and all individual eddies and their influences on the mean flow are treated explicitly. Because the predictability of synoptic eddies is limited to about one week (Lorenz, 1969), we can at best expect to produce long-range forecasts of mean fields. Therefore the use of a GCM is very time-consuming.

An alternative way of making long-range weather forecasts is to treat the time-averaged flow explicitly, whereas transient systems with periods less than the averaging period are treated as a kind of turbulence. This turbulence then has to be related to the mean flow. Models of this type are called Statistical Dynamical (SD)¹⁾ models.

The most direct way to derive equations for the time-mean flow is to take a time average of all terms in the primitive equations.

¹⁾Footnote. Here we adopt the terminology used by Kurihara (1970) and others, although the term statistical dynamical model is also used to describe the time evolution of the probability distribution of atmospheric states.

The resulting equations contain a set of unknown variables. These "eddy-statistics" describe the effects of the transient eddies on the time-mean atmosphere.

At first sight, this way of attacking the problem seems much more elegant than a straightforward integration with an explicit general circulation model. However, SD-models will only be successful in making long-range weather forecasts, if a reliable set of closure relations, diagnostic or prognostic, can be derived. It is well known that the transient eddies contribute substantially to the maintenance of the time-mean fields (Lorenz, 1967).

Most of the models discussed in the literature are zonally averaged. One of the few time-averaged and non-zonally averaged models was constructed by Adem (1964, 1970). Adem uses a time-dependent heat-balance model in which only the thermodynamic equation is used. The unknown eddy heat flux is assumed to be of a diffusive form. Recently Vernekar and Chang (1978) presented a linear time-averaged steady-state SD-model, which describes stationary perturbations. Their equations deal with both dynamical and thermodynamical processes and, again, eddy fluxes are approximated by diffusion terms.

The use of a diffusion concept in order to parameterize second-order eddy statistics is not based on much observational evidence. From diagnostic studies it becomes clear that it is very difficult to find closure relations. In order to avoid problems with second-order eddy statistics one can formulate equations for their evolution in time. In doing so we introduce new unknowns: third-order eddy statistics, this in the hope that these terms will be easier to deal with. Until now very little work has been published on this possibility. Exceptions are papers by Saltzman et al. (1961), Van den Dool (1975) and Savijärvi (1976).

Apart from very difficult problems concerning the closure of the system of equations one will have to deal with many other questions. Is there an optimum averaging period? What

are leading terms in the equations and can any of the terms be neglected?

There are many papers that touch on these problems. The purpose of some of these studies is to obtain a better insight in the maintenance of certain quantities, see for example Lau et al. (1978). But because prediction of time-mean quantities is the ultimate goal, one should also investigate the possibilities of prognostic equations. Therefore it makes sense to study a rather short period of a few months, instead of many years or many seasons.

A complete observational survey of the terms in all equations might be useful in the description of the time-averaged atmosphere. In this paper calculations are presented of the orders of magnitude of nearly all terms in the equations describing time mean quantities \bar{u} , \bar{v} , \bar{T} , $\bar{\omega}$ and the equations describing the horizontal second-order eddy statistics $\overline{u'^2}$, $\overline{v'^2}$, $\overline{u'v'}$, $\overline{u'T'}$, $\overline{v'T'}$. These calculations have been performed over Northwestern Europe, which, of course, is a rather small domain. We used radiosonde observations of wind, temperature and height at ten standard levels for one winter.

It is hoped that scaling considerations will provide a better insight into the following problems. First, the closure problem: can we neglect or easily parameterize the third-order terms in the equations for second-order terms? If this were the case, then it is advantageous to close the system at third-order, despite the fact that we introduce another five non-linear differential equations at the same time. And secondly, how can we find a way to modify the original set of equations such that they become easier to use?

2.2. Formulation of the problem for time-mean atmosphere

The set of equations for dry air which are commonly used in meteorology consists of the horizontal momentum balance, the hydrostatic assumption, the continuity equation, the first law of thermodynamics and the equation of state. Together these equations form a closed set in six unknowns, u , v , ω , T , ϕ and

α , the horizontal and vertical wind, temperature, geopotential height and specific volume respectively. Friction and diabatic heating have to be prescribed.

In order to obtain equations for the time-averaged flow we have to define a time average first.

$$\bar{F}(t) = \frac{1}{\Delta t} \int_{t' - \frac{1}{2}\Delta t}^{t' + \frac{1}{2}\Delta t} F(t') dt' \quad (2.1)$$

At any time F can be divided in its time average and a deviation

$$F = \bar{F} + F' \quad (2.2)$$

If (2.2) is substituted for all variables in all basic equations and consequently the time-averaging procedure is applied, then we obtain equations for the evolution of \bar{u} , \bar{v} , $\bar{\omega}$, $\bar{\phi}$, \bar{T} and $\bar{\alpha}$. In addition, we assume that $\overline{F'} = 0$, which is not necessarily true for running means.

The equations for averaged horizontal motion are completely comparable to the usual equations of motion, except that large-scale Reynolds' stresses are included now as additional forces. In the same way we find in the thermodynamic equation the large-scale eddies as additional heating. The subsequent terms of these three equations can be found in tables 1 and 2.

We now have a system of six equations in fourteen unknown variables. These variables are \bar{u} , \bar{v} , $\bar{\omega}$, \bar{T} , $\bar{\phi}$, $\bar{\alpha}$, and the eddy statistics $\overline{u'^2}$, $\overline{v'^2}$, $\overline{u'v'}$, $\overline{u'T'}$, $\overline{v'T'}$, $\overline{u'\omega'}$, $\overline{v'\omega'}$, $\overline{\omega'T'}$. Obviously we do not have a closed set of equations anymore. Because, in general, the eddy statistics are found to be important, one cannot simply neglect them. Unfortunately, satisfactory parameterizations of the second-order eddy statistics are not available. Therefore we shall try an alternative approach.

It is possible to add new equations for the time derivative of the horizontal eddy fluxes and variances. Such equations can be derived by simple manipulations with the non averaged

equations. For example, we multiply the u-momentum equations by u' and take a time average afterwards, then we obtain a prognostic equation for the variance of u . The subsequent terms of the equations for $\overline{u'^2}$, $\overline{v'^2}$, $\overline{u'v'}$, $\overline{u'T'}$ and $\overline{v'T'}$ can be found in tables 3 to 7.

The structure of these five equations is roughly the same and consists of five groups of terms. The first group represents advection of the eddy flux quantities by the mean wind. In the second group we find creation and destruction terms (ageostrophic terms, friction, diabatic heating). In the third group the influence of the curvature of the coördinate system is described, while the fourth group represents the interaction with the mean flow. Finally, the fifth group consists of the third-order terms, which describe the mean effect of advection of eddy flux quantities by eddy motion.

A derivation of similar equations for vertical fluxes like $\overline{u'\omega'}$ is impossible. The reason for this is that we have no prognostic equation for ω because of hydrostatic equilibrium. Through the introduction of the five eddy flux equations we have to accept 17 new unknown variables. Eleven of these are third order terms: $\overline{u'^3}$, $\overline{v'^3}$, $\overline{u'^2v'}$, $\overline{u'v'^2}$, $\overline{u'^2\omega'}$, $\overline{v'^2\omega'}$, $\overline{u'v'\omega'}$, $\overline{u'^2T'}$, $\overline{v'^2T'}$, $\overline{u'v'T'}$, $\overline{u'\omega'T'}$, $\overline{v'\omega'T'}$. The remaining unknowns have been expressed as ageostrophic terms: $\overline{u'v'_{ag}}$, $\overline{v'u'_{ag}}$, $\overline{u'u'_{ag}}$, $\overline{v'v'_{ag}}$, $\overline{T'v'_{ag}}$ and $\overline{T'u'_{ag}}$. It is more useful to write them as ageostrophic expressions than to maintain pressure and Coriolis terms separately. Because of the approximate geostrophic balance the latter two are in general very large, but only their small imbalance is relevant in the equations.

If we consider all terms involving friction and diabatic heating as known functions, then the problem as a whole is formulated as a set of 11 equations in 31 unknowns. At first sight the result is a very complex description even though we do not have to prescribe second-order eddy heating explicitly. To find closures we shall have to parameterize third-order terms, second-order vertical fluxes and ageostrophic terms. There is no doubt that this is a tremendous task.

There is very little information concerning the importance of third-order terms in the equations mentioned above. In a study of meridional transport of eddy kinetic energy Saltzmann (1961) found the third-order contribution to be important. Van den Dool (1975) found that the third-order terms in the eddy kinetic energy equation, though smaller than the leading terms, cannot be neglected. Moreover, a diffusion parameterization is not useful. Savijärvi (1976) arrived at the same conclusions. On the other hand, Lau et al. (1978) state that the third-order terms are small in the balance equation for the eddy momentum flux $\overline{u'v'}$.

Even less direct observational information is available concerning large-scale vertical eddy fluxes of momentum and heat. Holopainen (1964, 1973) studied the balance of time-averaged horizontal momentum over England. He calculated mean vertical fluxes with the kinematic and adiabatic methods. Holopainen calculated that the vertical fluxes are about one order of magnitude smaller than the leading terms in the equations. For zonally averaged flow vertical eddy fluxes have been determined as a residue; Hantel (1976) and Hantel and Hacker (1978) found that in this case vertical fluxes by eddies of all scales may become important.

Finally, the ageostrophic terms are doubtlessly important. For example, all kinetic energy in the atmosphere is produced by ageostrophic winds; in the context of the horizontal momentum flux equation Lau et al. (1978) find ageostrophic terms to be of major importance.

2.3. Data and Analysis

For our computations we chose 22 radiosonde stations in Northwestern Europe, see Fig. 1. Twice daily measurements of wind, temperature and geopotential height at 10 levels during the period 17 December 1976 00 GMT to 16 March 1977 12 GMT were used. The levels are the surface and 850, 700, 500, 400, 300, 250, 200, 150 and 100 mb. For our purpose it is convenient

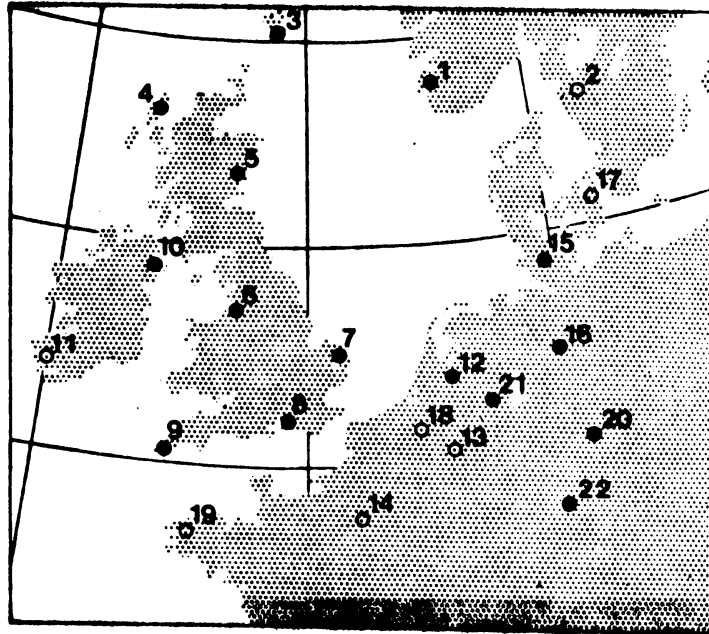


Fig. 1. The northwestern European area where the computations have been performed at radiosonde stations 1-22. Those stations that hardly could be used are denoted by open circles.

to look at these raw data as a collection of time series. So, at 22 stations and 10 levels we have time series of u , v , T and z , each consisting of at most 180 observations. Each time series was checked first. Missing data were filled in by linear interpolation. Elements that deviated more than four standard deviations from the mean were considered missing. If four or more consecutive data were missing, the complete series was rejected. Also, if the missing data totalled 10%, such a series was not used anymore.

For these reasons many series could not be used and for several stations it was hard to find any reliable series. It turns out that starting with 22 stations yields only 15 stations with more or less complete upper air data, (see Fig. 1). In all maps to be presented in the next section, those quantities that could be computed after the check are plotted near the stations.

As far as possible for each station, the following mean terms and eddy statistics were computed:

$$\begin{aligned} &\bar{u}, \bar{v}, \bar{T}, \bar{z}, \\ &\overline{u'^2}, \overline{v'^2}, \overline{u'v'}, \overline{u'T'}, \overline{v'T'}, \\ &\overline{u'^3}, \overline{v'^3}, \overline{u'^2v'}, \overline{u'v'^2}, \overline{u'^2T'}, \overline{v'^2T'}, \overline{u'v'T'} \text{ and} \\ &\frac{\partial \bar{u}}{\partial t}, \frac{\partial \bar{v}}{\partial t}, \frac{\partial \bar{T}}{\partial t}, \frac{\partial \overline{u'^2}}{\partial t}, \frac{\partial \overline{v'^2}}{\partial t}, \frac{\partial \overline{u'v'}}{\partial t}, \frac{\partial \overline{u'T'}}{\partial t}, \frac{\partial \overline{v'T'}}{\partial t} \end{aligned}$$

All terms were computed with an averaging period of 5, 10, 15, 30, 45 and 90 days. We hoped that, for example, the third-order terms would be very small in some properly chosen averaging period. However, from our computations we could not find the existence of such a period. Hence we shall restrict ourselves to a description of the results for an averaging period of 90 days.

From hand-analyses the gradients of mean and eddy quantities were estimated at four levels, namely 200, 300, 500 and 850 mb.

In order to have an estimate of large-scale vertical mean and eddy fluxes, vertical velocities were derived from a filtered quasi-geostrophic baroclinic three-level model. This model is in operational use in the Netherlands Weather Service;

it provides vertical velocities (ω) at three pressure levels: 300, 500 and 850 mb. From objective analyses of geopotential height at 00 and 12 GMT time series of vertical velocities were composed for the locations of the 115 radiosonde stations. If we combine the direct observations of u , v , T and the pseudo-observations of ω , the following eddy and mean quantities can be computed:

$$\overline{\omega},$$

$$\overline{\omega'u'}, \overline{\omega'v'}, \overline{\omega'T'} \text{ and}$$

$$\overline{u'^2\omega'}, \overline{v'^2\omega'}, \overline{u'v'\omega'}, \overline{u'\omega'T'}, \overline{v'\omega'T'}$$

The same objective analysis of geopotential height has been used to compute geostrophic winds at the locations of the 15 stations at the 300, 500 and 850 mb levels. Combined with really observed winds this allows us to estimate $\overline{u'v'}_{ag}$, $\overline{v'u'}_{ag}$, $\overline{u'u'}_{ag}$, $\overline{v'v'}_{ag}$, $\overline{T'v'}_{ag}$, $\overline{T'u'}_{ag}$.

2.4. Reliability of the eddy statistics

We investigated the sensitivity of the horizontal eddy statistics for errors in the wind components. For this purpose, random errors of 2 ms^{-1} were added to both the u and v component. The resulting new statistics showed small deviations of a few per cent.

It is likely, however, that measuring errors are dependent on wind strength. We have simulated this dependence by adding to both velocity components random errors to a maximum of 10% of the respective components. In this case the resulting differences amounted to 20% for $\overline{u'^2}$, $\overline{v'^2}$, $\overline{u'T'}$ and $\overline{v'T'}$, 50% for $\overline{u'v'}$ and 100% for the third-order statistics.

It is well known that the determination of vertical transports, using ω -time series derived with direct or indirect methods, results in large errors. There is no doubt that this applies also to our ω -series. The first reason is that only synoptic-scale vertical motion is considered. One cannot a priori neglect vertical transports by sub-synoptic motion. (Palmen en Newton, 1969). The second reason is the coarse resolution of our model,

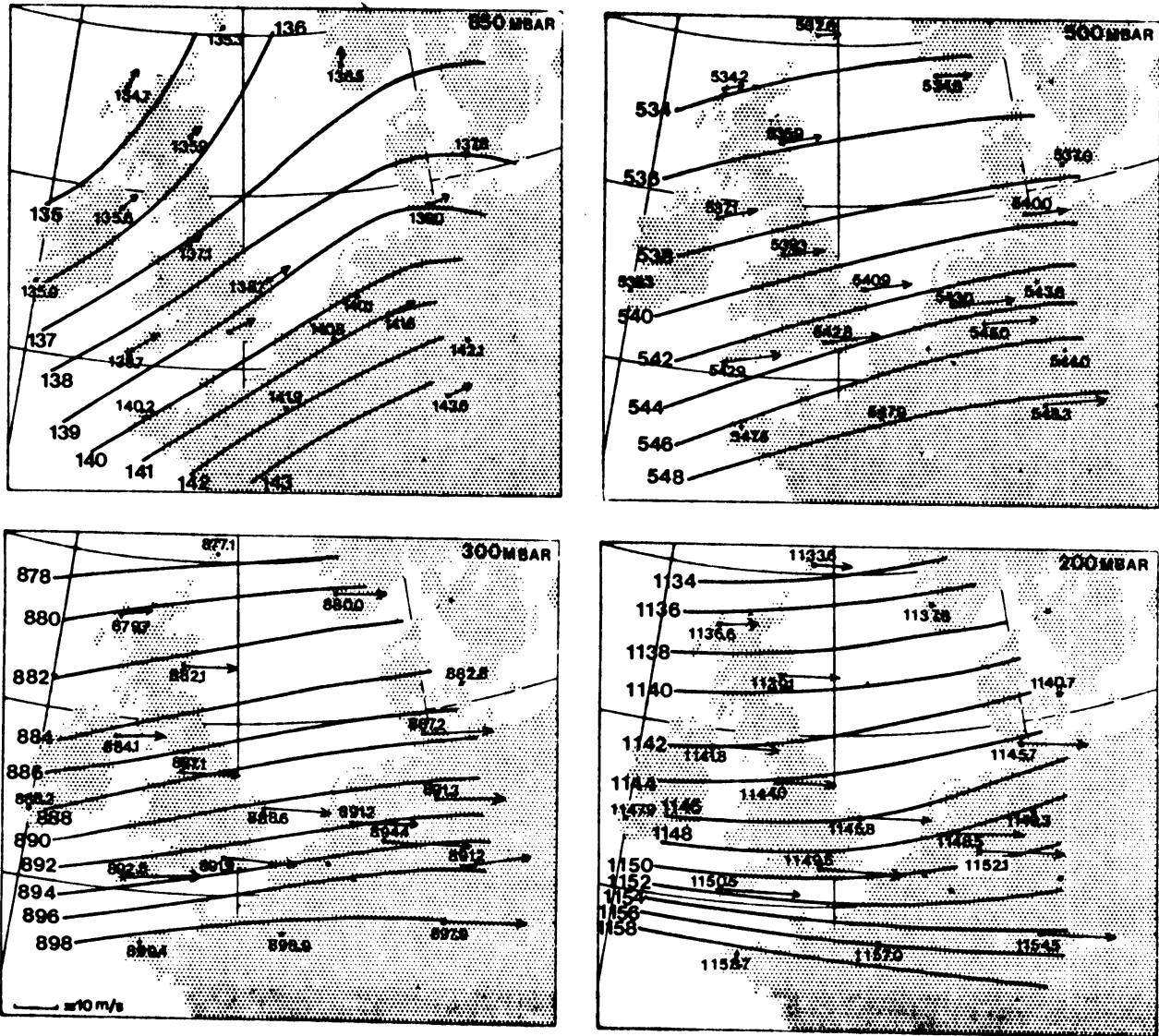


Fig. 2. Spatial distribution of time-mean geopotential height (\bar{z}) during the winter of 1976/77 at four pressure levels. Contour interval is 2 dm, except for 850 mb where it is 1 dm. Arrows indicate time-averaged wind vectors. The scale of these vectors is indicated in the lower left corner.

both horizontally and vertically. Moreover, surface friction, diabatic heating and ageostrophic effects are not taken into account. Therefore the vertical fluxes, even those averaged over a whole winter, contain large errors. Nevertheless, as far as the 90-day mean vertical velocity is concerned, it was found that there is a good agreement with vertical velocities derived from the 90-day mean divergence of the observed winds.

The last group of terms, which may contain large errors, are the ageostrophic terms. The ageostrophic wind is a small difference between two large quantities, which are poorly known, at least for this purpose. We can illustrate this for the time-mean geostrophic wind, because we have two estimates. The first is, of course, the average of the geostrophic wind derived from the objective analyses and used in all computations. A second estimate can be derived from a subjective analysis of time-averaged geopotential height (\bar{z}). As will be visualized in the next section (see Figures 2 and 3) these two estimates show differences which are important in the calculation of the ageostrophic wind.

From the foregoing it is clear that the composition of a reliable set of statistics is a tremendous task. This seems to be especially true for the third-order terms, vertical transport terms and ageostrophic terms. Hence one should be very careful in the interpretation of these statistics.

2.5. Mean state of the atmosphere over Northwestern Europe during the winter of 1976/1977.

We start our discussions of the results with a description of the time-mean atmosphere. In Fig. 2 the distribution of time-mean geopotential height is given for the 850, 500, 300 and 200 mb levels. Time-mean wind vectors are plotted as arrows. From these four maps it becomes clear that the time-averaged atmosphere is rather baroclinic; the mean winds veer with height, especially in the lower half of the troposphere.

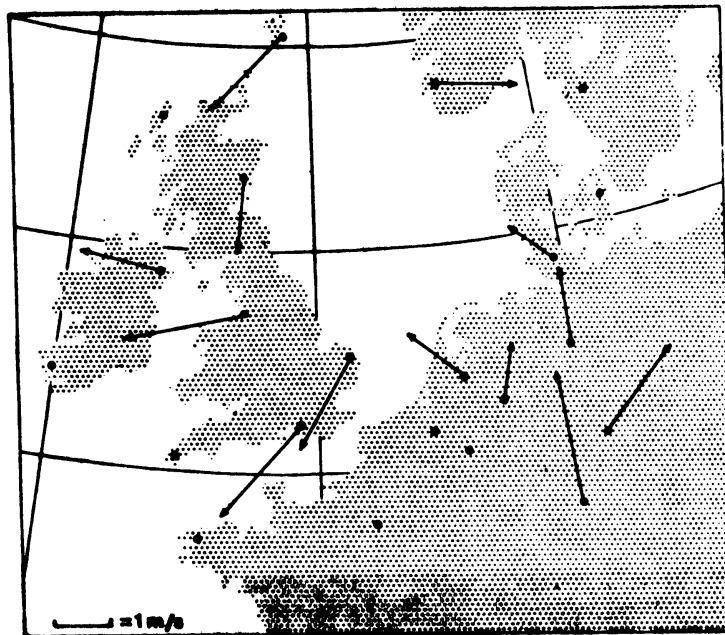


Fig. 3. Ageostrophic winds at 300 mb, determined with objective height analyses. Note that compared to Fig. 2 the length of the wind vectors is multiplied by 10.

At 200 and 300 mb there is considerable cross-isobaric flow; at many stations there is a small wind component towards high pressure. It turns out that the determination of the ageostrophic wind component is very sensitive to the choice of the height-field analysis. In Fig. 2 we used a subjective analysis derived from mean heights only; Fig. 3 shows ageostrophic winds determined with the use of our objective height analyses. In these latter analyses wind measurements are used to estimate local gradients of the height field. However, one must doubt whether this is a real improvement for our purpose; it is far less clear from Fig. 3 that there is a general cross-isobaric flow towards high pressure. This is an illustration of the uncertainties in the computation of ageostrophic winds, mentioned earlier.

Fig. 4 gives the spatial distribution of time-mean temperature at four levels. Again, the arrows are mean wind vectors. The most significant features of these maps are the strong warm air advection at 850 mb and the gradual decrease of horizontal temperature gradients with height. As usual at 200 mb the gradients become very weak or reverse sign.

The veering of the mean wind in the lower layers and the apparent phase difference between contours and isotherms indicate that standing eddies have a baroclinic structure.

The distribution of the vertical velocity \bar{w} at 500 mb is displayed in Fig. 5. Most of the area is characterized by upward motion. The heating due to warm advection is counteracted by cooling due to rising motion. Over the southern part of the British Isles these effects are equivalent to a temperature rise of 2.0 K per day and a temperature decrease of about 1.2 K per day respectively.

As an example, the vertical mean profiles of \bar{u} , \bar{v} and \bar{T} of station 9 (Camborne, Southwest England) are shown in Fig. 6. All profiles are compared with the averages at the 50-degree latitude circle (Oort and Rasmussen, 1971). The winds can also be compared with geostrophic approximations at three levels.

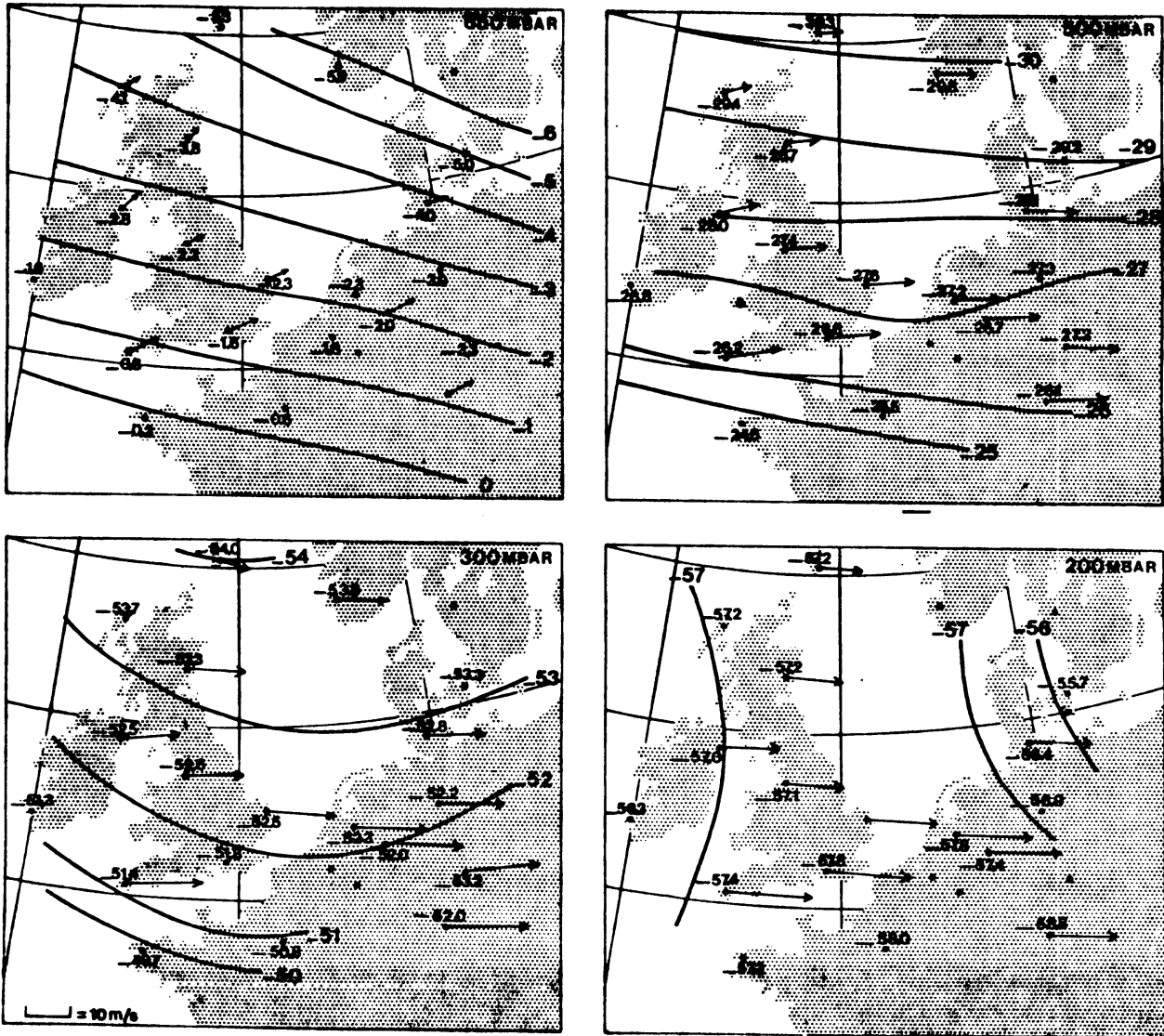


Fig. 4. Spatial distribution of time-mean temperature (\bar{T}) during the winter of 1976/77 at four pressure levels. Isotherms are drawn at intervals of 1 K. As in Fig. 2 arrows represent time-mean wind vectors.

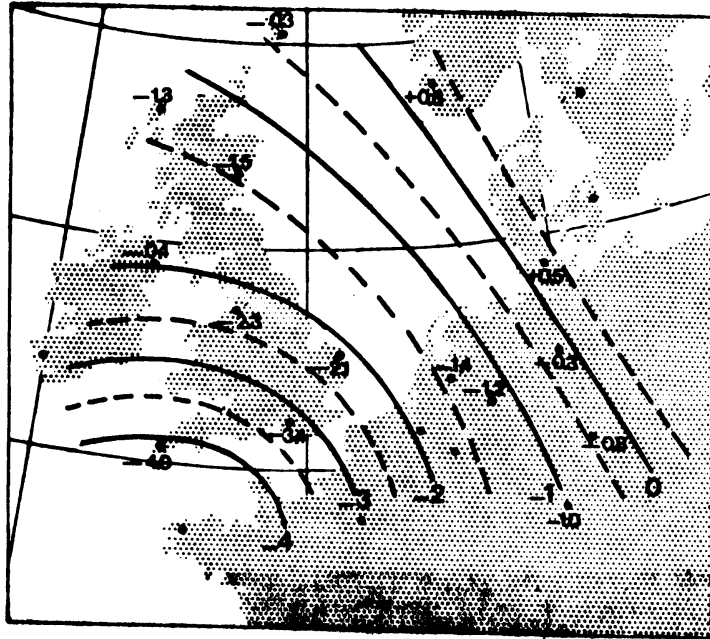


Fig. 5. Time-mean vertical velocity distribution at 500 mb ($\bar{\omega}$) during the winter of 1976/77. Negative values indicate upward large-scale motion. Isolines are drawn at intervals of $10^{-2} \text{ Nm}^{-2} \text{ s}^{-1}$.

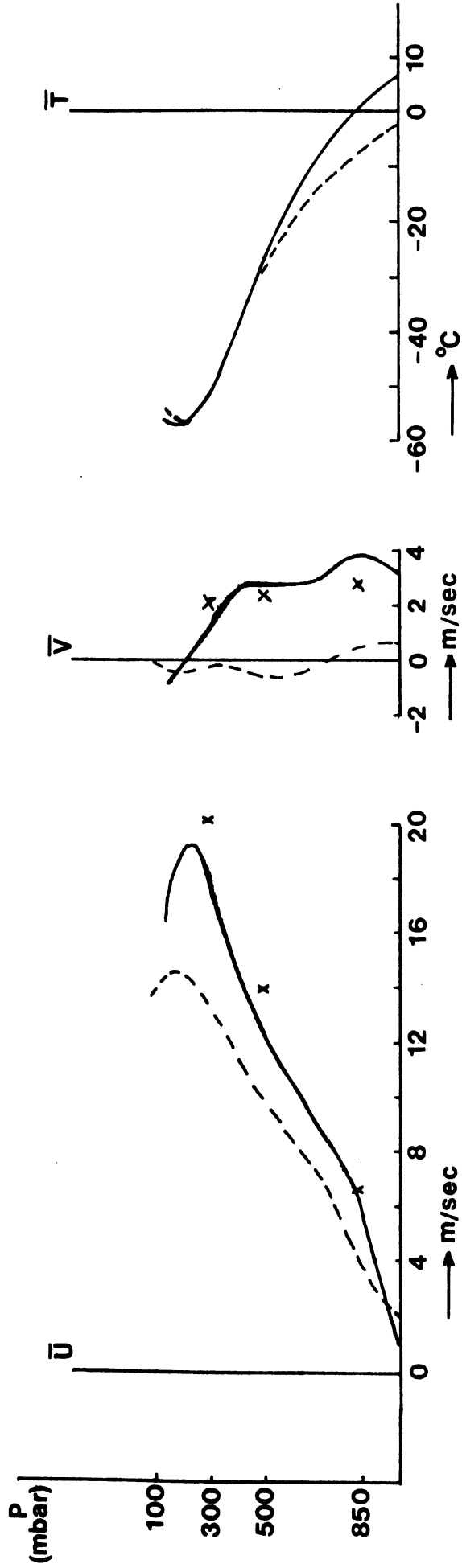


Fig. 6. Vertical profiles of \bar{u} , \bar{v} and \bar{T} (solid lines) at station 9 (Camborne, England), for the winter of 1976/77. Dashed lines give zonally averaged profiles for the same season and latitude (50 N) according to Oort and Rasmusson (1971). Crosses give geostrophic estimates of the time-mean wind at 850, 500 and 300 mb.

The zonal wind profile has a very distinct maximum at 250 mb, which is not uncommon for this latitude. Although much stronger than the zonal average, zonal winds in the upper troposphere are subgeostrophic by a few meters per second. This was also found by Holopainen for the autumn of 1954 (Holopainen, 1964). In the lowest 150 mb the shear in \bar{u} is remarkably stronger than in the zonal average.

Except at 850 mb the meridional wind is close to its geostrophic value. Of course this is in contrast with the zonally averaged meridional wind, which is entirely ageostrophic. The meridional wind found over Southwest England is about one order of magnitude larger than the zonally averaged value. Virtually all air is moving northwards in this area. Obviously, the almost geostrophic meridional mass circulation in horizontal standing eddies dominates the overturning in the ageostrophic Ferrel cell.

The mean temperature profile in the lower half of the atmosphere is locally much steeper than the corresponding zonal average. The temperatures over 500 mb are almost the same but the surface temperature is about 10 K above the zonal average.

An important aspect is the observed vertical shear of the zonal wind. Is the time-mean flow baroclinically stable in the traditional sense? This is an important question in the context of SD-modelling. The baroclinic stability properties were investigated with the help of a linearized version of the 3-level quasi-geostrophic baroclinic model. Using static stabilities and wind shear observed over Southwest England, wavelengths ranging from 1750 to 5000 km turned out to be unstable. Minimum doubling time of these waves amounts to 32 hours. But we are sure that the mean atmosphere does not show any wave growth in this part of the spectrum. How does one deal with this in an SD-model? Two arguments can be put forward. The first is, of course, the transient character of such unstable waves. Transient waves do not appear in time-mean flow and therefore a time-averaged model should be constructed such that these waves are suppressed or made

non-existent. A simple way to do this is the use of smoothing operators or alternatively heavy truncation of the spectrum. A second possibility is that the eddy terms in the model-equations drastically change the stability properties such that wave-growth does not occur anymore at those wavelengths.

2.6. Second-order eddy statistics over Northwestern Europe.

The influence of transient weather systems on the evolution of the mean atmosphere is represented as horizontal and vertical gradients of eddy fluxes of heat and momentum. An example of the vertical profiles of horizontal eddy terms is shown in Fig. 7. As in the previous section, data of station 03808 (Camborne, England) were used for this purpose. As far as possible a comparison is made with zonally averaged profiles at 50 N (Oort and Rasmusson, 1971) and with geostrophic eddy terms at three levels. Data of Oort and Rasmusson suggest that the profiles of $\overline{u'^2}$ and $\overline{v'^2}$ are very nearly the same. This means that large scale turbulence is isotropic, which is in agreement with almost negligible $\overline{u'v'}$ at these latitudes. However, our results indicate that local deviations of isotropy occur; at jet stream level the variances of u and v may differ by 25%. Furthermore, the meridional flux of zonal momentum is substantially larger than the zonal average.

These features can also be judged from maps of $\overline{u'^2}$, $\overline{v'^2}$ and $\overline{u'v'}$ at 300 mb (Figures 8 and 9).

The local (Southwest-England) meridional eddy temperature flux profile shows a maximum at 850 mb, a minimum at 300 mb and again strong poleward fluxes at stratospheric levels. This is qualitatively in good agreement with data of Oort and Rasmusson except that the stratospheric flux in this study is much stronger. The zonal eddy heat flux is predominantly eastward in the troposphere; this is undoubtedly related to the enormous heat input of the ocean into the atmosphere, which is consequently swept into the continent where the radiation balance is negative in winter.

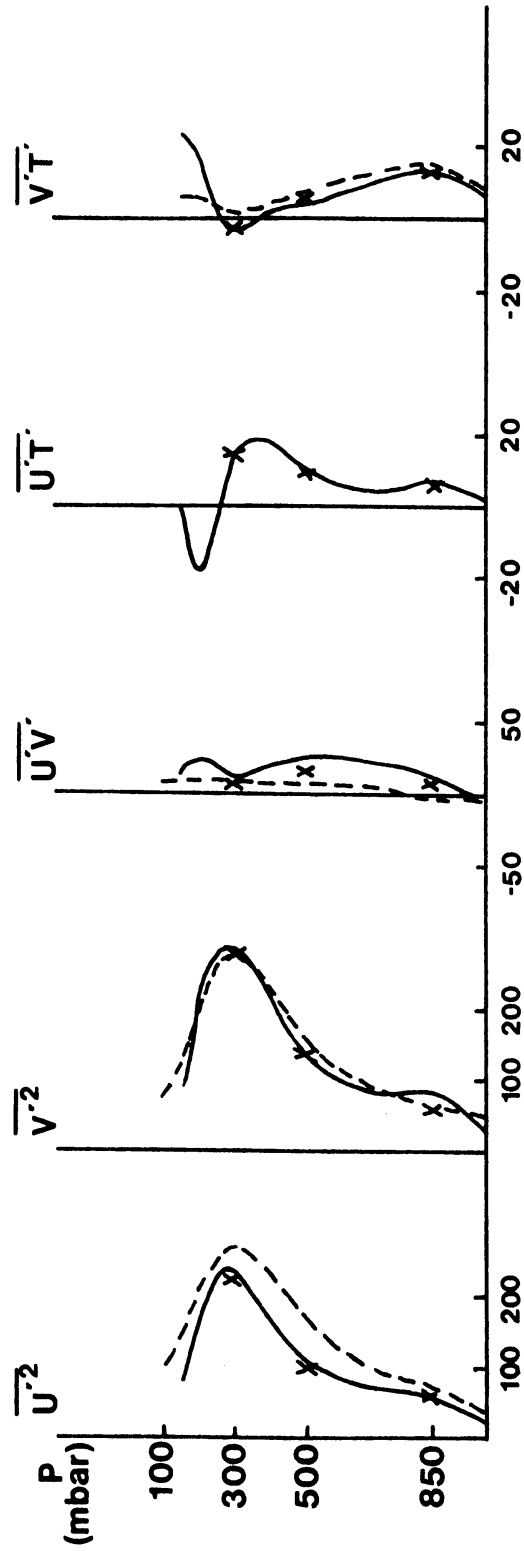


Fig. 7. Vertical profiles of $\overline{u'^2}$, $\overline{v'^2}$, $\overline{u'v'}$, $\overline{u'T'}$ and $\overline{v'T'}$ at station 9 (Camborne, England) for the winter of 1976/77. Dashed lines give zonally averaged values for 50 N according to Oort and Rasmusson (1971). Crosses give geostrophic fluxes at three levels. Units are $m^2 s^{-2}$ and mKs^{-1} .

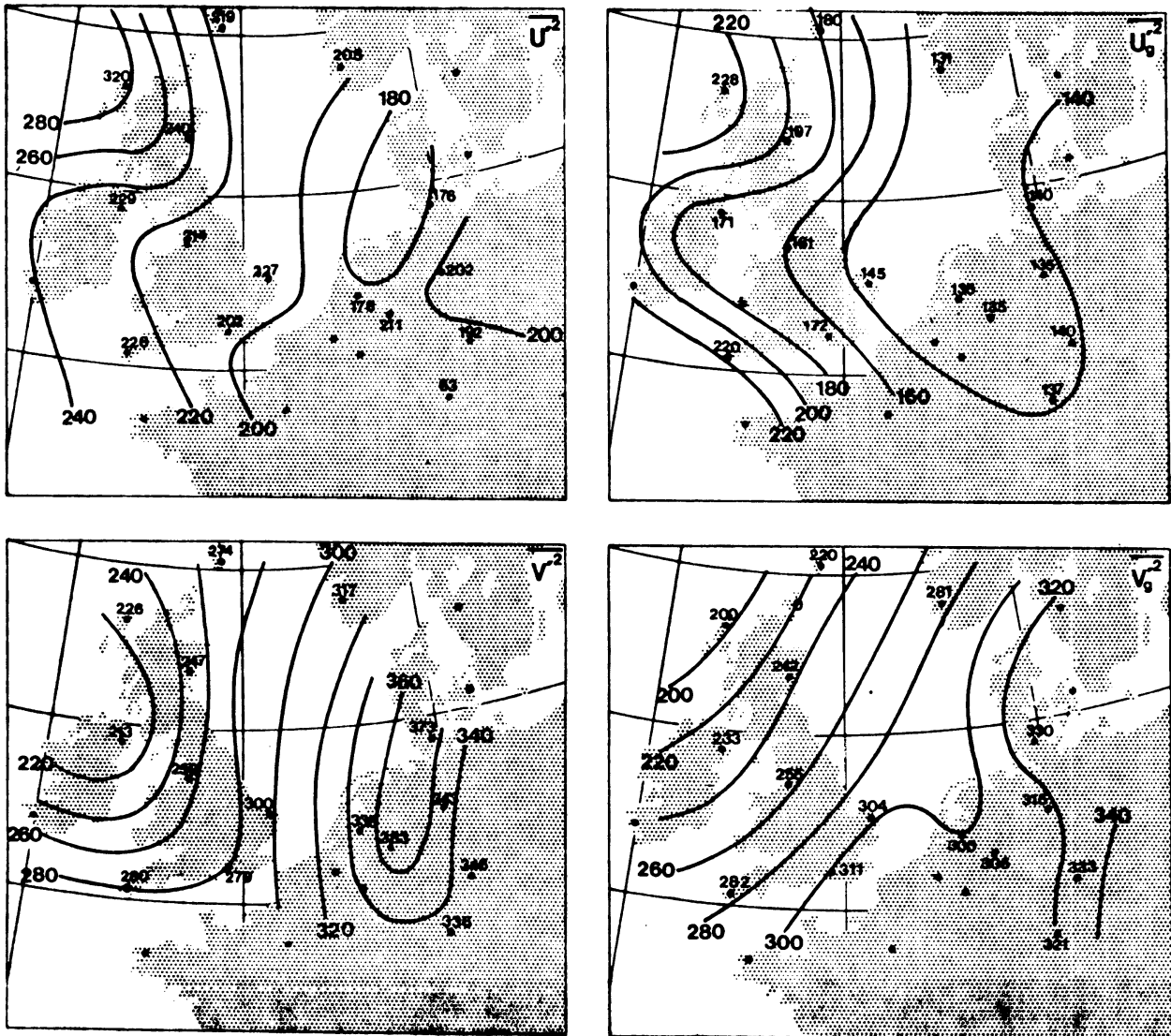


Fig. 8. Spatial distribution of the variances of u and v computed with real winds (left-hand side) and geostrophic winds (right-hand side). The level is 300 mb. Units are $m^2 s^{-2}$.

A peculiar phenomenon is the negative value of $\overline{v'T'}$ at 300 mb in Fig. 7. It is probably a real feature, as it is consistently shown at all radiosonde stations (Fig. 9). The northern latitudes on the average being colder than the southern this would mean a counter-gradient meridional eddy heat flux at 300 mb (the zonal eddy heat flux $\overline{u'T'}$ is nearly parallel to the isothermes). This result is confirmed by Lau (1978) and also by unpublished maps of Oort and Rosenstein. In fact, counter-gradient heat fluxes in the higher troposphere over the western parts of the continents in winter is a normal though unexplained feature of the general circulation. It is remarkable that if we cross the tropopause the rapid change in $\overline{v'T'}$ is accompanied by a similar change in $\overline{u'T'}$.

If we compare eddy fluxes computed with real winds to those computed with geostrophic winds, there is a general resemblance. This is certainly the case in Fig. 7. However, larger differences occur at other places and, moreover, small differences may lead to meaningful differences in the gradients of these fluxes. In Figures 8 and 9 horizontal distributions of $\overline{u'^2}$, $\overline{v'^2}$, $\overline{u'v'}$ and $\overline{v'T'}$, and $\overline{u_g'^2}$, $\overline{v_g'^2}$, $\overline{u_g'v_g'}$ and $\overline{v_g'T'}$ at 300 mb are given. Due to the noisy character of fluxes based on raw data, it is difficult to make a spatial analysis. The subjective analysis includes a certain degree of smoothing; sometimes we had to reject one or two stations. If we compare the analyses in Figures 8 and 9, it can be seen that the gross features are the same for real and geostrophic winds. The computation of horizontal gradients may lead to quite different results, however. It is not clear which of the two estimates of gradients is to be preferred. Fluxes based on real observations contain more small-scale structures, but some of this may be noise. Geostrophic fluxes have better spatial coherence and fewer small-scale features.

Fig. 10 shows the spatial distribution of $\overline{u'\omega'}$ and $\overline{v'\omega'}$ at 500 mb. Both zonal and meridional momentum are transported mainly upwards by synoptic eddies, the latter transport being almost three times larger than the first. The order of magnitude of the vertical eddy flux of zonal momentum at 500 mb ($10 \cdot 10^{-2} \text{ Nm}^{-1} \text{ s}^{-2}$) compares well to results of Holopainen (1964).

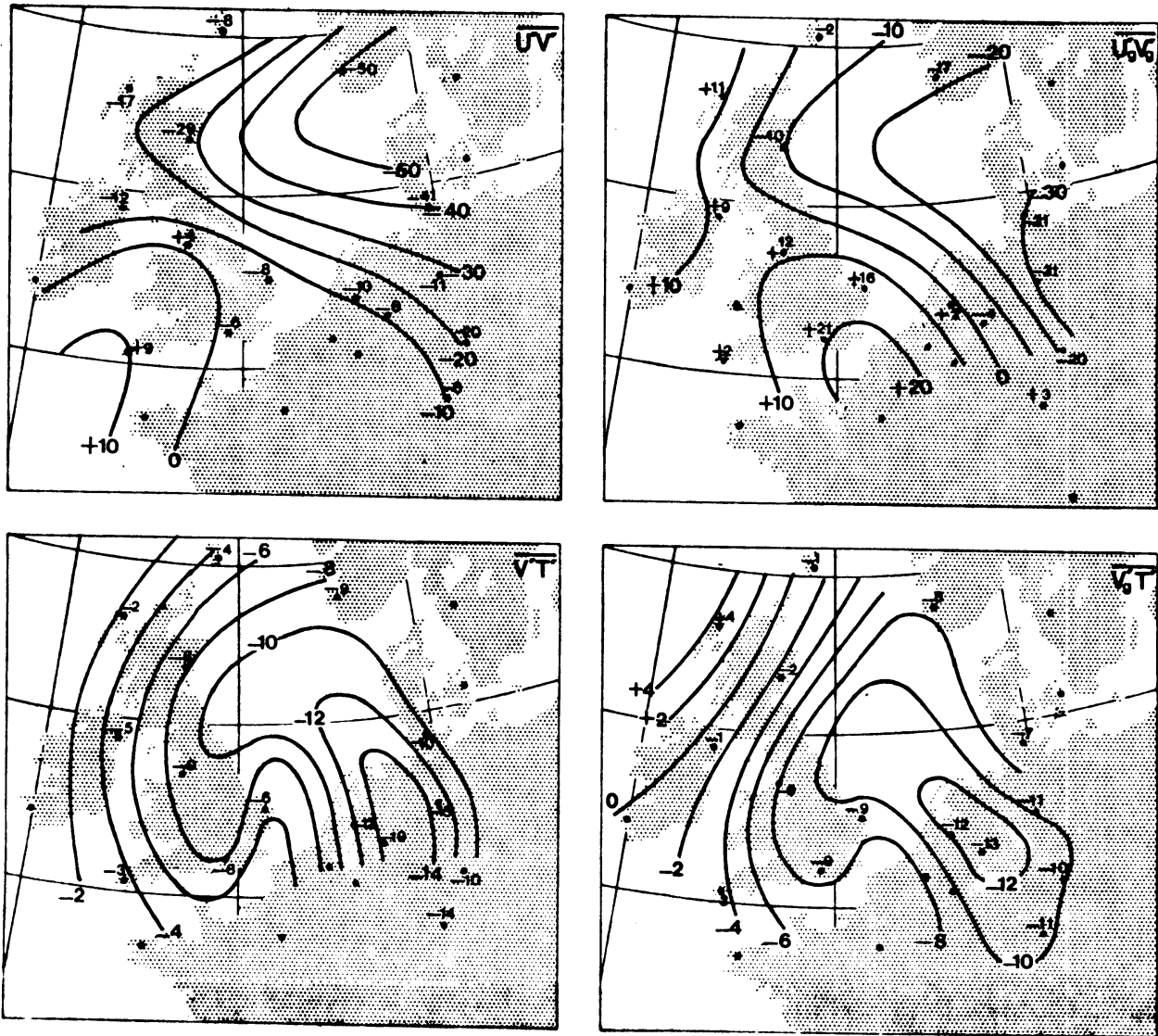


Fig. 9. Spatial distribution of meridional momentum and heat fluxes computed with real winds (left-hand side) and geostrophic winds (right-hand side). The level is 300 mb. Units are $\text{m}^2 \text{s}^{-2}$ and mKs^{-1} respectively.

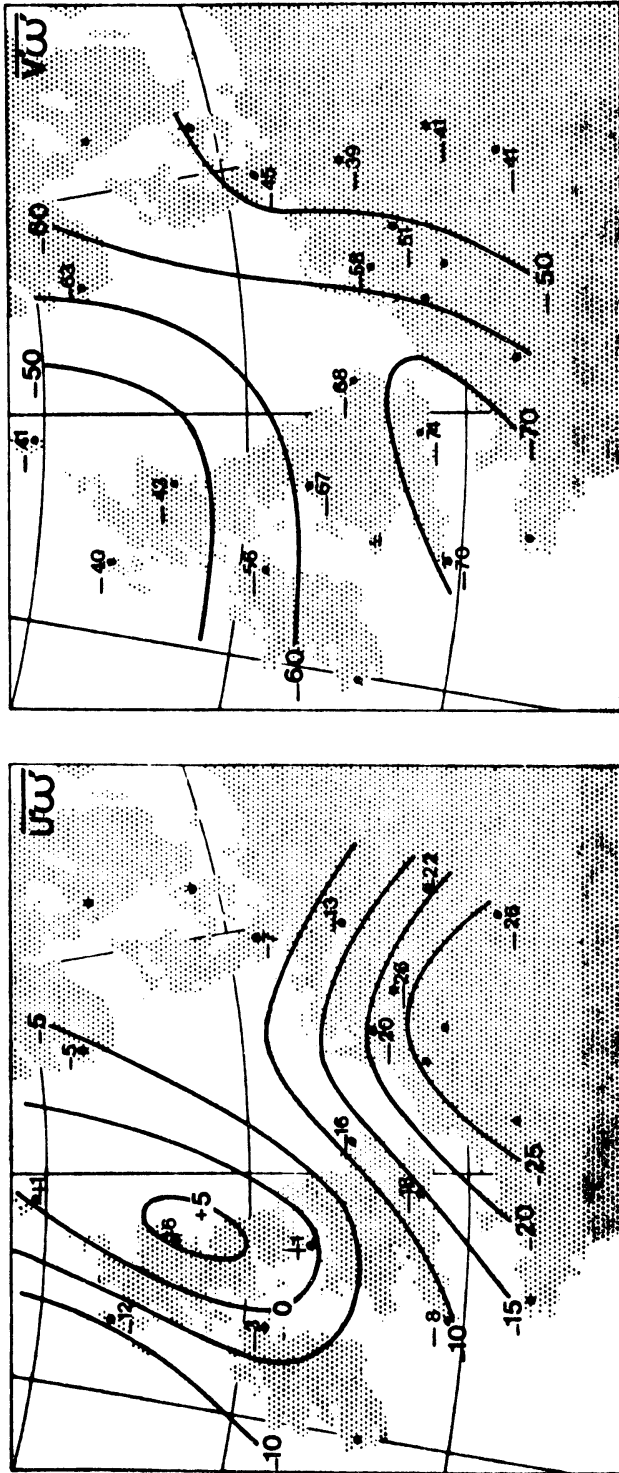


Fig. 10. Spatial distribution of vertical eddy fluxes of zonal (left-hand side) and meridional (right-hand side) momentum. The level is 500 mb. Units are $10^{-2} \text{ Nm}^{-1} \text{ s}^{-2}$.

2.7. Estimates of the terms in the equations for mean momentum and temperature

The statistical properties of time-averaged momentum and temperature balance equations have been investigated in several general circulation studies. For the zonally averaged conditions a rather complete picture can be derived from the atmospheric statistics of Oort and Rasmusson (1971). However, knowledge of the local features of the general circulation is far less complete. For a non-zonally averaged atmosphere a quantitative evaluation of the mean momentum and temperature equation has been given by Holopainen (1964, 1973) and Savijärvi (1966, 1977). Savijärvi's study is comparable to ours in the sense that his formulation of the equations is the same. However, he could not compute the vertical flux convergence terms, except terms involving $\bar{\omega}$ in the thermodynamic equation.

Our estimates of the various terms in both momentum equations are given in Table 1. As an estimate of all terms we have taken in a subjective way absolute values which are considered to be representative for the area. In most cases the estimates are close to the extreme values except when the extreme was suspect. This procedure has been followed also in Tables 2 - 7, discussed in the next sections. It is clear that no balance of all terms can be made from which friction or diabatic heating follows as a residue. The convergence of vertical fluxes is available only at 500 mb, while the ageostrophic terms are given only at 850, 500 and 300 mb.

It can easily be seen from Table 1 that the time rate of change of mean momentum is very small. We therefore conclude that the equations are essentially maintenance equations. The dominating balance in the equations is the geostrophic balance, which is eliminated by taking the ageostrophic term. This ageostrophic residue balances approximately with the advection part of the acceleration term, the eddy forces and possibly friction.

		850	500	300	200			850	500	300	200
	$\frac{\partial \bar{u}}{\partial t}$.3	.5	.6	.5		$\frac{\partial \bar{v}}{\partial t}$.3	.5	.6	.5
+	$\bar{v} \cdot \nabla \bar{u}$	4	7	9	9	+	$\bar{v} \cdot \nabla \bar{v}$	3	5	18	7
+	$\bar{\omega} \frac{\partial \bar{u}}{\partial p}$.8			+	$\bar{\omega} \frac{\partial \bar{v}}{\partial p}$.4		
-	$f \bar{v}_{ag}$	12	8	18		+	$f \bar{u}_{ag}$	10	14	24	
-	\bar{F}_x					-	\bar{F}_y				
-	$\bar{u} \bar{v} \frac{\tan \phi}{a}$.3	.4	.6	.6	+	$\bar{u}^2 \frac{\tan \phi}{a}$	1	2	5	5
-	$2\bar{u}'\bar{v}' \frac{\tan \phi}{a}$.4	.8	2	.8	+	$(\bar{u}'^2 - \bar{v}'^2) \frac{\tan \phi}{a}$	1	2	3	2
+	$\frac{\partial \bar{u}'^2}{\partial x}$	10	8	15	8	+	$\frac{\partial}{\partial x} \bar{u}'\bar{v}'$	2	5	5	10
+	$\frac{\partial \bar{u}'\bar{v}'}{\partial y}$	2	6	10	4	+	$\frac{\partial}{\partial y} \bar{v}'^2$	10	10	12	8
+	$\frac{\partial \bar{u}'\bar{\omega}'}{\partial p}$.5			+	$\frac{\partial}{\partial p} \bar{v}'\bar{\omega}'$		2		
=	0					=	0				

Table 1. Estimates of the terms in the equations for mean horizontal motion at four pressure levels. Units are 10^{-5}ms^{-2} . The complete equations can be read from the top to the bottom of the table.

Both vertical mean and eddy fluxes are about one order of magnitude smaller than the leading terms in this approximate balance. In the zonal momentum equation the curvature terms are very small; however, they are not negligible in the y-direction.

Estimates of the terms in the equation for mean temperature are given in Table 2.

From the information of Table 2 a mean temperature balance for Northwestern Europe can be derived. Again, we essentially deal with a maintenance equation. The balance consists of advection of mean temperature, heating due to dry adiabatic vertical motion, heating by horizontal eddies and probably diabatic heating. The effect of vertical eddies seems to be small; the same applies to curvature terms.

The estimates of the various terms in Tables 1 and 2 are in good agreement with estimates by Savijärvi (1976, 1977), which are valid for a large part of the northern hemisphere. Assuming that vertical transport terms are small he arrives at the same approximate balance equations for mean momentum and temperature.

The small values of vertical transports deserve more attention. Holopainen (1964) gives estimates of the transient eddy vertical momentum flux for autumn 1954 over the British Isles. For $\overline{u'\omega'}$ his kinematic and adiabatic estimates for 500 mbar are -0.23 and $0.05 \text{ Nm}^{-1}\text{s}^{-2}$ respectively. For the same level Holopainen estimates $\overline{v'\omega'}$ to be -0.92 and $-0.72 \text{ Nm}^{-1}\text{s}^{-2}$ according to the two methods. These values agree fairly well with our results (see Fig. 10). As far as the convergence of vertical fluxes is concerned, we must keep in mind that the vertical velocities used in this study are derived from a model with poor vertical resolution. This means that we can describe only the smoothly varying part of the synoptic-scale ω -profile. Therefore we easily might have underestimated the convergence of, for example, $\overline{u'\omega'}$. This seems to be the case if we compare the value for $\frac{\partial}{\partial p} \overline{u'\omega'}$ ($0.5 \cdot 10^{-5} \text{ ms}^{-2}$) obtained in this study with those of Holopainen. With a high resolution in the vertical he finds convergence

		850	500	300	200
	$\frac{\partial \bar{T}}{\partial t}$.1	.1	.2	.2
+	$\bar{v} \cdot \nabla \bar{T}$	3	3	5	4
-	$\bar{\omega} \left(\frac{R\bar{T}}{pc_p} - \frac{\partial \bar{T}}{\partial p} \right)$		2		
-	$\frac{ \bar{Q} }{c_p}$				
-	$\frac{\overline{v'T'}}{a} \tan \phi$.3	.2	.3	.7
+	$\frac{\partial}{\partial x} \overline{u'T'}$	1	1	2	2
+	$\frac{\partial}{\partial y} \overline{v'T'}$	1	2	2	1
+	$\frac{\partial}{\partial p} \overline{\omega'T'}$.2		
-	$\frac{R}{pc_p} \overline{\omega'T'}$.05		
=	0				

Table 2. Estimates of the terms in the equation for mean temperature. Units are 10^{-5}Ks^{-1} .

values of 1 to $4 \cdot 10^{-5} \text{ms}^{-2}$ in the lower half of the troposphere. If we accept these larger values, there is not sufficient reason to neglect vertical momentum fluxes.

2.8. Third-order eddy statistics

In the equations for the eddy variances and covariances third-order eddy statistics appear as new variables. Van den Dool (1975) and Savijärvi (1976) have investigated third-order terms appearing in the transient eddy kinetic energy equation. They used geostrophic winds derived from NMC height-field analyses; in both studies it was concluded that third-order terms are somewhat smaller than the leading terms, but by no means negligible. Attempts to parameterize the influence of third-order terms as a diffusion of eddy kinetic energy failed. In a recent paper by Lau et al. (1978) the maintenance of the eddy momentum flux ($\overline{u'v'}$) is investigated. For this purpose they used NMC wind analyses. The wind analysis procedure yields essentially gradient winds in data-sparse areas. In their paper the role of third-order terms is discussed only qualitatively; third-order terms are said to be small.

Before we start the presentation of our results it is necessary to discuss whether or not third-order terms can be computed reliably. Let us look at $\overline{u'^3}$ for example. The non-zero value of this term is a result of the skewness of the probability distribution of u' . It is obvious that an asymmetry in the extreme values of u' can contribute substantially to $\overline{u'^3}$. As an example the probability distribution of u' is given for station 01415 (Sola, Southwest Norway) at 300 mb (Fig. 11). The mean value of u' amounts to 12.5 m/s, while $\overline{u'^3}$ has a value of $1583 \text{ m}^3 \text{ s}^{-3}$ for this winter. It can be seen from the figure that there are about four positive extremes, which are not cancelled by negative extremes. These extremes, with a typical value of 40 m/s for u' , account for almost the entire value of $\overline{u'^3}$. This strongly

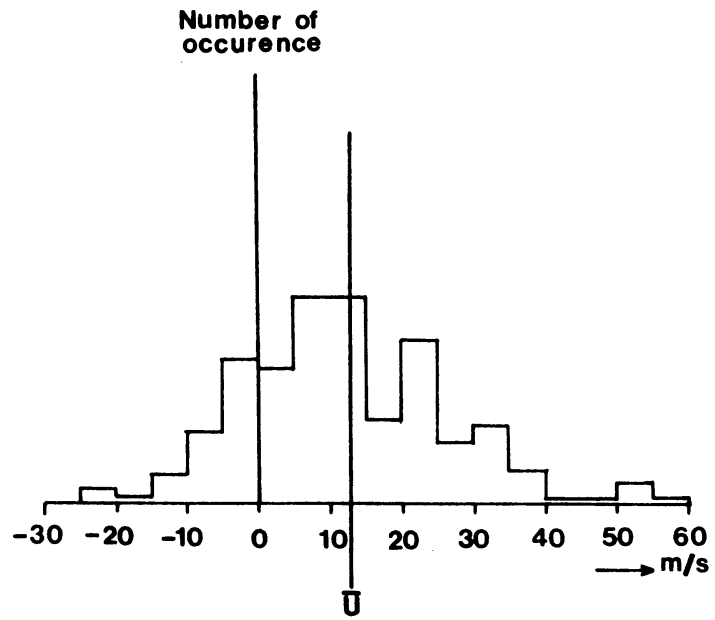


Fig. 11. Probability distribution of the zonal wind at station 1 (Sola, Norway) for 300 mb during the winter of 1976/77. Number of occurrence is given for intervals of 5 ms^{-1} .

indicates the large uncertainty in the computed value of third-order terms for individual stations. First of all, there are sampling errors. All wind values, including the extremes, are assumed to be representative for equal intervals in time (12 hour). If some of the strong winds persisted only for a few hours, we can expect a large dependence of third-order terms on the specific sampling, which is at 00 and 12 GMT. Secondly, one or two large erroneous wind measurements in the time series can obviously have great influence. This last source of errors is probably absent in third-order terms determined on the basis of geostrophic winds. The reason for this is the rejection by the objective analysis procedure of large winds which are not spatially coherent.

Fig. 12 shows the distribution of $\overline{u'^3}$ at 300 mb computed with real and with geostrophic winds. In spite of the rather noisy character in the real wind case, it can easily be seen that there is an overall predominance of positive values with a maximum over East Anglia and the North Sea. The spatial distribution of geostrophic values of $\overline{u'^3}$ shows the same general character, but the field is smoother. A comparison of the two fields also shows that the spatial gradients can be larger by a factor 2 to 4 if we use real winds. This is mainly due to unexpectedly large values of stations 03005 (3) and 03496 (7), which are probably due to a few large winds or wind errors. Therefore it might be better to derive the spatial gradients from the geostrophic estimates of third-order terms. Hence in the next section, when we discuss the order of magnitude of all terms in the eddy flux equations, gradients of third-order terms are estimated with geostrophic winds rather than real winds.

Fig. 13 displays vertical profiles of a variety of third-order terms for station 03808, together with geostrophic values at 300, 500 and 850 mb. These vertical profiles are fairly representative for the whole area. Those third-order terms that

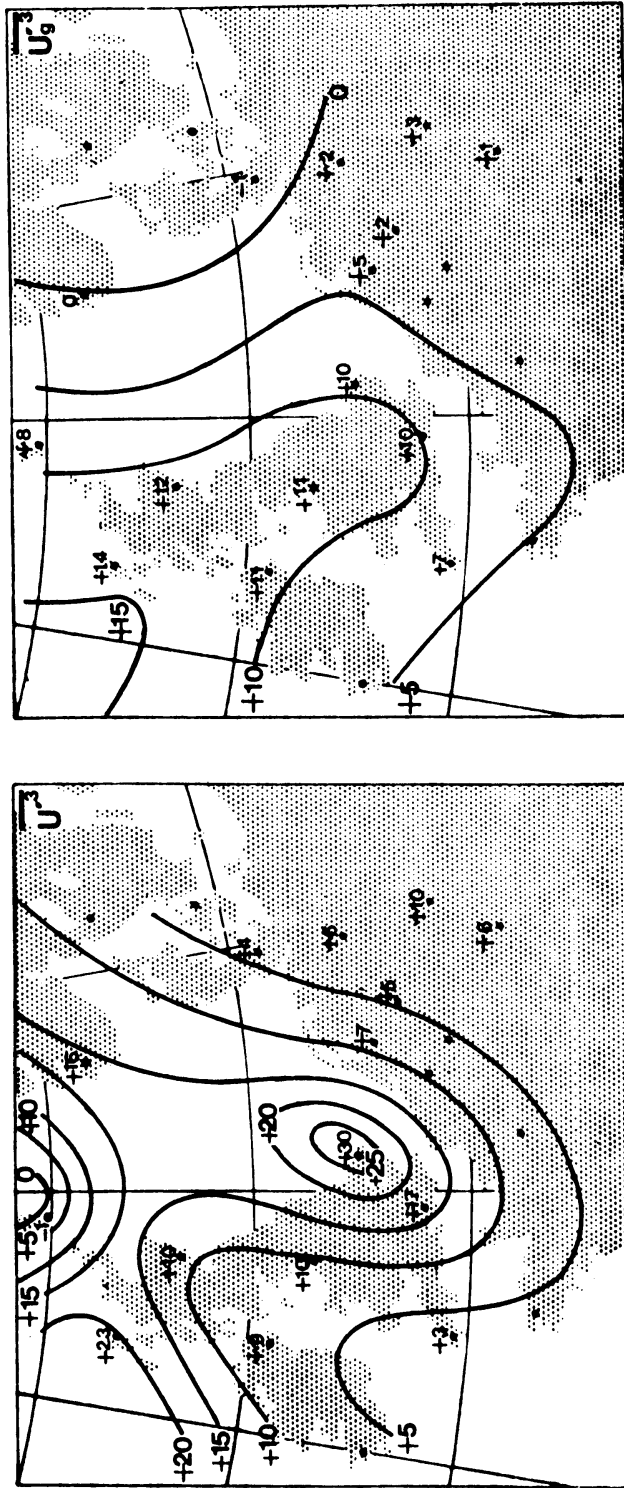


Fig. 12. Spatial distribution of $\overline{u^3}$ at 300 mb computed with real winds (left-hand side) and with geostrophic winds (right-hand side). Units are $10^2 m^3 s^{-3}$.

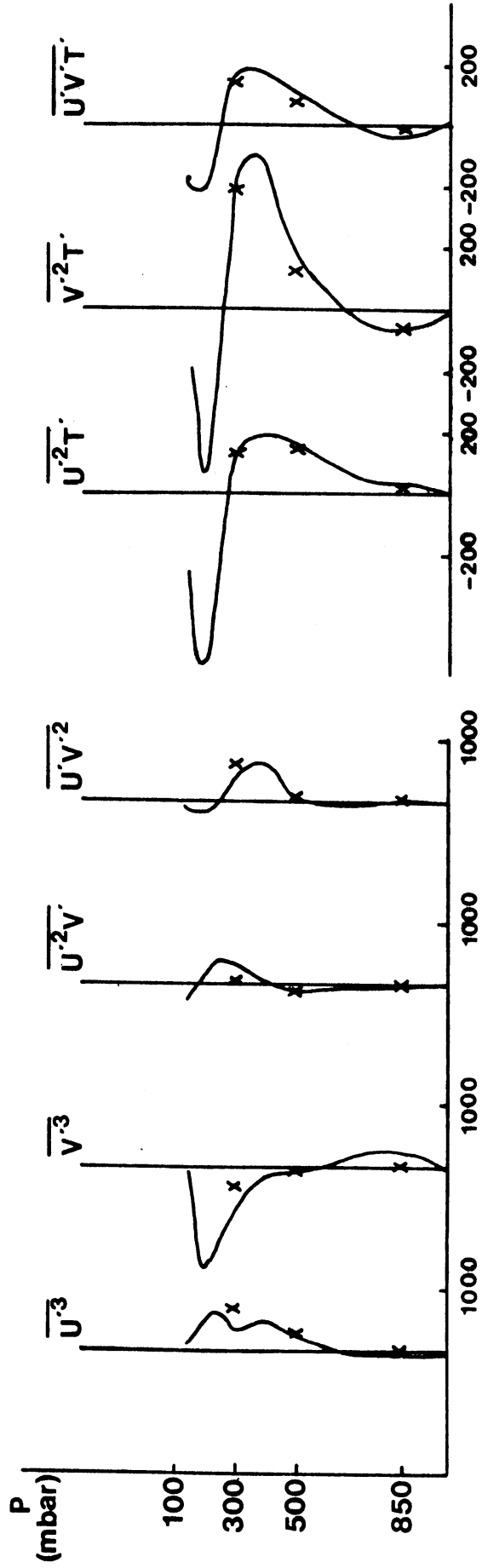


Fig. 13. Vertical profiles of third-order terms at station 9 (Camborne, England). Crosses denote geostrophic estimates. Units are $m^3 s^{-3}$ and $m^2 K s^{-2}$.

contain only velocity components are small below 500 mb; beyond this level they show a rapid increase and peak at about 300 mb. Above 300 mb a sharp decrease can be observed. This behaviour is not unlike vertical profiles of the second-order terms. The third-order terms involving T' show interesting vertical profiles. The sharp peak at 300 mb is accompanied by a rapid transition to a peak of opposite sign if we cross the tropopause. This is of course related to change of sign of both $\overline{u'T'}$ and $\overline{v'T'}$ at these levels (Fig. 7).

The geostrophic estimates (crosses in Fig. 13) compare well with the profiles. It should be emphasized that at some of the other stations the deviations are much larger.

When we started this study, one of our hopes was to find an averaging period for which third-order terms would turn out to be small. If the averaging period was increased from 5 to 90 days, we found a general decrease with a factor of about 2.

Finally, concerning third-order terms containing ω , we restrict ourselves in the next section to give orders of magnitude only. We do not believe that their spatial distribution is very informative.

2.9. Estimates of the terms in the horizontal eddy flux equations

The estimates of the various terms in the equations for the horizontal eddy fluxes $\overline{u'^2}$, $\overline{v'^2}$, $\overline{u'v'}$, $\overline{u'T'}$ and $\overline{v'T'}$ are given in Tables 3 to 7. In these tables we have condensed the significance of each term into one numerical value.

In the equations for $\overline{u'^2}$ and $\overline{v'^2}$ there is an approximate balance between the advection of these quantities by the mean flow, ageostrophic momentum fluxes, horizontal third-order advection and, finally, the interaction with the mean flow. (See Tables 3 and 4). Terms containing vertical velocity and curvature terms turn out to be relatively small. As was the case in the mean momentum equations, the time derivatives are very small and therefore we are essentially dealing with maintenance equations, which as such have no predictive value.

	850	500	300	200
$\frac{\partial}{\partial t} \frac{1}{2} \overline{u'^2}$	1	5	8	5
+ $\overline{v \cdot \nabla} \frac{1}{2} \overline{u'^2}$	30	50	200	80
+ $\overline{\omega} \frac{\partial}{\partial p} \frac{1}{2} \overline{u'^2}$		8		
- $f \overline{u'v'}$	40	100	300	
- $\overline{u'F'_x}$				
- $\overline{u u'v'} \frac{\tan \phi}{a}$	1	4	10	6
- $\overline{v u'^2} \frac{\tan \phi}{a}$	5	5	10	6
- $\frac{3}{2} \overline{u'^2 v'} \frac{\tan \phi}{a}$	6	10	20	
+ $\overline{u'^2} \frac{\partial \overline{u}}{\partial x}$	30	40	100	50
+ $\overline{u'v'} \frac{\partial \overline{u}}{\partial y}$	10	20	40	20
+ $\overline{u'\omega'} \frac{\partial \overline{u}}{\partial p}$		4		
+ $\frac{1}{2} \frac{\partial \overline{u'^3}}{\partial x}$	40	80	100	
+ $\frac{1}{2} \frac{\partial}{\partial y} \overline{u'^2 v'}$	20	40	90	
+ $\frac{1}{2} \frac{\partial}{\partial p} \overline{u'^2 \omega'}$		5		
= 0				

Table 3. Estimates of the terms in the equation for the variance of the zonal wind. Units are $10^{-5} \text{ m}^2 \text{ s}^{-3}$.

	850	500	300	200
$\frac{\partial}{\partial t} \frac{1}{2} \overline{v'^2}$	1	5	10	10
+ $\overline{V \cdot \nabla} \frac{1}{2} \overline{v'^2}$	30	80	200	200
+ $\overline{\omega} \frac{\partial}{\partial p} \frac{1}{2} \overline{v'^2}$		8		
+ $\overline{f v' u'_{ag}}$	50	50	200	
- $\overline{v' F'_y}$				
+ $2 \overline{u' v'} \frac{\tan \phi}{a}$	2	8	20	10
+ $\overline{u'^2 v'} \frac{\tan \phi}{a}$	4	8	10	
- $\frac{1}{2} \overline{v'^3} \frac{\tan \phi}{a}$	2	10	30	
+ $\overline{u' v'} \frac{\partial}{\partial x} \overline{v}$	6	10	40	6
+ $\overline{v'^2} \frac{\partial}{\partial y} \overline{v}$	50	100	100	60
+ $\overline{v' \omega'} \frac{\partial}{\partial p} \overline{v}$		7		
+ $\frac{1}{2} \frac{\partial}{\partial x} \overline{u' v'^2}$	10	40	100	
+ $\frac{1}{2} \frac{\partial}{\partial y} \overline{v'^3}$	20	60	100	
+ $\frac{1}{2} \frac{\partial}{\partial p} \overline{v'^2 \omega'}$		10		
= 0				

Table 4. Estimate of the terms in the equation for the variance of the meridional wind. Units are $10^{-5} \text{ m}^2 \text{ s}^{-3}$.

Concerning the $\overline{u'v'}$ maintenance, Lau et al. (1978) concluded that the most important terms are the ageostrophic terms and the so-called mixing term $\overline{v'^2} \frac{\partial \bar{u}}{\partial y}$. From Table 5 it will become clear that at least for the Northwestern European area a role in the balance is also played by terms other than the destruction and creation term. The approximate balance is between advection of $\overline{u'v'}$ by the mean wind, ageostrophic terms, horizontal third-order terms and interaction with the mean flow by two "mixing terms", namely $\overline{v'^2} \frac{\partial \bar{u}}{\partial y}$ and $\overline{u'^2} \frac{\partial \bar{v}}{\partial x}$. The latter term was estimated by Lau et al. to be at least three times smaller. Our finding is based on the fact that $\frac{\partial \bar{v}}{\partial x}$ can be as large as $\frac{\partial \bar{u}}{\partial y}$ even though it is the smaller one in general, see Fig. 14. Vertical advection terms and some of the terms describing interaction with the mean flow seem to be negligible. The same holds for many of the curvature terms, with the exception of $\frac{\tan \phi}{a} \bar{u} (\overline{2u'^2} - \overline{v'^2})$, which is of some importance and cannot be neglected.

In the equation for the zonal eddy temperature flux the main balance is composed of the ageostrophic term, horizontal third-order terms and two mean flow interaction terms, namely $\overline{v'T'}$ $\frac{\partial \bar{u}}{\partial y}$ and $\overline{u'^2} \frac{\partial \bar{T}}{\partial x}$. See Table 6. Terms of minor importance but non-negligible are advection $\bar{v} \cdot \nabla \overline{u'T'}$, and $\overline{u'v'} \frac{\partial \bar{T}}{\partial y}$ and $\bar{\sigma} \overline{u'\omega'}$. All the other terms are at least one order of magnitude smaller than the leading terms.

The equation for $\overline{v'T'}$ proves to be puzzling. Recently, Wallace (1978) investigated this flux equation for the lower stratosphere. He assumed an approximate balance between $\overline{v'^2} \frac{\partial \bar{T}}{\partial y}$, $\bar{\sigma} \overline{v'\omega'}$ and $\overline{f u' T'}$ in his attempt to explain the maintenance of counter-gradient heat flux from the structure of waves in the lower stratosphere. In this paper we must first of all make a clear distinction between the lower and upper troposphere. In the lower troposphere a balance like the one proposed by Wallace seems to be valid except that advection and third-order terms cannot be neglected altogether. In the upper troposphere we find $\overline{v'^2} \frac{\partial \bar{T}}{\partial y}$ to be $200 \cdot 10^{-5}$, which is much larger than any of the other computed terms. The question now arises, how is this mixing term balanced.

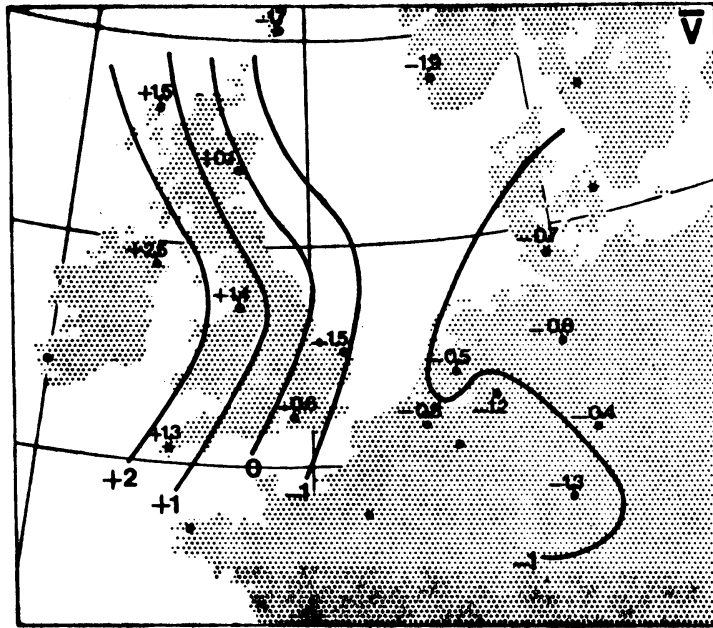


Fig. 14. Spatial distribution of the mean meridional wind at 300 mb. Units are ms^{-1} . Note the large gradients in zonal direction.

	850	500	300	200
$\frac{\partial}{\partial t} \overline{u'v'}$	1	5	20	20
+ $\overline{v \cdot \nabla} \overline{u'v'}$	20	60	200	200
+ $\overline{\omega} \frac{\partial}{\partial p} \overline{u'v'}$		4		
- $f(\overline{v'v'_{ag}} - \overline{u'u'_{ag}})$	100	100	400	
- $(\overline{v'F'_x} + \overline{u'F'_y})$				
+ $\overline{u}(2\overline{u'^2} - \overline{v'^2}) \frac{\tan \phi}{a}$	10	20	50	30
- $\overline{v} \overline{u'v'} \frac{\tan \phi}{a}$.6	.8	2	.8
+ $\overline{u'^3} \frac{\tan \phi}{a}$	8	20	30	
- $2\overline{u'v'^2} \frac{\tan \phi}{a}$	2	10	30	
+ $\overline{u'v'} \frac{\partial \overline{u}}{\partial x}$	3	6	10	6
+ $\overline{v'^2} \frac{\partial \overline{u}}{\partial y}$	80	200	400	200
+ $\overline{v'\omega'} \frac{\partial \overline{u}}{\partial p}$		10		
+ $\overline{u'^2} \frac{\partial \overline{v}}{\partial x}$	50	70	300	40
+ $\overline{u'v'} \frac{\partial \overline{v}}{\partial y}$	6	10	20	6
+ $\overline{u'\omega'} \frac{\partial \overline{v}}{\partial p}$		2		
+ $\frac{\partial}{\partial x} \overline{u'^2 v'}$	30	70	200	
+ $\frac{\partial}{\partial y} \overline{u'v'^2}$	20	80	200	
+ $\frac{\partial}{\partial p} \overline{u'v'\omega'}$		10		
= 0				

Table 5. Estimate of the terms in the equation for the meridional momentum flux by large-scale eddies. Units are $10^{-5} m^2 s^{-3}$.

	850	500	300	200
$\frac{\partial}{\partial t} \overline{u'T'}$.5	1	2	2
+ $\overline{V \cdot \nabla u'T'}$	5	10	30	30
+ $\overline{\omega \frac{\partial}{\partial p} u'T'}$.8		
- $\overline{fT'v'_{ag}}$	20	40	60	
- $\overline{T'F'_x}$				
- $\frac{\overline{u'Q'}}{c_p}$				
- $\overline{u v'T'} \frac{\tan \phi}{a}$	2	2	5	10
- $\overline{v u'T'} \frac{\tan \phi}{a}$.9	.7	.8	.8
- $2\overline{u'v'T'} \frac{\tan \phi}{a}$	1	3	6	
+ $\overline{u'T'} \frac{\partial \overline{u}}{\partial x}$	5	5	6	6
+ $\overline{v'T'} \frac{\partial \overline{u}}{\partial y}$	20	10	20	40
+ $\overline{\omega'T'} \frac{\partial \overline{u}}{\partial p}$		2		
+ $\overline{u'^2} \frac{\partial \overline{T}}{\partial x}$	20	10	60	40
+ $\overline{u'v'} \frac{\partial \overline{T}}{\partial y}$	5	10	20	8
- $\overline{u'\omega'} \left(\frac{R\overline{T}}{pc_p} - \frac{\partial \overline{T}}{\partial p} \right)$		8		
- $\frac{R}{pc_p} \overline{\omega u'T'}$.4		
+ $\frac{\partial}{\partial x} \overline{u'^2 T'}$	7	40	40	
+ $\frac{\partial}{\partial y} \overline{u'v'T'}$	10	20	20	
+ $\frac{\partial}{\partial p} \overline{u'\omega'T'}$		2		
- $\frac{R}{pc_p} \overline{u'\omega'T'}$.1		
= 0				

Table 6. Estimate of the terms in the equation for the zonal temperature flux by large-scale eddies.

Units are 10^{-5}mKs^{-2} .

	850	500	300	200
$\frac{\partial}{\partial t} \overline{v'T'}$.8	2	3	3
+ $\overline{V \cdot \nabla} \overline{v'T'}$	10	20	30	30
+ $\overline{\omega} \frac{\partial}{\partial p} \overline{v'T'}$		2		
+ $\overline{r'T'u'_{ag}}$	40	40	40	
- $\frac{\overline{T'F'_y}}{c_p}$				
- $\frac{\overline{v'Q'}}{c_p}$				
+ $2\overline{u'u'T'} \frac{\tan \phi}{a}$	3	7	10	10
+ $\overline{u'^2T'} \frac{\tan \phi}{a}$	1	4	6	
+ $\overline{v'^2T'} \frac{\tan \phi}{a}$	1	6	10	
+ $\overline{u'T'} \frac{\partial \overline{v}}{\partial x}$	9	10	20	6
+ $\overline{v'T'} \frac{\partial \overline{v}}{\partial y}$	9	6	6	10
+ $\overline{\omega'T'} \frac{\partial \overline{v}}{\partial p}$		1		
+ $\overline{u'v'} \frac{\partial \overline{T}}{\partial x}$	2	2	8	6
+ $\overline{v'^2} \frac{\partial \overline{T}}{\partial y}$	40	90	200	80
- $\overline{v'\omega'} \left(\frac{R\overline{T}}{pc_p} - \frac{\partial \overline{T}}{\partial p} \right)$		30		
- $\frac{R}{pc_p} \overline{\omega v'T'}$.2		
+ $\frac{\partial}{\partial x} \overline{u'v'T'}$	10	20	20	
+ $\frac{\partial}{\partial y} \overline{v'^2T'}$	10	30	30	
+ $\frac{\partial}{\partial p} \overline{v'\omega'T'}$		1		
- $\frac{R}{pc_p} \overline{v'\omega'T'}$.1		
= 0				

Table 7. Estimate of the terms in the equation for the meridional temperature flux by large-scale eddies. Units are 10^{-5}mKs^{-2} .

A first counteracting term is $f \overline{u'_{ag} T'}$, for which we have computed a maximum value of $40 \cdot 10^{-5} \text{ mKs}^{-2}$. It could be that we have underestimated this term. However, looking at the total value of $f \overline{u' T'}$, which has been computed direct from the measurements, we find values of up to $100 \cdot 10^{-5} \text{ mKs}^{-2}$ in regions where the mixing term has it's maximum. The bulk of this flux must be geostrophic. Hence it is very unlikely that our estimate of $f \overline{u'_{ag} T'}$ is too low.

A second contributing term is $\overline{\sigma v' \omega'}$, which also acts to destroy a positive eddy heat flux, and therefore counteracts the creation of northward flux by the "mixing term". Although the static stability at 300 mb is about two times larger than at 500 mb, the vertical momentum flux, however, is probably smaller than at 500 mb. Hence $\overline{\sigma v' \omega'}$ cannot be much larger than $50 \cdot 10^{-5} \text{ mKs}^{-2}$. This means that there must be a third contributing term with a value of the order of $100 \cdot 10^{-5} \text{ mKs}^{-2}$.

A candidate which was not numerically evaluated, is $\overline{v' Q' / c_p}$. How large can this term be? We can try to answer this question from our knowledge that v and ω are correlated ($\rho = -0.5$). Therefore, southerly flow seems to be connected with rising motion and, consequently, clouds in a thick layer of the troposphere. It is well known that in the layer above the clouds heat is rapidly lost due to an increase of outgoing IR radiation. According to Paltridge and Platt (1976) the associated cooling may amount to several degrees per hour. If we accept 10 K per day as a typical value for a rather thick layer above the clouds, then Q' / c_p is about $10 \cdot 10^{-5} \text{ K/s}$. Combined with a typical value for v' , say 15 m/s, it seems that $\overline{v' Q' / c_p}$ can be of the order of $100 \cdot 10^{-5} \text{ mKs}^{-2}$. Therefore, this diabatic heating term is important and should be taken into account.

Perhaps we also have the key to the explanation of the counter-gradient eddy heat fluxes at 300 mb over Northwestern Europe, whereas in the zonal average this flux is small but down-gradient. At every level in the troposphere the mixing term tries to establish a poleward heat flux. The diabatic heating term $\overline{v'Q'}/c_p$ is important everywhere where v' is correlated to ω' . Above the cloud layer the diabatic term tends to counteract the northward heat flux, which may reverse sign if the cloud layer is sufficiently thick. It is not impossible that cloud layers over Northwestern Europe have a considerable vertical extent, because the air that rises in the cyclones is warmer, see Fig. 6, and probably moister than in the zonal average.

Concerning the lower stratosphere, represented here by 200 mb, it is difficult to draw any conclusion. The mixing term becomes smaller because the temperature gradient has vanished. Because we have no vertical velocities and ageostrophic terms for 200 mb, we cannot examine the balance.

To summarize the results of the five flux equations the following overall picture can be composed: Important terms are advection by the mean flow, ageostrophic processes, some of the many mean flow interaction terms, especially the mixing terms that try to produce down-gradient fluxes and horizontal third-order advection terms. Small terms are the time derivatives of the fluxes, curvature terms and all processes depending on vertical velocities except $\overline{\sigma v'\omega'}$ and $\overline{\sigma u'\omega'}$.

2.10. Discussion and concluding remarks

In the introduction we have explained that the purpose of this study is to investigate possibilities of making long-range weather forecasts. More specifically we consider the question of whether or not one can predict the anomalies in monthly or seasonal mean circulation patterns with and SD-model. In order to derive model equations we have scaled the original equations that describe the evolution of the time-mean state of the atmosphere. Closure of these equations has to be done somehow. By scaling the

equations for the evolution of the horizontal second-order eddy statistics we have tried to derive these closure relations.

The results of the scaling are given in Tables 3 to 7. We are not going to repeat all details, but only summarize and discuss the most important features.

First, we can conclude that starting from initial mean conditions an integration in time towards the next month or season is completely useless. This holds for every equation investigated in the previous sections. The reason is that the time derivatives are negligible compared to, for example, advection and therefore the system loses its prognostic ability. This does not mean, however, that general circulation experiments with a time-dependent SD-model are also useless (Kurihara, 1970), but in this kind of experiments we only have to parameterize the eddies such that the resulting model atmosphere behaves well in a statistical sense. The path in the phase space is realistic but not applicable to the development of the real atmosphere. The above-mentioned conclusion seems at first sight to imply that time-averaged SD-models cannot be used for prediction. There is an escape however. At best these models can be used to describe stationary solutions which result from known internal or external forcing. This makes sense only if the variability of monthly or seasonal mean patterns is not completely caused by day-to-day weather fluctuations.

Simple closure relations for the horizontal eddy fluxes cannot be derived from eddy flux equations. Scaling arguments show that new unknowns in these eddy flux equations are large and therefore the set of equations has again to be closed in a, probably, more complicated way. The first reason is that third-order terms are large and cannot simply be neglected. They are determined by a few extremes in the wind field. Because these extremes are deterministically unpredictable, it is probably impossible to find parameterization relations. Hence the existence of extremes is a limiting factor in long-range predictability. A second reason

for difficulties with the closure scheme are the ageostrophic terms in the eddy flux equations. They are in almost every case the dominant terms and it is not clear at all how to deal with them in an SD-model. The foregoing implies that the possibility of parameterizing second-order eddy statistics directly, should be explored in greater depth.

Vertical fluxes are small in general, with the exception of $\overline{\sigma \bar{\omega}}$ in the equation for \bar{T} and $\overline{\sigma u' \omega'}$ and $\overline{\sigma v' \omega'}$ in the equations for $\overline{u'T'}$ and $\overline{v'T'}$.

The equation for $\overline{v'T'}$ proves to be puzzling. In the upper troposphere it was found that the mixing term $\overline{v'^2 \frac{\partial T}{\partial y}}$ is much larger than any of the other investigated terms. Although we did not compute the diabatic term $\overline{v'Q'}/c_p$, it seems that this must be an important counteracting term at these levels. This diabatic term is probably responsible for the occurrence of counter-gradient eddy heat fluxes over Northwestern Europe at 300 mb.

For this study we used about 15 radiosonde stations for one winter and for a small spot in the atmosphere. Can we derive any general conclusion from such a limited attack of the problem? Of course, many of the features arrived at in this paper are valid only in this small area. But each SD-model must be able to describe these features for, among other things, this particular area. Besides, we are convinced that much of the scaling presented in Tables 3 to 7 is valid for a great part of the extra-tropics. The fact that we used one winter only is not a serious objection. It is not only important to know, for instance, whether third-order terms are climatologically significant, it is more meaningful to know how important third-order terms are for one season or one month. After all that is what we want to predict: one individual case.

Acknowledgement. We thank our colleagues for the stimulating discussions we had during the course of this study. We also thank A. Grendel and G. Brouwer for drafting the figures and Mrs. A. Krabman for typing the manuscript. We finally thank the reviewers for their useful suggestions.

2.11. References

- Adem, J., 1964: On the physical basis for the numerical prediction of monthly and seasonal temperatures in the troposphere-ocean-continent system. Mon. Wea. Rev., 92, 91-103.
- Adem, J., 1970: On the prediction of mean monthly ocean temperatures. Tellus, 22, 410-430.
- Dool, H.M. van den, 1975: Three studies on spectral structures of the horizontal atmospheric motion in the time domain. Thesis, University of Utrecht. 128 pp.
- Hantel, M., 1976: On the vertical eddy transports in the northern hemisphere - 1 Vertical eddy heat transport for summer and winter. J. Geophys. Res., 81, 1577-1588.
- Hantel, M. and J.M. Hacker, 1978: On the vertical eddy transports in the northern hemisphere - 2 Vertical eddy momentum transport for summer and winter. J. Geophys. Res., 83, 1305-1318.
- Holopainen, E.O., 1964: Investigation of friction and diabatic processes in the atmosphere. University of Helsinki, Department of Meteorology, paper no. 101.
- Holopainen, E.O., 1973: An attempt to determine the effects of turbulent friction in the upper troposphere from the balance requirements of the large-scale flow: A frustrating experiment. Geophysika, 12, 151-176.
- Kurihara, Y., 1970: A statistical-dynamical model of the general circulation of the atmosphere. J. Atmos. Sci., 27, 847-870.
- Lau, N.G., H. Tennekes and J.M. Wallace, 1978: Maintenance of the momentum flux by transient eddies in the upper troposphere. J. Atmos. Sci., 35, 139-147.

- Lau, N.G., 1978: On the three-dimensional structure of the observed transient eddy statistics of the Northern hemisphere wintertime circulation. J. Atmos. Sci., 35, 1900-1923.
- Lorenz, E.N., 1967: The nature and theory of the general circulation of the atmosphere. WMO-N.218.TP.115, Geneva.
- Lorenz, E.N. 1969: The predictability of a flow which possesses many scales of motion. Tellus, 21, 289-307.
- Oort, A.H. and E.M. Rasmusson, 1971: Atmospheric circulation statistics. NOAA, Professional paper 5, pp. 323.
- Paltridge, G.W. and C.M.R. Platt, 1976: Radiative processes in meteorology and climatology. Developments in Atmospheric Science 5. Elsevier Scientific Publishing Company, pp. 318.
- Saltzman, B., R.M. Guttuso and A. Fleisher, 1961: The meridional eddy transport of kinetic energy at 500 mbar. Tellus, 13, 293-295.
- Savijärvi, H., 1976: The interaction of the monthly mean flow and large-scale transient eddies in two different circulation types. Part 1: The forcing effect of large-scale turbulence and kinetic energy balance. Geophysika, 14, 23-46.
- Savijärvi, H., 1977: The interaction of the monthly mean flow and large-scale transient eddies in two different circulation types. Part 2: Vorticity and temperature balance. Geophysika, 15, 207-230.
- Vernekar, A.D. and H.D. Chang, 1978: A statistical-dynamical model for stationary perturbations in the atmosphere. J. Atmos. Sci., 35, 433-444.
- Wallace, J.M., 1978: Trajectory slopes, counter-gradient heat fluxes and mixing by lower stratosphere waves. J. Atmos. Sci., 35, 554-558.

- III. Seasonal differences in the stationary response of a linearized primitive equation model: prospects for long range weather forecasting?[†]

J.D. Opsteegh and H.M. van den Dool

[†]Published in J. Atmos. Sci., 1980, 37, 2169-2185.

Abstract

A linear steady-state primitive equation model has been developed for the computation of stationary atmospheric waves that are forced by anomalies in surface conditions. The model has two levels in the vertical. In the zonal direction the variables are represented by Fourier series, while in meridional direction a gridpoint representation is used. The equations governing atmospheric motion are linearized around a zonally-symmetric state, which depends on latitude and height according to Oort (1980).

We have studied the amplitude and phase relations of the model response as a function of latitude for a very simple heating, which is sinusoidal in the zonal direction, with zonal wavenumber m ($m = 1, 10$) and constant in the meridional direction, using February mean conditions.

The response of the model indicates that a heating in the tropics can have a substantial influence on the middle and high latitudes, provided that part of the heating is in the westerlies. We have compared the model response for such a heating with the results of similar experiments with a GCM and a linear barotropic model and also with mean anomaly patterns at middle and high latitudes derived from observations for Northern Hemispheric winters with a warm equatorial Pacific. In all cases we find strong similarities of hemispheric wave patterns.

We plan to test the model for the prediction of that part of the anomalies in the monthly or seasonal mean circulation that comes from persistent abnormal surface conditions. In order to predict more than a persistent atmospheric response, such an anomaly in the surface conditions must have different effects in different months or seasons. We have tested the hypothesis that due to a changing zonally-symmetric state, the response to a prescribed heating will be different in the four seasons. This effect is computed for a heating in the tropics and in the middle latitudes. Both in amplitude and phase the response to exactly the same heating can change very much from one season to the next.

3.1. Introduction

The belt of westerlies at middle and high latitudes of the northern hemisphere has been documented for a long time. When looking at a sequence of hemispheric streamline maps, large meanders in the predominantly westerly winds become visible. Some of these meanders have a quasi-stationary character. They are clearly seen on maps of the long-term averaged circulation. The nature of these standing waves is often studied by assuming that they arise as a linear atmospheric response to zonal asymmetries in the earth surface conditions. This makes it possible to study the standing waves with simple linear steady-state models. Saltzman (1968) has given an extensive analysis of this approach. The response of these models to forcing by the earth orography (Charney and Eliassen, 1949; Sankar Rao, 1965) and the exchange of sensible heat with the earth surface (Smagorinsky, 1953; Döös, 1962) shows good agreement with the observed standing wave pattern.

Until 1968 most of the studies had been performed with analytical methods, and therefore the model atmosphere had to be further simplified to a quasi-geostrophic β -plane, with a zonally-symmetric state that is only dependent on height. Saltzman (1968) suggested to incorporate the ageostrophic and nonlinear effects and to use a zonally-symmetric state which depends on latitude and height according to observations. Webster (1972) and Egger (1976a) presented two-level models based on the primitive equations in which winds can be ageostrophic. Webster applied his model only in the tropics, while Egger (1976b, 1978) simulated the standing wave pattern for January and July for the whole northern hemisphere. Recently Ashe (1979) simulated the standing waves with a nonlinear steady-state model.

In this paper we will present a model similar to the one used by Egger with special emphasis on the prospects of making long-range weather forecasts with these models. From the point of view of a long-range weather forecaster it would be interesting to know the stationary response caused by local anomalies in

the earth surface conditions, that is, deviations from their long-term mean value. This makes sense only when we know this anomalous forcing beforehand, for example in case of persistent anomalies. In the earth surface conditions, persistent anomalies are often found in the large-scale distribution of the sea surface temperature (SST), which maintains its character for many months. It is often thought that SST anomalies may act as heat sources or sinks, producing anomalies in the circulation pattern of the atmosphere. It has been shown by many authors that there is indeed some statistical relation (Ratcliffe and Murray, 1970; Namias, 1978; Davis, 1978; Harnack and Landsberg, 1978). In various studies with GCM's it was tried to simulate and quantify this relation (Houghton et al., 1974; Rowntree, 1976; Huang, 1978). But the response produced by the SST anomalies is generally small and hard to distinguish from the noise in the model statistics caused by the transient weather systems.

Egger (1977) has studied the atmospheric response to SST anomalies with a linear steady-state model. He computed the atmospheric response to a pool of warm water near Newfoundland and found some agreement with surface pressure maps constructed from observations by Ratcliffe and Murray.

The value of such a description depends of course very much on the magnitude of the contribution of SST anomalies to anomalies in the mean circulation. There are indications that for middle latitudes most of the variance in the monthly mean circulation can be explained from the transient weather systems (Madden, 1976) and therefore in general only a small part is caused by external forcing. This means that only on those occasions that SST anomaly distributions give rise to large responses, the model results can be used to predict future weather.

A limitation on the use of a persistent forcing anomaly for prediction purposes might be that only persistent anomalies in the circulation are produced. In that case the model predicts persistence. However, the zonally-symmetric component of the circulation shows important changes from one month to the next. Therefore it

is likely that, due to interaction with the zonally-symmetric flow, persistent heating will have a different effect in different months or seasons.

The model described in this paper has two levels and is based on the primitive equations. It is linearized around a zonally symmetric state, that depends on height and latitude, according to Oort (1980). The zonal symmetry allows us to expand the model variables in Fourier series along latitude circles; a forcing in zonal wavenumber m leads to a model response in zonal wavenumber m only. In meridional direction a gridpoint representation is used with 23 points between equator and pole. The heating is prescribed at the intermediate atmospheric level. To obtain a clear picture of the model response, we will use a prescribed heating rather than an interactive heating scheme.

First we will describe the results of some experiments to show the behaviour of the model for different zonal wavenumbers. The model response to a heating that is sinusoidal in zonal direction with zonal wavenumber m ($m = 1, 10$) and an infinite wavelength in meridional direction is computed. Because the zonal mean winds, the zonal mean temperature, the zonal mean static stability and the Coriolis parameter are functions of latitude, the amplitude and phase of the resulting disturbances will also depend on latitude. So a plot of amplitude and phase against latitude will be the most suitable way of discussing the results for each of the wavenumbers. In a second experiment, we will study the influence of an anomalous heating in the tropics on the atmospheric response in middle latitudes. We try to get a better understanding of this response by comparing the model results with the properties of a quasi-geostrophic model. Finally, the prospects of using this model for the prediction of the anomalous monthly or seasonal mean circulation, caused by persistent SST anomalies, are investigated by testing the hypothesis that a persistent heating will have different effects in different months or seasons.

The response of the model is computed for each of the four seasons, using a heating distribution that is the same in each season. We have done one experiment with a heating in middle latitudes and one with a heating in the tropics. The differences between the eight model runs are carefully studied.

3.2. Derivation of the model equations

The model equations can be derived by first applying a time average to the basic laws governing the instantaneous atmosphere. Apart from new unknowns that appear in the momentum and thermodynamic equations as additional forcing and heating, the resulting equations look very much the same as the original ones (Opsteegh and Van den Dool, 1979). In order to construct model equations, we follow roughly the approach by Egger (1976a).

The equations for the monthly mean flow are linearized around a basic state, which is the normal (or long-term) monthly mean circulation. For example

$$\bar{U} = U_n + \hat{u} \quad (1)$$

Here, \bar{U} , U_n and \hat{u} are the monthly mean zonal wind for a particular month, the normal monthly mean zonal wind and the anomalous component. All three quantities depend on latitude, longitude and height.

We now substitute (1) in the equations for the time-averaged quantities and neglect the tendency term and terms nonlinear in \hat{u} , \hat{v} etc. Further we subtract from the equations the terms describing the normal monthly mean atmospheric state. We then obtain a set of linear stationary equations in the deviations (\hat{u} , \hat{v} , etc.). In order to derive tractable model equations, the normal flow is divided further into a zonal symmetric and a zonal asymmetric part. For example

$$U_n = U_{sn} + U_{an} \quad (2)$$

Here, U_{sn} and U_{an} are the symmetric and the asymmetric part of the normal zonal wind. After substitution of (2) we get the final anoma-

ly (or perturbation) equations. Because we will not deal in this study with the terms describing the interaction of the perturbations with both the mean meridional flow and the normal standing eddies, we transfer these terms to the right-hand side of the perturbation equations. The equations are expressed in curvilinear coordinates with pressure as vertical coordinate. They read as follows:

Zonal momentum balance

$$U_{sn} \frac{\partial \hat{u}}{\partial x} + \hat{v} \frac{\partial U_{sn}}{\partial y} + \hat{\omega} \frac{\partial U_{sn}}{\partial p} - f \hat{v} + \frac{\partial \hat{\phi}}{\partial x} - U_{sn} \hat{v} \frac{\tan \phi}{a} - \hat{F}_{Wx} = \hat{F}_{Ex} - \hat{M}U - \hat{S}U \quad (3)$$

Meridional momentum balance

$$U_{sn} \frac{\partial \hat{v}}{\partial x} + f \hat{u} + \frac{\partial \hat{\phi}}{\partial y} + 2U_{sn} \hat{u} \frac{\tan \phi}{a} - \hat{F}_{Wy} = \hat{F}_{Ey} - \hat{M}V - \hat{S}V \quad (4)$$

First law of thermodynamics

$$U_{sn} \frac{\partial \hat{T}}{\partial x} + \hat{v} \frac{\partial T_{sn}}{\partial y} - \sigma_{sn} \hat{\omega} = \frac{\hat{Q}}{c_p} + \hat{Q}_E - \hat{M}T - \hat{S}T \quad (5)$$

Continuity equation

$$\frac{\partial \hat{u}}{\partial x} + \frac{\partial \hat{v} \cos \phi}{\cos \phi \partial y} + \frac{\partial \hat{\omega}}{\partial p} = 0 \quad (6)$$

Hydrostatic approximation

$$\frac{\partial \hat{\phi}}{\partial p} = - \hat{\alpha} \quad (7)$$

Equation of state

$$p \hat{\alpha} = R \hat{T} \quad (8)$$

where $\partial x = a \cos \phi \partial \lambda$ and $\partial y = a \partial \phi$.

The symbols $u, v, \omega, x, y, p, f, \phi, T, \alpha$ and R have their conventional meaning. \hat{F}_{Wx} and \hat{F}_{Wy} are the dissipation terms and

will be specified below. \hat{F}_{Ex} , \hat{F}_{Ey} and \hat{Q}_E are the internal eddy sources of momentum and heat, \hat{MU} , \hat{MV} and \hat{MT} describe the interaction of the perturbations with the mean meridional flow. \hat{SU} , \hat{SV} and \hat{ST} describe the interaction with the normal standing eddies. Of all the terms at the right-hand side only the anomalous diabatic heating \hat{Q}/c_p will be retained. In this study the heating, which drives the model, will be prescribed.

Vertical discretization. The vertical discretization of the model is shown in the upper part of Fig. 1. The momentum and continuity equations are applied at level 1 (400 mb) and 3 (800 mb), while the thermodynamic equation is applied at level 2 (600 mb). In the last equation \hat{T}_2 is eliminated and expressed in $\hat{\phi}_1$ and $\hat{\phi}_3$, with the hydrostatic equation and the equation of state. The boundary condition at levels 0 and 4 is:

$$\hat{\omega} = 0. \quad (9)$$

By using a rigid top at the tropopause, the propagation of the waves into the stratosphere is prevented. This may cause spurious reflection of wave energy, which affect amplitude and phase of the response in the troposphere (Shutts, 1978; Laprise, 1978). We now have a set of seven equations in the seven variables \hat{u}_1 , \hat{u}_3 , \hat{v}_1 , \hat{v}_3 , $\hat{\phi}_1$, $\hat{\phi}_3$, and $\hat{\omega}_2$. For the friction terms Egger's (1976a) approach is followed. So at level 3 we have surface friction and vertical diffusion, while at level 1 there is only vertical diffusion. In the zonal momentum equations they have the following form:

$$\hat{F}_{Wx3} = K_D(\hat{u}_1 - \hat{u}_3) - K_W\hat{u}_3 \quad (10)$$

$$\hat{F}_{Wx1} = -K_D(\hat{u}_1 - \hat{u}_3) \quad (11)$$

K_D and K_W are vertical diffusion and surface friction coefficients respectively. They are constants in the model. The friction terms in the meridional momentum equations are obtained by replacing \hat{u}_1 and \hat{u}_3 by \hat{v}_1 and \hat{v}_3 in (10) and (11).

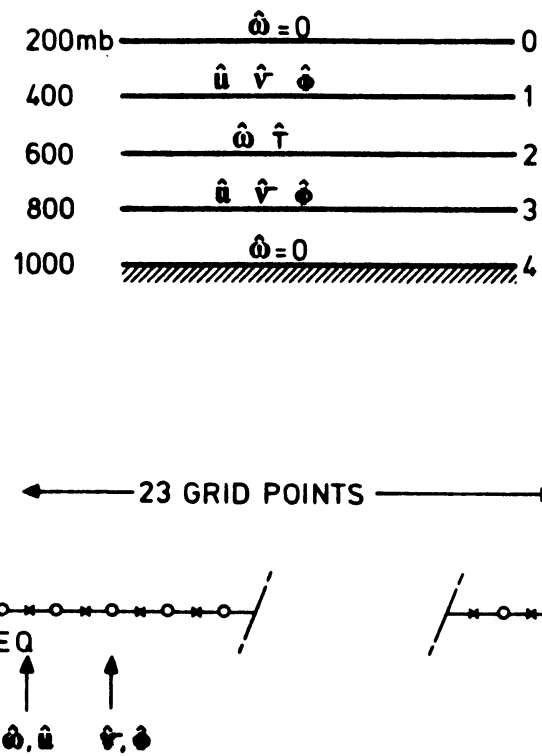


Fig. 1 : Discretization of the two-level model in the vertical (upper part) and in the meridional direction (lower part).

Horizontal discretization. The various terms in the seven model equations contain coefficients that do not depend on longitude. Therefore the perturbation quantities are expanded in Fourier series along latitude circles. In the meridional direction we have chosen a gridpoint representation, with 23 gridpoints between pole and equator. As an example of the Fourier expansion we write:

$$\hat{u}_1 = \sum_{m=1}^N \hat{u}_{1m}(\phi) e^{-im \lambda} \quad (12)$$

where \hat{u}_{1m} is a complex coefficient. By substitution of these relations into the model equations we get new equations for the complex Fourier coefficients. These equations are given in Appendix A. Finally, we have N sets of 14 linear first-order differential equations for the real and imaginary parts of the Fourier coefficients.

The equations are solved on the grid that is shown in the lower parts of Fig. 1. There are 23 gridpoints, indicated as crosses with a grid distance of slightly less than 4° . \hat{v} and $\hat{\phi}$ are formulated at intermediate points, indicated with open circles. The boundary conditions are:

$$\begin{aligned} \hat{v} \cos(\phi) &= 0 & \text{at } \phi &= \pi/2 \\ \frac{\partial \hat{\phi}}{\partial \phi} &= 0 & \text{at } \phi &= 0 \end{aligned} \quad (13)$$

Here, $\hat{v} \cos \phi$ is a variable which is used in the model, instead of \hat{v} ; it is zero at the pole. At the equator we use a symmetry condition. Some of our experiments have been repeated with the boundary conditions used by Egger (1976a), with almost the same results.

3.3. Behavior of the model in the zonal wavenumber domain

In order to investigate the characteristic behavior of the model, we solve the system of equations for a heating distribution that is sinusoidal in the zonal direction and constant

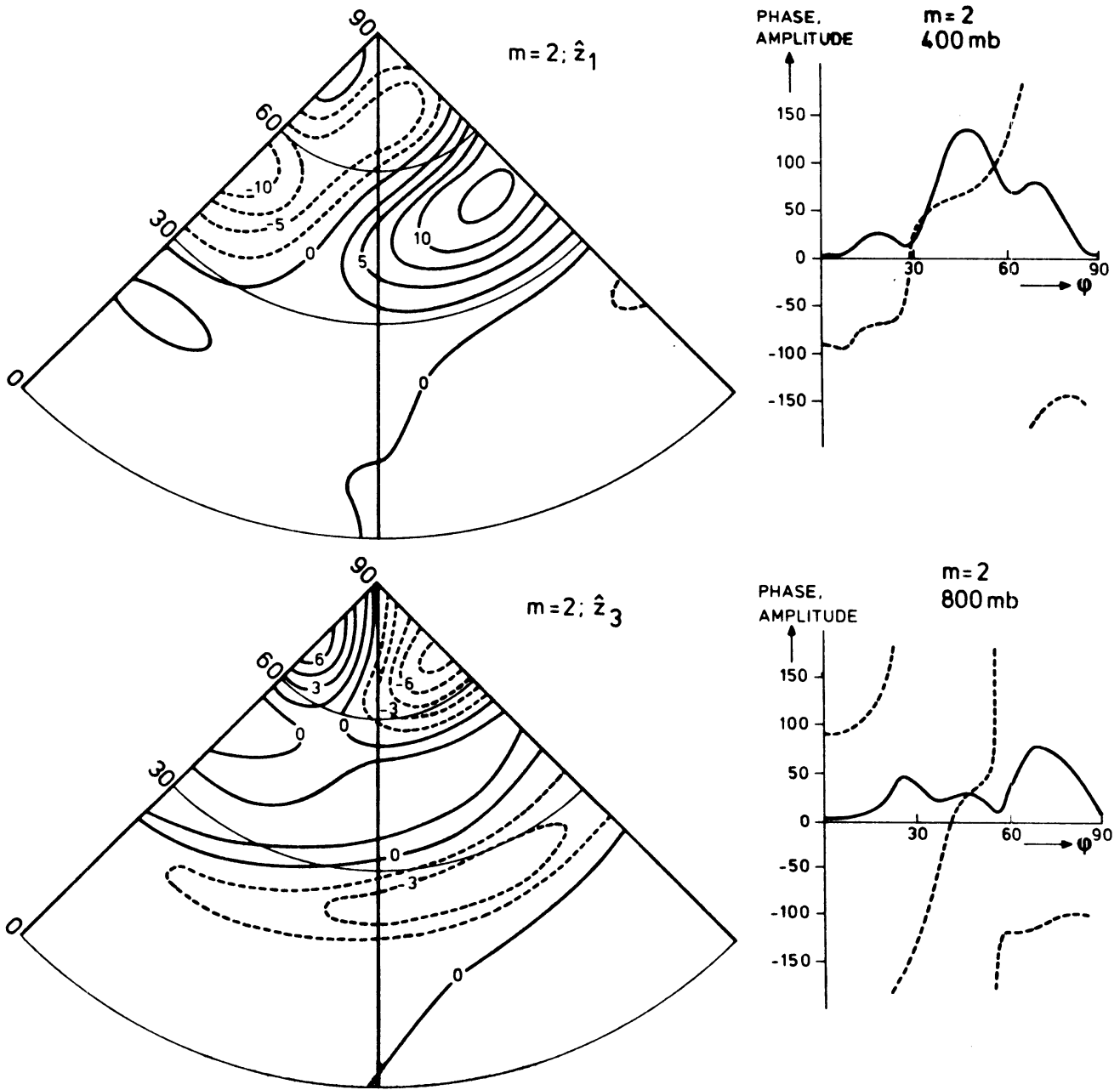


Fig. 2 : The geopotential height response of the model at 400 and 800 mb to a heating that is sinusoidal in longitudinal direction (zonal wavenumber 2) and uniform with latitude. The amplitude of the heating is 10^{-5} K s^{-1} . In the left part the response is presented as a geographical distribution, while in the right part amplitude and phase are plotted against latitude.

in the meridional direction. Hence

$$\hat{Q}_2/c_p = A \cos (m\lambda) ,$$

with $A = 1.10^{-5} \text{ Ks}^{-1}$. The model solution is derived separately for zonal wavenumbers from 1 to 10. The zonally-symmetric fields U_{sn1} , U_{sn3} , T_{sn1} , T_{sn3} and σ_{sn2} have been computed from the data of Dort (1980), while $(\frac{\partial U}{\partial p})_1$ and $(\frac{\partial U}{\partial p})_3$ are derived from the normal temperature fields by applying the thermal wind relation. In this section we have chosen the February mean conditions. The numerical value of the friction coefficient (K_W) is 2.10^{-7} s^{-1} , which is close to the value taken by Egger (1976a). For the vertical diffusion coefficient (K_D) we have chosen a value of 1.10^{-7} s^{-1} . We have neglected the terms that describe the convergence of the meridians, because in a linear model they generate spurious energy. This is outlined in Appendix B.

Most of the experiments with steady-state models have been performed on a β -plane, with zonally-symmetric fields that are independent of latitude. As a consequence, the forced wave will have the same wavelength in the zonal and meridional directions as the heating wave. In the present model the zonally-symmetric state and the derivative of the Coriolis parameter are functions of latitude. Therefore, a heating with wavenumber (m,n) will create a response with the same zonal wavenumber m , but with a complex meridional structure.

As an example we will discuss at some length the geopotential height response in $m = 2$. In the left part of Fig. 2 the horizontal distribution of the geopotential height of 400 and 800 mb is shown. Units are decameters. Because of the symmetry and periodicity of the solution we show only 90 degrees of geographical longitude. In this area the cosine bell-shaped heating is $1.10^{-5} \text{ Ks}^{-1}$ at $\lambda = -45^\circ$. At 800 mb low pressure is found everywhere over the heating in the subtropics, whereas at 70° N the low pressure is observed downstream of the maximum of the heating.

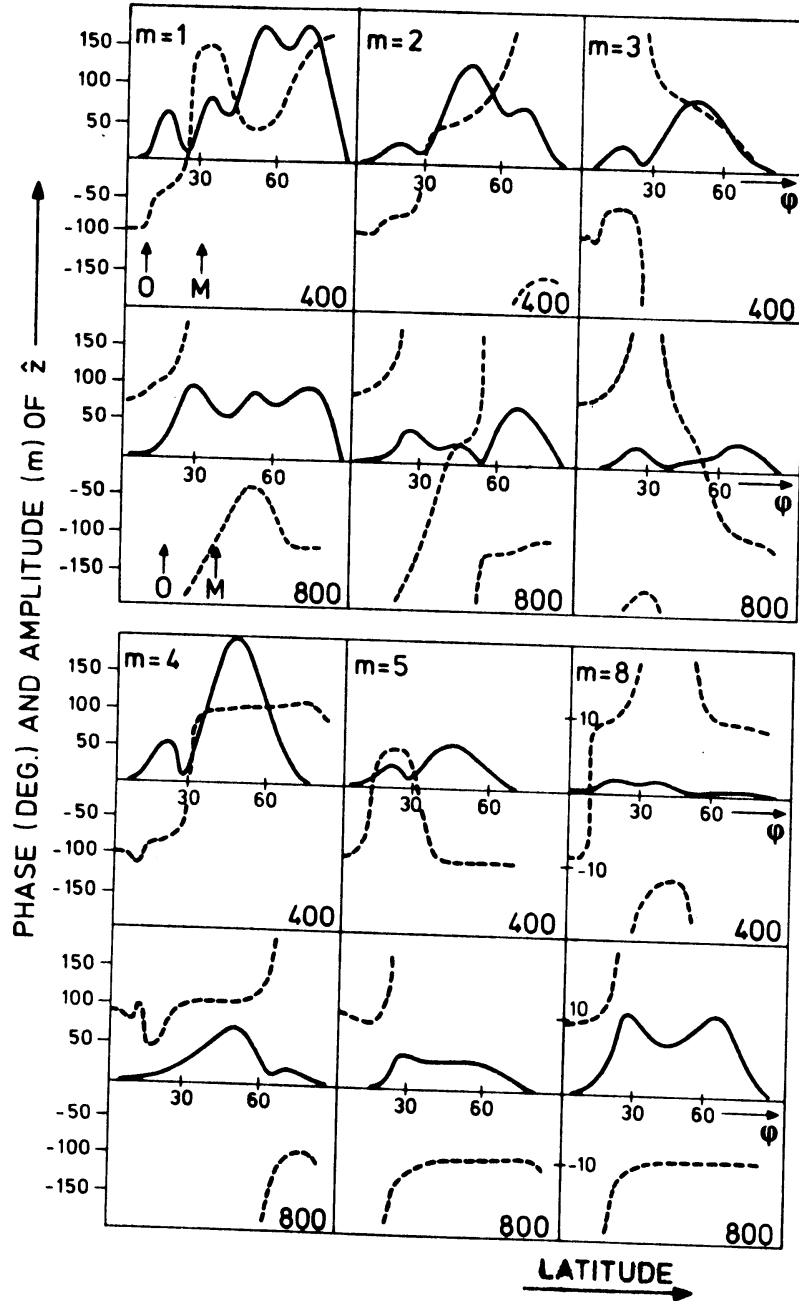


Fig. 3 : Amplitude and phase of the geopotential height response at 400 and 800 mb as a function of latitude and wave-number. The heating has zonal wavenumber m ($m = 1, 2, 3, 4, 5$ and 8) and infinite meridional wavelength; the amplitude is $1.10^{-5} \text{ K s}^{-1}$ for all m . The latitudes where the mean wind is zero (O) and where it reaches its maximum (M) are indicated by arrows in the graph of $m = 1$.

At 400 mb there is a system of high pressure downstream of the heating maximum at 50° N. The upstream low pressure system has an extension to the high northern latitudes.

In the right part of Fig. 2 the same responses are represented in a more informative and concise way: amplitude and phase are plotted as a function of latitude. The amplitude is in meters and the phase in degrees of the wavelength in question (-180 to $+180$). The phase measures the distance of the geopotential ridge to the maximum of the heating. The phase is positive (negative) if the geopotential ridge is found to the east (west) of the heating maximum. It is clear that amplitude and phase show a remarkable dependence on latitude although the heating is the same everywhere. The reason is the latitude-dependence of U_{sn} , T_{sn} , σ_{sn} and $\beta (= \frac{df}{dy})$.

Before we discuss amplitude/phase diagrams for all wavenumbers, it should be noted that the resonance wavenumber is very close to $m = 4$ and 5 . This wavenumber separates the ultralong waves from the long waves. For the ultralong waves the β -term in the vorticity equation dominates over the advection terms, while the opposite is true for the long waves (see e.g. Salzman, 1965). In Fig. 3 the geopotential height responses are shown for $m = 1, 2$ and 3 (ultralong waves), $m = 4$ and 5 (near-resonance) and $m = 8$ (long wave). The results are complicated but some general features can be seen in Fig. 3.

In the tropical belt of easterlies, the amplitudes are very small for all wavenumbers. The heating (cooling) is almost completely balanced by strong upward (downward) motion, while horizontal temperature advection is negligible. This thermally direct circulation was also found by Webster (1972).

In subtropical regions the amplitude and phase of the ultralong waves increase very fast north of the latitude of zero mean wind. The phase of the subtropical maximum at 800 mbar is about 180° , which means that for $m = 1, 2$ and 3 the troughs are found over the heating; the phase of the maximum at 400 mb varies between -70 and -30° .

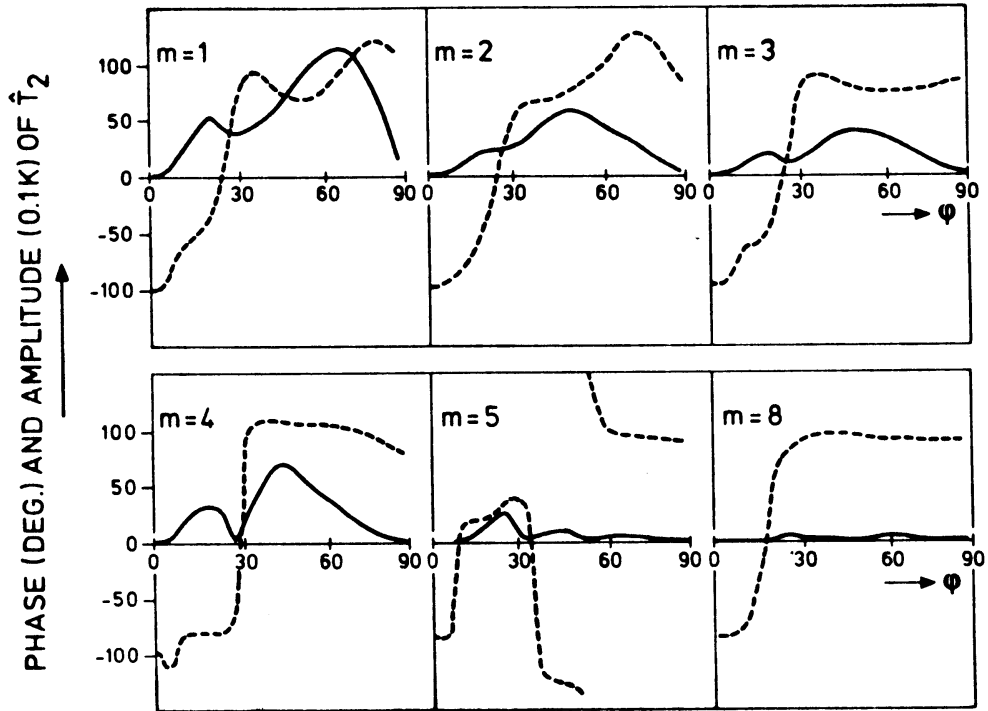


Fig. 4 : As in Fig. 3, but now for the temperature response at 600 mb. The vertical scales for the phase (degrees) and temperature (0.1 K) are the same.

Going north to the mid-latitudes, the amplitude and phase are different for the first three wavenumbers. Nevertheless, looking at the maxima, we find the same general picture that can be derived from experiments with quasi-geostrophic models; at 800 (400) mb a high is found up(down)stream of the heating.

For infinite meridional wavelength of the heating, wavenumbers 4 and 5 are close to resonance. They exhibit a quite different behavior than the ultralong waves. The smooth decrease of amplitude with wavenumber is interrupted at $m = 4$.

As a representative of the long waves we have chosen $m = 8$. The most prominent feature in its response is that the amplitude is at least one order of magnitude smaller than that of the ultralong waves. (Note the difference in vertical scale for $m = 8$).

The height response at 400 and 800 mb can, of course, be combined into a temperature response at 600 mb. In Fig. 4 amplitude/phase diagrams are shown for \hat{T}_2 . Some clear conclusions can be drawn now:

- (1) The temperature wave can be found downstream of the heating wave. This is perfectly true for $m = 8$, nearly true for $m = 1, 2$ and 3 and only at the resonance wavelength deviations of the simple concept occur.
- (2) The phase of temperature wave has a bimodal distribution with peaks at $+90^\circ$ and -90° . This indicates that the zonal advection of \hat{T}_2 by the climatological wind cools the area of maximum diabatic heating (\hat{Q}/c_p) as much as possible.

A good impression of the way in which the diabatic heating is balanced is given in Fig. 5. Here we show the value of the three terms in the thermodynamic equation as a function of latitude at the longitude of maximum heating. The sum of the three terms equals the heating that is indicated by the dashed straight line ($\hat{Q}/c_p = 1.10^{-5} \text{Ks}$). From this figure it is clear that at the very low latitudes the heating is almost completely balanced by vertical motion, whereas temperature advection plays a minor role. This holds for all wavenumbers. For the ultralong waves the advection

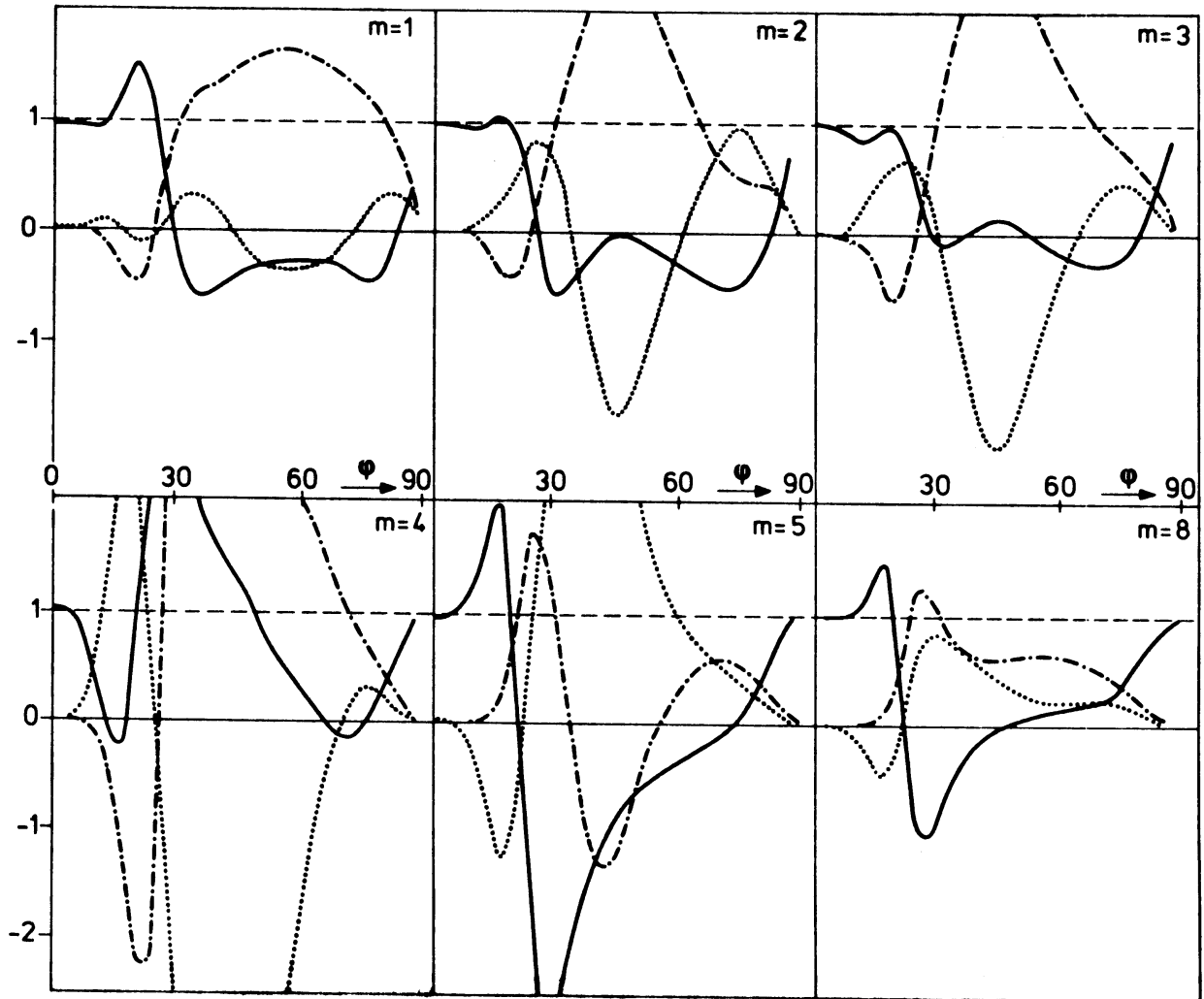


Fig. 5 : Thermodynamic balance as a function of latitude at the longitude of maximum heating. The heating is indicated with a dashed line ($\hat{Q}/c_p = 1.10^{-5}$), the vertical motion term with a solid line, the zonal temperature advection with a dashed-dotted line and the meridional advection with a dotted line. Units are $1.10^{-5} \text{ K s}^{-1}$.

terms are dominant at middle latitudes. This balance is not very efficient, because the zonal temperature advection is counteracted by the meridional temperature advection and the vertical motion term. At many latitudes the latter two processes warm the air, whereas cooling is required in order to oppose the diabatic heating. From the balance in wavenumber 4 and 5 it can be seen that they are close to resonance. The terms are very large and mainly counteract each other. Wavenumber 8 shows a different picture at mid-latitudes. Here the heating is balanced efficiently, because all terms have a positive contribution.

To summarize the results, we have found that there is some agreement with the results of studies with a local heating at mid-latitudes and in the tropical regions. However, the general picture is much more complicated than can be deduced from local experiments. It turns out that even for a simple heating distribution (heating is kept constant with latitude) the amplitude as well as the phase of the response is strongly dependent on latitude.

3.4. The influence of heating in the tropics on the standing waves in the middle latitudes

In most of the experiments that have been performed with steady-state models so far, the nature of the standing eddies at mid-latitudes has been investigated without the influence of heating in the tropics. However, at present it is not clear how important the heating in the tropics is and whether a steady-state model can handle it properly.

Egger (1977) investigated the influence of an anomalous warm region in the tropical Atlantic and the Pacific on the standing eddies in middle latitudes with a steady-state PE model. In the Pacific experiment the heating was restricted to the belt of easterlies, whereas in the Atlantic experiment part of the heating region was situated in the westerlies. The mid-latitude response to the

heating in the Pacific was negligible, but the warm spot in the Atlantic Ocean results in a significant response, although it is smaller than the one derived with a GCM for the same tropical Atlantic sea surface temperature anomaly (Rowntree, 1976). Egger did not investigate in detail the differences between the two experiments, although he suggested that the critical line where the zonally averaged mean wind changes sign, as well as the equatorial easterlies might have a profound influence on the intensity and position of the standing waves at mid-latitudes.

We have made similar experiments with the two-level steady-state PE model. However, in order to get a better understanding of the responses, we will start with a theoretical study of the behavior of the simpler quasi-geostrophic two-level model on a β -plane.

Response of a quasi-geostrophic model. Let us consider tropical heating south of latitude ϕ_0 . North of ϕ_0 the heating is zero everywhere. Hence at latitudes north of ϕ_0 the response must be a solution of the homogeneous equations. Stationary Rossby-waves are solutions of these homogeneous equations. The question is whether forcing at these low latitudes will excite these waves. In the following we will show how this depends on the zonally-symmetric conditions and on the particular value of β and f .

The equations of the quasi-geostrophic two-level model on a β -plane are:

$$U_{sn1} \frac{\partial^2 \hat{v}_1}{\partial x^2} + U_{sn1} \frac{\partial^2 \hat{v}_1}{\partial y^2} + \beta \hat{v}_1 = \frac{f_0}{2\Delta p} \hat{w}_2 \quad , \quad (14)$$

$$U_{sn3} \frac{\partial^2 \hat{v}_3}{\partial x^2} + U_{sn3} \frac{\partial^2 \hat{v}_3}{\partial y^2} + \beta \hat{v}_3 = - \frac{f_0}{2\Delta p} \hat{w}_2 \quad , \quad (15)$$

$$U_{sn1} \hat{v}_3 - U_{sn3} \hat{v}_1 + \frac{2\Delta p \sigma_{sn2}}{f_0} \hat{w}_2 = 0 \quad , \quad (16)$$

where (14) and (15) are the vorticity equations, applied at 400 and 800 mb, and (16) is the homogeneous thermodynamic

equation applied at 600 mb. For simplicity we have replaced the polar coordinates λ and ϕ by the rectangular coordinates x and y . In order to get tractable equations, $\hat{\omega}_2$ is eliminated from (14) and (15), using (16), while the remaining variables are expanded in Fourier series in x direction as follows:

$$\begin{pmatrix} \hat{v}_1 \\ \hat{v}_3 \end{pmatrix} = \sum_{m=1}^M \begin{pmatrix} \hat{v}_{1m} \\ \hat{v}_{3m} \end{pmatrix} \exp\left(\frac{2\pi}{L} imx\right)$$

where $L = 2\pi a \cos \phi$ is the length of the latitude circle, a is the earth radius. The vorticity equations for the m -th Fourier component now have the following form:

$$\frac{\partial^2 \hat{v}_{1m}}{\partial y^2} + K_1 \hat{v}_{1m} + K_3 \hat{v}_{3m} = 0 \quad (17)$$

$$\frac{\partial^2 \hat{v}_{3m}}{\partial y^2} + K_2 \hat{v}_{3m} + K_3 \hat{v}_{1m} = 0 \quad (18)$$

where

$$K_1 = \frac{\beta}{U_{sn1}} - \frac{4\pi^2}{L^2} m^2 - \frac{f_o^2}{4\Delta p^2 \sigma_{sn2}} \frac{U_{sn3}}{U_{sn1}} \quad (19)$$

$$K_2 = \frac{\beta}{U_{sn3}} - \frac{4\pi^2}{L^2} m^2 - \frac{f_o^2}{4\Delta p^2 \sigma_{sn2}} \frac{U_{sn1}}{U_{sn3}} \quad (20)$$

$$K_3 = \frac{f_o^2}{4\Delta p^2 \sigma_{sn2}} \quad (21)$$

If a stationary Rossby-wave with zonal wavenumber m exists, it is a solution of (17) and (18). Given a set of constants on the β -plane (β , f_o , U_{sn1} , U_{sn3} , and σ_{sn2}), we will investigate for all zonal wavenumbers whether such solutions exist. Hence we look for solutions that are periodic in the y -direction:

$$\begin{pmatrix} \hat{v}_{1m} \\ \hat{v}_{3m} \end{pmatrix} = \begin{pmatrix} A_{1m} \\ A_{3m} \end{pmatrix} \exp(iny) \quad (22)$$

Substitution of (22) in (17) and (18) gives two homogeneous equations in A_{1m} and A_{3m} . These equations have only a nonzero solution if the determinant is zero.

That is,

$$(K_1 - n^2)(K_2 - n^2) - K_3^2 = 0$$

hence

$$2n^2 = (K_1 + K_2) \pm \sqrt{(K_1 - K_2)^2 + 4K_3^2} \quad (23)$$

For a positive n^2 (n is real), the solution is periodical in the y -direction and stationary Rossby-waves with zonal wave-number m are possible. Once excited, such waves will influence the mid-latitudes. When n^2 is negative, n will be complex and one growing plus a decaying exponential solution is obtained. Such solutions can only exist for nonzero boundary conditions, in contrast with the Rossby-waves. When the conditions are such that exponential solutions occur, a nonzero perturbation at latitude ϕ_0 , which arises as a result of the forcing south of ϕ_0 , will be damped exponentially. The amplifying branch has zero amplitude because the solution must satisfy the homogeneous boundary condition at the pole ($\hat{v}_m = 0$ at $\phi = \Pi/2$). In this case the mid-latitudes will not feel the heating in the tropics. So by investigating (23) in more detail, we are able to gain some insight into the conditions that are favorable for a tropical disturbance to propagate into the mid-latitudes.

From (23) it can easily be seen that in case $(K_1 + K_2)$ is positive, there is always at least one positive solution of n^2 . The only positive contribution to K_1 and K_2 comes from the β -term, provided that the mean wind is westerly. So if the β term is positive and large compared to the other two contributions to K_1 and K_2 , we will get periodic solutions. On the other hand, if the zonal wavenumber m is large enough, both solutions for

n^2 become negative and the forced disturbance at latitude ϕ_0 will damp exponentially. Hence from a first glance at (23) we can learn that, given a set of local conditions U_{sn1} , U_{sn3} , β , f_0 and σ_{sn2} , we can expect a critical zonal wavenumber m_c . For wavenumbers smaller than m_c the β -term dominates and stationary Rossby-waves are excited. Wavenumbers larger than m_c will be damped.

We will quantify this qualitative understanding by determining the critical wavenumber for local β plane conditions at each gridpoint. So we take the observed February mean condition at a particular gridpoint, together with the real value of β at that point and assume that they are independent of latitude. Now K_1 , K_2 and K_3 are constant and we can determine the solution for m_c from (23).

Fig. 6 shows the critical zonal wavenumber as a function of latitude. In the belt of easterlies, m_c is zero and no stationary Rossby-waves exist. Just to the north of the latitude where U_{sn1} changes sign all wavenumbers have stationary Rossby-wave solutions (the β term is very large and positive). Going to the north, m_c decreases until it reaches a value of approximately 7 at the latitude where U_{sn3} is zero. North of that latitude, again all wavenumbers have stationary Rossby-wave solutions. At mid-latitudes zonal wavenumbers higher than 5 will be damped. Only zonal wavenumbers 1 and 2 have stationary Rossby-wave solutions up to the polar regions.

Response of the PE model. With this picture in mind, we now turn to the tropical experiment with the two-level PE model. We have placed a heating in the tropics with zonal wavenumber m ($m = 1, 10$), which decreases linearly with latitude. The heating has a maximum at the equator of $1.10^{-5} \text{ K s}^{-1}$ and it is zero at 16° N . Fig. 7 shows the response of the model as a function of latitude for $m = 1$ to 10 at 400 mb . Friction and vertical diffusion have been excluded in this experiment.

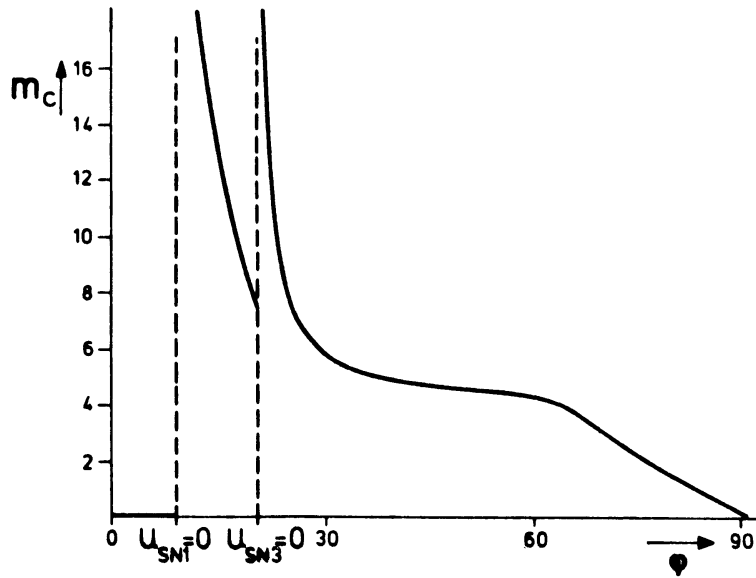


Fig. 6 : The critical zonal wavenumber (m_c) as a function of latitude. This wavenumber defines the largest zonal scale that allows periodic solutions in the meridional direction.

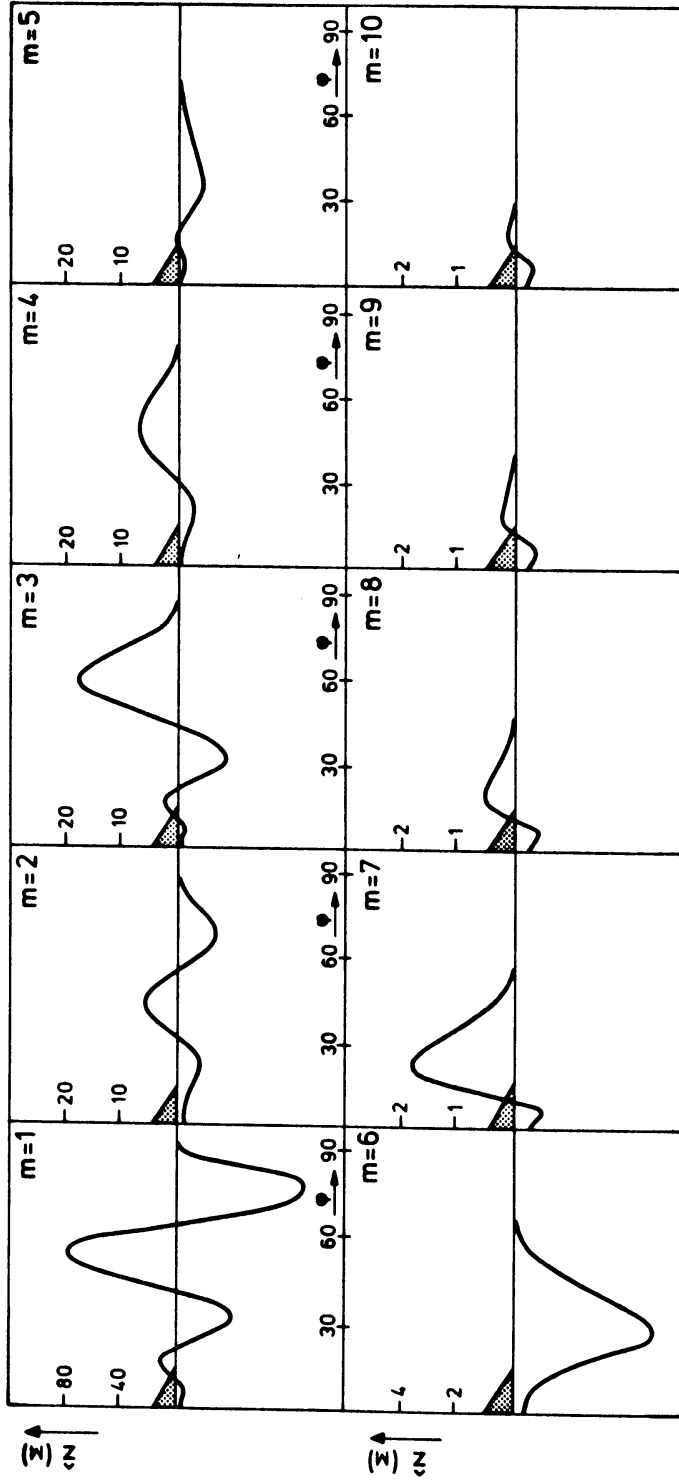


Fig. 7 : Geopotential height response at 400 mb for a tropical heating (indicated by the shaded triangle) with zonal wavenumber $m = 1, \dots, 10$. The amplitude of the height response is given as a function of latitude. The vertical scales are adapted to the magnitude of the amplitude.

Clearly wavenumbers 1 and 2 have a periodic solution in the y-direction, up to high northern latitudes. Wavenumbers 3, 4 and 5 are damped north of the middle latitudes, while wavenumbers higher than 5 start their damped behavior already north of the subtropics. This is perfectly in agreement with the behavior that was predicted by the critical wavenumber. The amplitudes of the lowest wavenumbers are quite large. However, when friction and vertical diffusion are included, it reduces to a few gpdam.

A major feature of this response, which could not be deduced from our simple analysis of the quasi-geostrophic system, is that the amplitudes increase with increasing latitude. As a consequence, the largest response to a heating in the tropics is found in the polar regions.

From this experiment we draw the conclusion that, even if only linear effects are incorporated, a heating in the tropical regions can have a significant influence on middle and high latitudes, especially when much of the forcing energy is in the low wavenumbers. However, when the heating is situated completely in the belt of easterlies, the disturbance will be damped, according to the critical wavenumber there. This explains the difference in response in Egger's tropical Pacific and Atlantic experiment (Egger, 1977). We are not quite sure yet whether the stationary wave patterns created by our linear model as a response to tropical forcing are realistic in the sense that they can be found also in the response of the real atmosphere or in the results of GCM experiments. We will go into that subject in the next section.

3.5. The influence of different zonally-symmetric states in different seasons

We mentioned in the introduction that our main interest is in the anomalies that frequently occur in the normal standing

wave pattern in a particular month or season. We want to describe these anomalies with a linear steady-state PE model as a response to observed abnormal surface conditions. We have planned to apply the model for the prediction of that part of the anomalous mean circulation that can be explained from the presence of persistent components in the anomalous surface conditions. We have a chance of predicting more than persistence only when these conditions produce a different effect in different months.

Here we demonstrate that due to a changing zonally-symmetric state, the response to a prescribed heating differs from season to season. This effect is computed for a rectangular heating of $1.10^{-5} \text{ K s}^{-1}$ in middle latitudes and in the tropics. The area enclosed by the heating is 20° latitude and 45° longitude. In this section we discuss all results in the space domain.

The tropical heating. Fig. 8 shows the results at 800 mb for the tropical heating. The heating is indicated by the shaded area. Apart from differences in amplitudes and position of the various lows and highs, the overall picture of the response in winter, spring and fall is comparable. However, in summer, the responses in middle and high latitudes are almost zero. Here we can see very clearly the influence of the easterlies. In summer the tropical heating is completely in the zonal belt of easterlies, which prevents the excitement of stationary Rossby-Haurwitz waves. The response in the other three seasons in middle latitudes shows low pressure upstream of the longitude of the heating, while high pressure is found downstream. The most dominant pressure system is however the low at high latitudes, approximately 90° downstream of the longitude of the heating. This low is most intense in spring and fall, with minor phase changes from one season to the other. The low pressure system at mid-latitudes is most intense in spring with three separate centers.

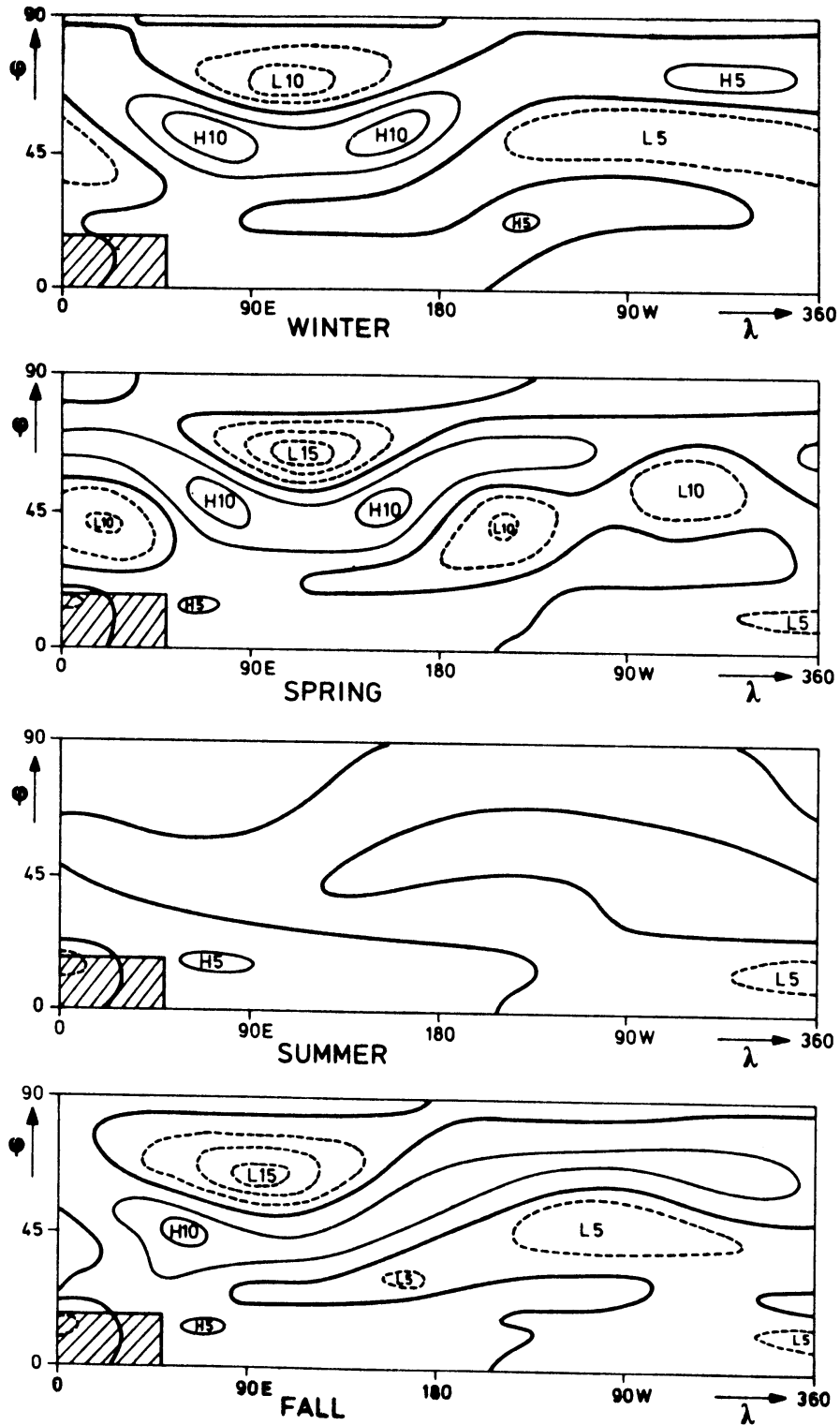


Fig. 8 : Geopotential height response (gpm) in four seasons at 800 mb for a rectangular heating of $1 \cdot 10^{-5} \text{ K s}^{-1}$ in the tropics (shaded area). The net response of the first ten zonal wavenumbers is given in a geographical display.

Comparison with other studies. We have compared the winter response with the results of experiments performed by Rowntree (1976). He computed the mean response of a GCM to the forcing produced by abnormally high SST's during the winter of 1963. The anomaly was in the tropical Atlantic near the Cape Verde Islands, with maximum deviations of 2.7 K. The response as given by Rowntree consists of the signal produced by the SST anomaly plus the noise of the transients. He gives surface pressure anomaly patterns only near the longitudes of the SST anomaly. Low pressure is found over and to the north of the anomaly up to a latitude of about 60° N and high pressure north of that latitude. Our winter response at 800 mb shows a similar pattern. However, we are especially interested in the planetary hemispheric wave structure produced by the GCM. Rowntree gives one hemispheric map of the results at 300 mb. In Fig. 9 his results are compared with our response at 400 mb (in stereographic maps). Of course, the absolute values of the responses cannot be compared, because the magnitude of the atmospheric heating in both experiments is not the same. It turns out that the middle and high latitude wave patterns are very similar. Apparently, a significant part of the anomaly patterns of the GCM can be interpreted in terms of stationary Rossby-Haurwitz waves, arising as a linear atmospheric response to a tropical heating.

Hoskins (1978)¹ computed the steady-state solution of the linear barotropic vorticity equation on the sphere. The tropical SST anomaly was simulated with a negative vorticity source at 300 mb. The computed anomaly pattern at middle and high latitudes has a very strong resemblance to our results at 400 mb. Indeed the vertical structure of the mid-latitude response of the two-level model is nearly equivalent barotropic and the agreement is therefore not surprising.

¹Hoskins, B.J., 1978: Horizontal wave propagation on a sphere. "The General Circulation: Theory, Modelling, and Observations". NCAR Summer 1978 Colloquium. p. 144-153. NCAR/CQ-6+1978-ASP.

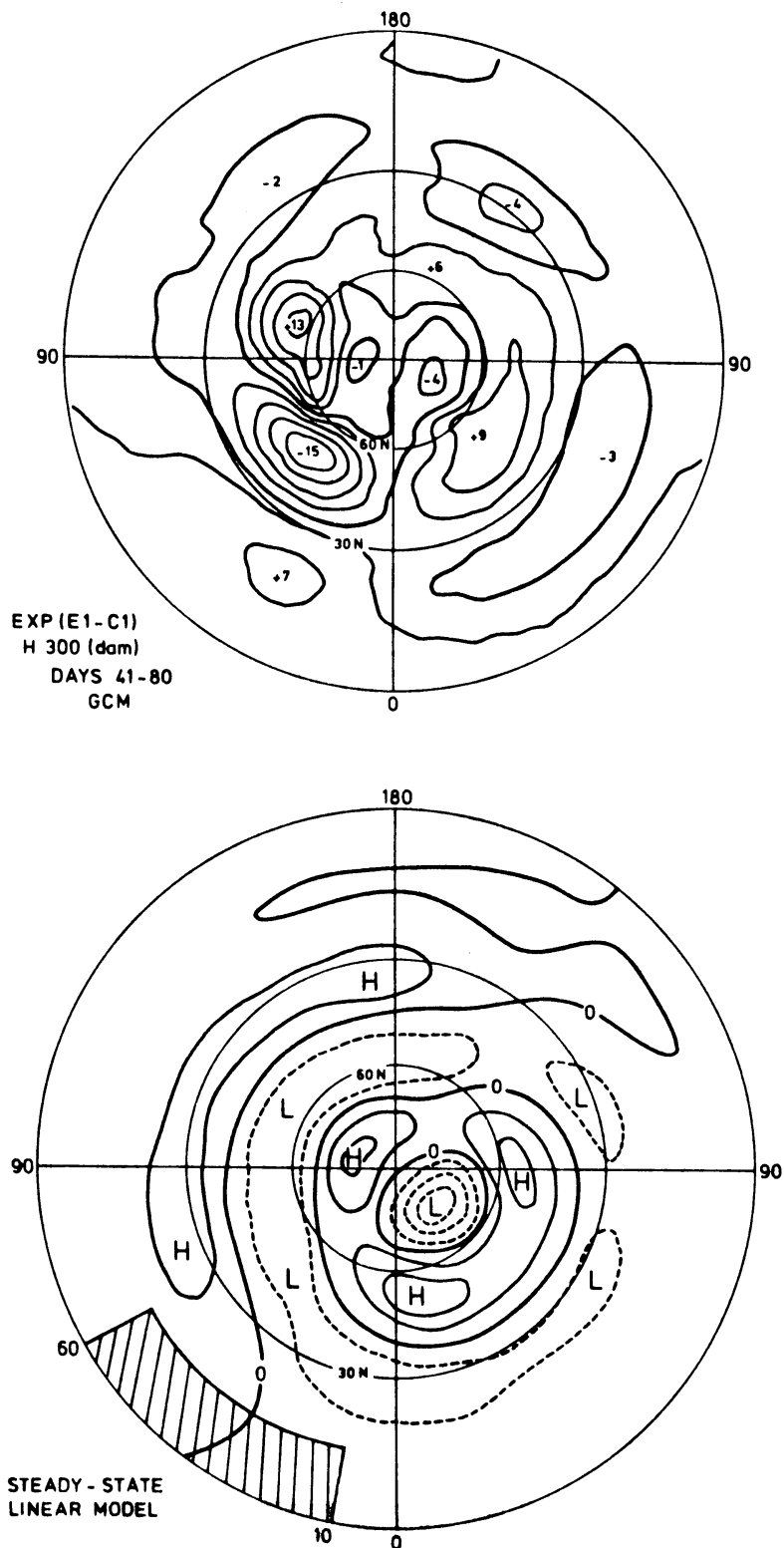


Fig. 9 : Geopotential height response at 300 mb of a GCM to a positive SST anomaly in the tropical Atlantic Ocean (Rowntree, 1976) and the steady-state response at 400 mb of the two-level linear model to a similar prescribed heating in the same area. Isolines are drawn at intervals of 3 and 1 gpdam for the GCM and linear model respectively.

Very recently Horel and Wallace (1981) computed from observations the mean anomaly pattern at middle and high latitudes for Northern Hemispheric winters in which the sea surface temperatures were above normal in the equatorial Pacific. The resemblance of these hemispheric wave patterns with the above mentioned model results is remarkable. We therefore think that the response of a linear model to a forcing in the tropics is meaningful.

The mid-latitude heating. Fig. 10 shows the seasonal responses for the middle latitude heating. Apart from some agreement in the neighborhood of the heated area, the hemispheric wave patterns show very large differences. Downstream of the heating we find a low and upstream a high in all seasons. This downstream low is very strong in summer, when its position is somewhat to the south of the heating center. In winter it is rather weak. The general character of the winter response is a wavenumber 1 wave, although the forcing is distributed over many wavenumbers. This changes completely in spring when higher wavenumbers are present, which results in low and high pressure systems that can hardly be detected in the winter-response. For instance in spring the low at (60° N, 120° E) is a dominant system, whereas in winter it is rather weak. The same applies for the low at (40° N, 150° W). The summer responses are very strong, with even higher wavenumbers present. The responses in fall are dominated again by wavenumber 1. In this season we find low pressure downstream of the heating at all latitudes, whereas in winter this low is flanked by a high at low and high latitudes. The same applies for the upstream high.

The large response in summer is surprising, because the strength of the observed anomalies in summer is usually weak compared to those in the other seasons. Because also the amplitudes of the normal standing eddies are small in summer, part of this discrepancy can possibly be explained by the much weaker heating in summer. The fact that the zonally averaged mean winds are weak in summer, is the

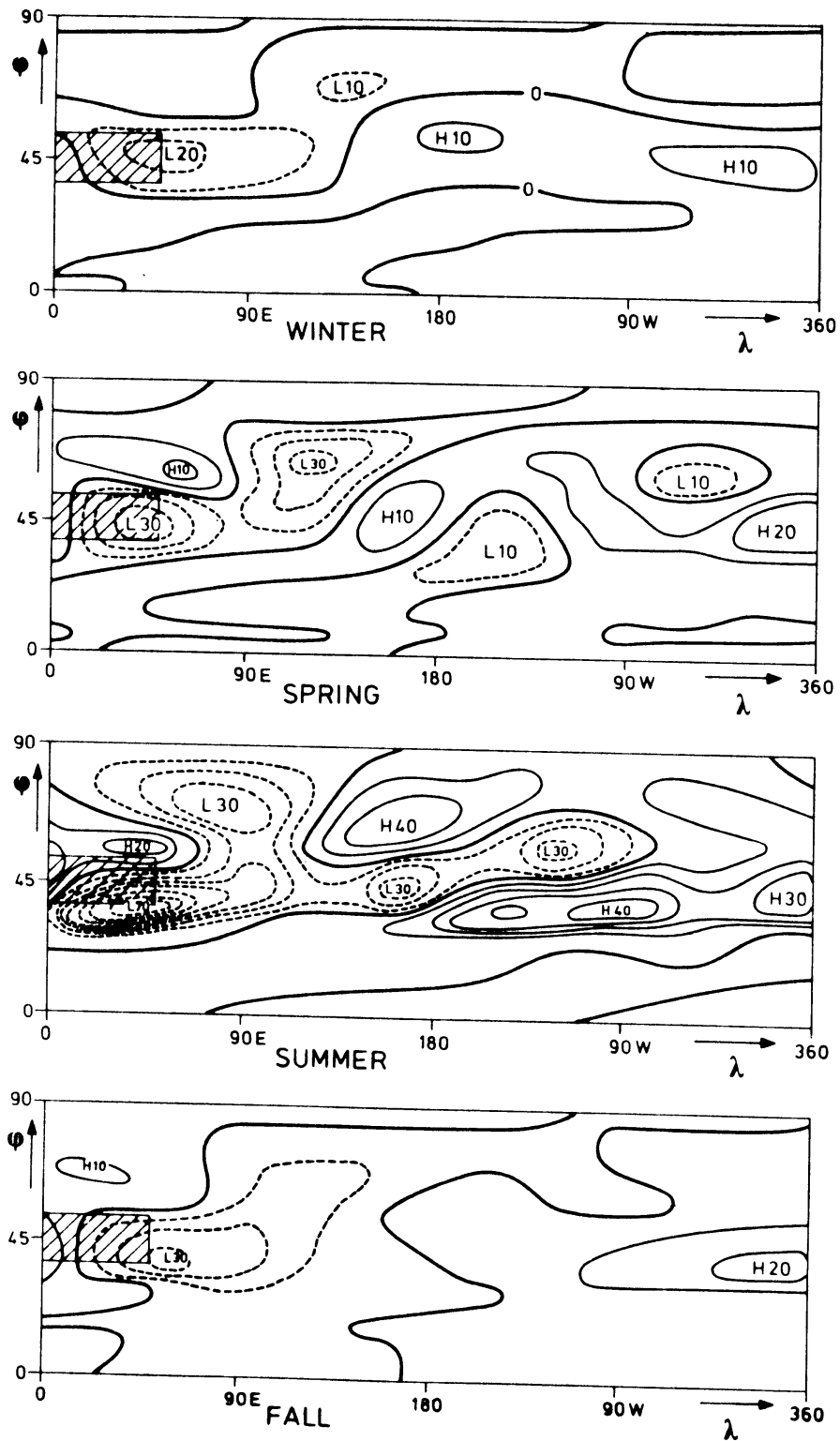


Fig. 10 : As Fig. 8, but now for a rectangular heating in the mid-latitudes.

reason that the model responses to a prescribed heating are large. However, it is likely that for large responses nonlinear processes have to be considered.

We have shown that if only a changing zonally-symmetric mean state is considered, a prescribed heating will have a different response in different seasons. Furthermore, we have shown that the region where we have to specify the heating is larger in winter than in summer. Processes that might influence the response and have not been considered here are, among other things, the interaction of the perturbation with the standing waves (which are different in each season) and the fact that the same anomaly in the surface boundary conditions will certainly cause a different atmospheric heating in different seasons.

3.6. Discussion

Linear steady-state models have proved to be useful for the description of the normal standing eddies forced by zonally-asymmetric surface conditions. Egger (1977) argued that the assumption of linearity would be even better if one is interested in the relatively small anomalies from the normal standing wave pattern in a particular month or season. We have shown that the linear steady-state response to a prescribed anomalous heating distribution is different from one season to the other and therefore we have a possibility of using such a model for the prediction of that part of the anomalies in the mean circulation that comes from persistent abnormal surface conditions.

Egger (1977) computed the linear steady-state response for an SST anomaly near Newfoundland, using January mean conditions. He found some agreement with surface pressure maps constructed by Ratcliffe and Murray (1970) from observations. The very crude approach that Egger used can be improved in many ways. The most obvious thing to do seems the incorporation of the entire geographical distribution of persistent abnormal surface conditions,

instead of one anomalous region in the Atlantic Ocean. We have shown in section V that an anomalous heating in the tropics can have significant effects on the circulation in middle and high latitudes, unless it is situated south of the zero mean wind line. This probably means that it is sufficient to deal only with anomalous forcing in the westerlies of the northern hemisphere. Apart from SST anomalies one can think of incorporating the effects of anomalous snow cover, or anomalies in sea ice conditions.

A second improvement is the use of heating schemes for the computation of atmospheric heating due to anomalies in the surface conditions, instead of prescribing the heating as we have done in this paper. Döös (1962) showed that the inclusion of atmospheric feed-back mechanisms in such a heating scheme is very important, both for the amplitude and for the phase of the resulting atmospheric pressure systems. An example of a heating scheme that is probably appropriate for this purpose is the one used by Vernekar and Chang (1978).

Other improvements, although probably difficult to accomplish, are the incorporation of the interaction of the anomalies with (i) the normal standing eddies and (ii) the mean meridional flow and the use of a friction coefficient that differs for land and sea. It would also be interesting to compute the contribution that arises from the anomalous internal forcing (caused by transients). This part of the response is considered unpredictable. In doing so, we will get an impression of the relative importance of the response produced by persistent abnormal surface conditions (signal-to-noise-ratio). It will be interesting to compare such signal-to-noise-ratio estimates with those computed in a completely different way by Madden (1976).

We have planned to develop our model along these lines and next to investigate its potential value for the prediction of anomalies in the time mean circulation. We think that this approach will lead at least to a better understanding of the statistical relations

between abnormal surface conditions and future weather, which are presently in use in weather services. These statistical rules have indeed some skill (Nap et al., 1981). If the statistical methods are replaced by a dynamical model of the kind described in this paper, the skill of long-range weather forecasts can perhaps be improved.

Acknowledgement. We thank our colleagues for the stimulating discussions we had during the course of this study. We also thank Mrs. A. Krabman for typing the manuscript. We finally thank the reviewers for their useful suggestions.

3.7. References

- Ashe, S., 1979: A nonlinear model of the time-average axially asymmetric flow induced by topography and diabatic heating. J. Atm. Sci., 36, 109-126.
- Charney, J.G., and A. Eliassen, 1949: A numerical method for predicting the perturbations of the middle latitude westerlies. Tellus, 1, 38-55.
- Davis, R.E., 1978: Predictability of sea level pressure anomalies over the North Pacific Ocean. J. Phys. Oceanogr., 8, 233-246.
- Döös, B.R., 1962: The influence of sensible heat with the earth's surface on the planetary flow. Tellus, 14, 133-147.
- Egger, J., 1976a: The linear response of a hemispheric two-level primitive equation model to forcing by topography. Mon. Wea. Rev., 104, 351-363.
- Egger, J., 1976b: On the theory of steady perturbations in the troposphere. Tellus, 28, 381-389.
- Egger, J., 1977: On the linear theory of the atmospheric response to sea surface temperature anomalies. J. Atm. Sci., 34, 603-614.
- Egger, J., 1978: On the theory of planetary standing waves: July. Beiträge zur Physik der Atmosphäre, 51, 1-14.
- Harnack, R.P., and H.E. Landsberg, 1978: Winter season temperature outlooks by objective methods. J. Geophys. Res., 83, 3601-3616.
- Horel, J.D., and J.M. Wallace, 1981: Planetary scale atmospheric phenomena associated with the interannual variability of sea-surface temperature in the Equatorial Pacific. Submitted to Mon. Wea. Rev., 109, 813-829.

- Houghton, D.D., J.E. Kutzbach, M. McClintock, and D. Suchman, 1974: Response of a general circulation model to a sea temperature perturbation. J. Atmos. Sci., 31, 857-868.
- Huang, J.C.K., 1978: Response of the NCAR general circulation model to North Pacific sea surface temperature anomalies. J. Atmos. Sci., 35, 1164-1179.
- Laprise, R., 1978: On the influence of stratospheric conditions on forced tropospheric waves in a steady-state primitive equation model. Atmosphere-ocean, 16, 300-314.
- Madden, R.A., 1976: Estimates of the natural variability of time-averaged sea-level pressure. Mon. Wea. Rev., 104, 942-952.
- Namias, J., 1978: Multiple causes of the North American abnormal winter 1976-1977. Mon. Wea. Rev., 106, 279-295.
- Nap, J.L., H.M. van den Dool, and J. Cerlemans, 1981: A verification of long range weather forecasts in the seventies. Mon. Wea. Rev., 109, 306-312.
- Oort, A.H., 1980: Global atmospheric circulation statistics, 1958-1973, NOAA professional paper, U.S. government printing office, Washington, D.C. (in preparation).
- Opsteegh, J.D., and H.M. van den Dool, 1979: A diagnostic study of the time-mean atmosphere over Northwestern Europe during winter. J. Atmos. Sci., 36, 1862-1879.
- Ratcliffe, R.A.S., and R. Murray, 1970: New lag associations between North Atlantic sea temperature and European pressure applied to long range weather forecasting. Quart. J. R. Met. Soc., 96, 226-246.
- Rowntree, P.R., 1976: Response of the atmosphere to a tropical Atlantic Ocean temperature anomaly. Quart. J. R. Met. Soc., 102, 607-625.

- Saltzman, B., 1965: On the theory of the winter average perturbations in the troposphere and stratosphere. Mon. Wea. Rev., 93, 195-211.
- Saltzman, B., 1968: Surface boundary effects on the general circulation and macroclimate: a review of the theory of the quasi-stationary perturbations in the atmosphere. Meteor. Monogr., No. 30, Amer. Meteor. Soc., 4-19.
- Sankar Rao, M., 1965: Continental elevation influence on the stationary harmonics of the atmospheric motion. Pure Appl. Geophys., 60, 141-159.
- Shutts, G.J., 1978: Quasi-geostrophic planetary wave forcing Quart. J. R. Met. Soc., 104, 331-350.
- Smagorinsky, J., 1953: The dynamical influence of large-scale heat sources and sinks on the quasi-stationary mean motions in the atmosphere. Quart. J. R. Met. Soc., 100, 342-366.
- Vernekar, A.D., and H.D. Chang, 1978: A statistical-dynamical model for stationary perturbations in the atmosphere. J. Atmos. Sci., 35, 433-444.
- Webster, P.J., 1972: Response of the tropical atmosphere to local steady forcing. Mon. Wea. Rev., 100, 518-541.

3.8. Appendix A

The model equations

Zonal momentum balance at level 1 :

$$\begin{aligned}
 & - \frac{im U \text{sn}1}{a \cos \phi} \hat{u}_{1m} + \frac{\partial U \text{sn}1}{a \partial \phi} \hat{v}_{1m} + \left(\frac{\partial U \text{sn}}{\partial p} \right)_1 \frac{\hat{\omega}_{2m}}{2} - f \hat{v}_{1m} \\
 & - \frac{im \hat{\phi}_{1m}}{a \cos \phi} - U \text{sn}1 \frac{\tan \phi}{a} \hat{v}_{1m} + K_D (\hat{u}_{1m} - \hat{u}_{3m}) = 0 . \quad (A1)
 \end{aligned}$$

Zonal momentum balance at level 3 :

$$\begin{aligned}
 & - \frac{im U \text{sn}3}{a \cos \phi} \hat{u}_{3m} + \frac{\partial U \text{sn}3}{a \partial \phi} \hat{v}_{3m} + \left(\frac{\partial U \text{sn}}{\partial p} \right)_3 \frac{\hat{\omega}_{2m}}{2} - f \hat{v}_{3m} \\
 & - \frac{im \hat{\phi}_{3m}}{a \cos \phi} - U \text{sn}3 \frac{\tan \phi}{a} \hat{v}_{3m} - K_D (\hat{u}_{1m} - \hat{u}_{3m}) + K_w \hat{u}_{3m} = 0 . \quad (A2)
 \end{aligned}$$

Meridional momentum balance at level 1 :

$$\begin{aligned}
 & - \frac{im U \text{sn}1}{a \cos \phi} \hat{v}_{1m} + f \hat{u}_{1m} \\
 & + \frac{\partial \hat{\phi}_{1m}}{a \partial \phi} + 2 U \text{sn}1 \frac{\tan \phi}{a} \hat{u}_{1m} + K_D (\hat{v}_{1m} - \hat{v}_{3m}) = 0 . \quad (A3)
 \end{aligned}$$

Meridional momentum balance at level 3 :

$$\begin{aligned}
 & - \frac{im U \text{sn}3}{a \cos \phi} \hat{v}_{3m} + f \hat{u}_{3m} \\
 & + \frac{\partial \hat{\phi}_{3m}}{a \partial \phi} + 2 U \text{sn}3 \frac{\tan \phi}{a} \hat{u}_{3m} - K_D (\hat{v}_{1m} - \hat{v}_{3m}) + K_w \hat{v}_{3m} = 0 . \quad (A4)
 \end{aligned}$$

Thermodynamic balance at level 2 :

$$\frac{im p_2 U \sin 2\phi}{2 R \Delta p a \cos \phi} (\hat{\phi}_{3m} - \hat{\phi}_{1m}) + \frac{\partial T \sin 2\phi}{a \partial \phi} \left(\frac{\hat{v}_{1m} + \hat{v}_{3m}}{2} \right) - \sigma \sin 2\phi \hat{w}_{2m} - \hat{Q}_{2m}/c_p = 0 , \quad (A5)$$

where p_2 and Δp are 600 mb and 200 mb respectively.

Continuity equation at level 1 :

$$- \frac{im \hat{u}_{1m}}{a \cos \phi} + \frac{\partial(\hat{v}_{1m} \cos \phi)}{a \cos \phi \partial \phi} - \frac{\hat{w}_{2m}}{2\Delta p} = 0 \quad (A6)$$

Continuity equation at level 3 :

$$- \frac{im \hat{u}_{3m}}{a \cos \phi} + \frac{\partial(\hat{v}_{3m} \cos \phi)}{a \cos \phi \partial \phi} + \frac{\hat{w}_{2m}}{2\Delta p} = 0 . \quad (A7)$$

These seven equations have been reduced to four by eliminating \hat{u} and \hat{w} by substitution of (A5) to (A7) in (A1) to (A4). Expressed in the real and imaginary parts of the m'th Fourier coefficients we finally have N sets of eight equations. The equations can be solved by discretization of the differential equations and inverting the matrix of the resulting system of linear equations.

3.9. Appendix B

Terms related to the convergence of the meridians

The terms related to the convergence of the meridians appear in the momentum equation as non-linear terms:

$$\begin{aligned} \frac{\partial u}{\partial t} &= \frac{u v \tan \phi}{a} + \dots , \\ \frac{\partial v}{\partial t} &= \frac{u^2 \tan \phi}{a} + \dots . \end{aligned} \tag{B1}$$

So they have to be linearized in the model:

$$\begin{aligned} \frac{\partial \hat{u}}{\partial t} &= \frac{U_{sn} \hat{v} \tan \phi}{a} + \dots , \\ \frac{\partial \hat{v}}{\partial t} &= \frac{-2 U_{sn} \hat{u} \tan \phi}{a} + \dots . \end{aligned} \tag{B2}$$

When the kinetic energy equation is formed by adding $\hat{u} \partial \hat{u} / \partial t$ and $\hat{v} \partial \hat{v} / \partial t$ it can easily be seen that (B2) leads to an extra term: $U_{sn} \hat{u} \hat{v} \frac{\tan \phi}{a}$. Hence the convergence terms may act as a source or sink of kinetic energy. This is an artificial result of the linearization that does not occur in (B1). On beforehand we do not know how serious this energetic inconsistency is for a stationary model ($\partial \hat{u} / \partial t = \partial \hat{v} / \partial t = 0$). Therefore we have performed three experiments. For the heating described in section 3 we computed the model response with (Exp. 1) and without (Exp. 2) the convergence terms, while in the third experiment (Exp. 3) we retain these terms in such a way that they do not appear anymore in the kinetic energy balance of the perturbations. This can be done by taking half the value of the convergence term in the meridional momentum balance and leaving the term in the zonal momentum balance unaffected.

The differences in the results of the three experiments are very small for the higher wavenumbers. However, for the lower wavenumbers the differences are significant, especially in high

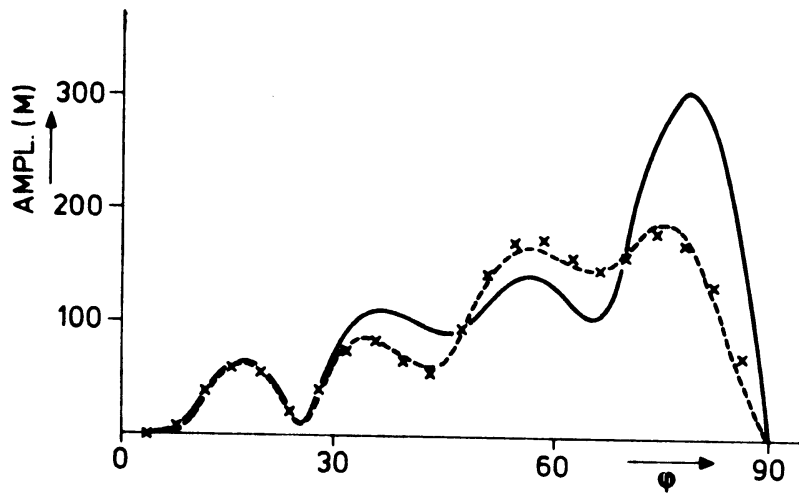


Fig. B1 : Amplitude of the geopotential at 400 mb as a function of latitude. The heating is sinusoidal in longitudinal direction ($m = 1$) and uniform with latitude. Three experiments can be distinguished: (1) convergence terms included, solid line; (2) convergence terms dropped, crosses, and (3) modified convergence terms, dashed line.

latitudes. The amplitudes of the geopotential height for Exp. 1 are very large at high latitudes compared to Exp. 2 and 3. This can be seen in Fig. B1 for wavenumber 1. The figure shows the amplitude of the geopotential height at 400 mb as a function of latitude. The results for Exp. 3 hardly differ from those obtained with Exp. 2, whereas the amplitudes of the response for Exp. 1 are much larger. Apparently, they only have large effects in polar regions when they appear artificially in the perturbation kinetic energy balance. We conclude that it is better to drop these terms altogether.

IV. On the Importance of the Hadley and Ferrel circulation
for Teleconnections forced by Low-Latitude Heat Sources.

J.D. Opsteegh.

ABSTRACT

The influence of the Hadley and Ferrel circulation on teleconnection patterns forced by heating in low latitudes is investigated with a linear model for stationary waves. The model is linearized around the observed zonally averaged January mean state. This prescribed mean state includes the mean meridional circulation (MMC). The influence of the cells is investigated by comparing the behavior of the model with a model that is identical but does not include the MMC in the zonal mean state.

First simulations have been performed with a hemispheric model. For a local heat source, placed completely in the easterlies, large differences are found between simulations with and without the MMC. Without MMC the remote response at middle and high latitudes is almost zero. With MMC a mid-latitude teleconnection pattern shows up. The sensitivity of this pattern for the strength of the easterlies is investigated. It is found that with increasing strength of the easterlies the mid-latitude response is damped dependent on the particular zonal wavenumber. This scale selective damping causes a shift in the response towards lower zonal wavenumbers.

Next a heat source is considered that reaches approximately to the zero wind line at the lower level of the model. Simulations with and without MMC give a remote response, but the results show large differences.

In a third tropical forcing experiment a large part of the heat source is in the westerlies. The resulting geopotential height patterns are very similar. The only difference is that the amplitude of the remote response is damped by the MMC. The geopotential height response is in good agreement with observed tropically forced teleconnection patterns, in contrast with the results of the first two experiments.

The results of forcing with a subtropical heat source also show some damping of the amplitude by the MMC. But the phase of the waves is not significantly affected.

The influence of the MMC on the ability of stationary waves to propagate wave energy through a region of easterlies from one hemisphere to the other is investigated with a global version of the model.

Without MMC no cross equatorial propagation of the waves occurs but with MMC a remote response in the other hemisphere shows up, especially in zonal wavenumber 1. A heat source in the southern hemisphere (SH), which is the summer hemisphere, gives a large response in the northern hemisphere (NH) and a significant reduction in the high latitude response of the SH. Forcing in the NH only shows a small response in the SH and a minor damping in the NH.

A dispersion relation is derived for barotropic Rossby waves embedded in a mean flow which has a zonal as well as a meridional component. From the dispersion relation it is shown that free stationary Rossby wave solutions exist, which are perturbations of an easterly mean flow. These waves have a very long wavelength in zonal direction and a short wavelength in meridional direction. The meridional component of the group velocity has the same sign as the meridional wind of the Hadley cell. This means that energy can be transported in only one direction. In the northern-hemisphere winter wave energy is transported from SH to NH in the upper troposphere and from NH to SH in the lower troposphere. As the strength and width of the easterlies decreases with height, cross equatorial propagation from SH to NH is much easier than vice versa.

The one way filtering activity of the Hadley cell may provide part of the explanation for the fact that tropically forced teleconnection patterns are so easily found in the NH winter, but less so in the NH summer.

4.1. Introduction

In Opsteegh and van den Dool (1980), hereafter referred to as OD, the effects of anomalous diabatic heating on stationary planetary waves were studied with a two-level steady-state primitive equation model. This model was linearized around a prescribed zonally averaged basic state. The assumption that the linear part of the advection dominates the nonlinear part has been used by several authors, studying the observed normal standing wave pattern. It has been justified from observations, at least for the upper part of the troposphere, by Lau (1979). Egger (1977) argued that the assumption of linearity is even more true for relatively small amplitude planetary waves resulting from anomalies in the surface conditions of the earth.

In OD the sensitivity of the solutions to the basic state was studied for a local heat source in the middle latitudes and in the tropics. For the basic state we used observed seasonal mean data. It was shown that the response is sensitive to differences in the zonal mean conditions when the heat source is in the middle latitudes.

For a tropical heat source the results are much less sensitive, provided that part of the heat source is in the westerlies. The mid-latitude response to this tropical heating is significant, except for the summer season when the heating is completely in the easterlies. It was shown in OD that only the longest waves propagate into middle and high latitudes. High wavenumbers are trapped in the subtropics. The remote response has an almost equivalent barotropic structure with weakly increasing amplitude in geopotential height towards the north. A comparison of the resulting hemispheric wave pattern with observational evidence for the existence of teleconnections due to tropical forcing (Horel and Wallace 1981) shows surprisingly good agreement. The meridional propagation of Rossby waves has been demonstrated before by Grose and Hoskins (1979) with a barotropic model. In Hoskins and Karoly (1981) it is shown that wave energy is transported approximately along great circle routes.

Considering the importance of heat sources in the tropics on the pressure pattern in middle latitudes it is interesting to study whether or not the remote response is still present (or stronger) if the zonally averaged state is replaced by a more realistic basic state. In this paper we enrich the zonally averaged state, used before, with mean meridional cells (MMC). Neglecting this circulation may be a good approximation in the strong westerlies at middle latitudes, but this is much less evident in the weak easterlies of tropical regions. Especially the influence of zero wind lines in OD makes it interesting to study the effect of the MMC on tropically forced teleconnection patterns.

In Egger's (1977 anomaly experiments the MMC was included. However, he does not discuss the sensitivity of his results to this circulation. In the present study the importance of the mean meridional cells is investigated with a hemispheric and a global model. Runs with a model with MMC will be compared with an identical model that does not include the MMC. We are especially interested whether the remote response to forcing in the tropics is affected by the

MMC and in the ability of the stationary waves to propagate wave energy from one hemisphere to the other through a region of easterlies in the presence of the MMC.

4.2. Description of the model

For a detailed description of the model the reader is referred to OD but for reason of convenience the important features will be repeated here.

The model is formulated in the primitive equations on the sphere with pressure as vertical coordinate. It has two levels in the vertical. The momentum equations and the continuity equation are applied at 400 and 800 mb, while the thermodynamic equation is applied at 600 mb. The hydrostatic approximation and equation of state close the system.

The upper and lower boundaries are 200 and 1000 mb, where we use the condition of vanishing vertical velocities.

We drop the tendency terms and solve for stationary waves excited by thermal forcing. The equations are linearized around a zonally averaged basic state. The model's zonally averaged basic state depends on latitude and height according to observations. We now have a set of stationary linear perturbation equations for asymmetrical components of the circulation.

The variables are expanded in Fourier series along a latitude circle. This leads to sets of equations in terms of Fourier coefficients which can be solved for each of the zonal waves independently. The response of the first five zonal wavenumbers is computed in this study. Higher wavenumbers only give a very small contribution to the geopotential height response (see fig. 3 in OD).

In meridional direction a gridpoint representation is used with 23 gridpoints between Equator and Northpole. The boundary conditions are:

$$\hat{\phi} = 0 \quad \text{at} \quad \phi = \pm \Pi/2.$$

For the hemispheric model we need a boundary condition at the equator. Here we chose a symmetry condition:

$$\hat{v} = 0 \quad \text{at} \quad \phi = 0.$$

At the lower level of the model (800 mb) Rayleigh friction is applied. In the global model the damping coefficient is constant and has a value of $2 \times 10^{-6} \text{ s}^{-1}$. In the hemispheric model the damping coefficient is inversely proportional to the strength of the zonal mean wind. This is done to simulate singular line dissipation (Simmons 1981). In the zonal momentum equation at 800 mb (level 3) this leads to the following expression for the friction term:

$$\hat{F}_{wx_3} = - \frac{K_w}{|U_{sn}(\phi)|} \cdot \hat{u}_3(\phi) \quad (1)$$

The value K_w is such that in the jet maximum K_w/U_{sn} has a value of $1 \cdot 10^{-6} \text{ sec}^{-1}$. Experiments performed to test what difference it makes to include a variable damping coefficient do not show a high sensitivity of the solutions to this change in the description of the damping.

In OD the terms describing the influence of the MMC on the planetary waves were not taken into account. This process is described by adding the following terms in the equations:

1. Zonal momentum equation

$$v_{sn} \frac{\partial \hat{u}}{a \partial \phi} + \omega_{sn} \frac{\partial \hat{u}}{\partial p} \quad (2)$$

2. Meridional momentum equation

$$v_{sn} \frac{\partial \hat{v}}{a \partial \phi} + \hat{v} \frac{\partial v_{sn}}{a \partial \phi} + \omega_{sn} \frac{\partial \hat{v}}{\partial p} + \hat{\omega} \frac{\partial v_{sn}}{\partial p} \quad (3)$$

3. Thermodynamic equation

Here no terms are added, because this equation is applied at 600 mb where the mean meridional circulation is assumed to be negligible. The subscript sn is used for the parameters describing the zonally averaged basic state.

In order to be able to express the term $\frac{\partial \hat{u}}{\partial p}$ in the model variables \hat{u}_1 and \hat{u}_3 (1 = 400 mb, 3 = 800 mb), it is assumed that \hat{u} increases linearly with height so that $\frac{\partial \hat{u}}{\partial p}$ is constant and the same expression can be used in the zonal momentum balance at levels 1 and 3. We use:

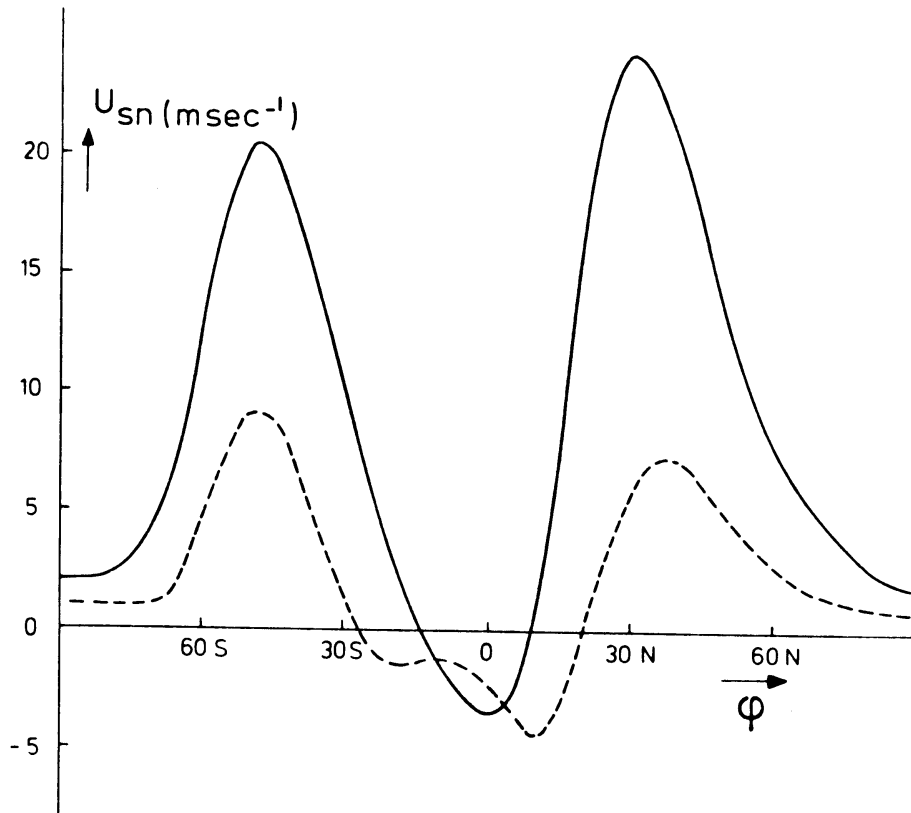


Fig. 1 : The January mean zonally averaged wind at 400 mb (solid line) and at 800 mb (dashed line) as a function of latitude.

$$\frac{\partial \hat{u}}{\partial p} = \frac{\hat{u}_3 - \hat{u}_1}{2\Delta p} \quad (4)$$

The same procedure is followed for $\frac{\partial \hat{v}}{\partial p}$.

Finally $\hat{\omega}$ at level 1 and 3 is expressed in $\hat{\omega}_2$ as follows:

$$\hat{\omega}_1 = \hat{\omega}_3 = \frac{\hat{\omega}_2}{2} \quad (5)$$

4.3. Description of the zonally averaged mean state

For the basic state, observed January mean conditions of zonal and meridional wind, temperatures and static stability are used. These data were kindly supplied by Dr. A.H. Oort. It is the mean state for the years 1969-1973. Fig. 1 shows the zonal wind at 400 and 800 mb as a function of latitude. In the hemispheric model the NH part of the zonal mean state is used.

As the model has only two levels, continuity considerations demand that the mean meridional wind at 400 mb has equal strength and is opposite to the mean wind at 800 mb. Fig. 2 shows v_{sn} and ω_{sn} at 400 mb. The vertical velocities of the MMC are computed from v_{sn} as follows:

$$\omega_{sn_1} = \omega_{sn_3} = - \Delta p \cdot \frac{\partial v_{sn_1}}{a \partial \phi} \quad (6)$$

In the hemispheric model symmetric boundary conditions are used at the equator. Using these conditions implies that the MMC has to be symmetric too. This was achieved by shifting the January Hadley cell to the north, such that the mean meridional wind is zero at the equator. Fig. 3 shows the profiles for v_{sn} and ω_{sn} at 400 mb, used in the hemispheric model.

4.4. Experiments with the hemispheric model

I will start the numerical simulations with a heating which is completely located in the easterlies. The heat source covers a region from 4N to the equator and in longitudinal direction from 157.5E to 157.5W (45°). The heating rate in this area is 1 Kday⁻¹.

Fig. 4 shows the geopotential height response at 400 mb with and without MMC. The remote response in the experiment without MMC is negligible, but when the MMC is included a teleconnection pattern shows up. The wave train is similar in structure to the results of

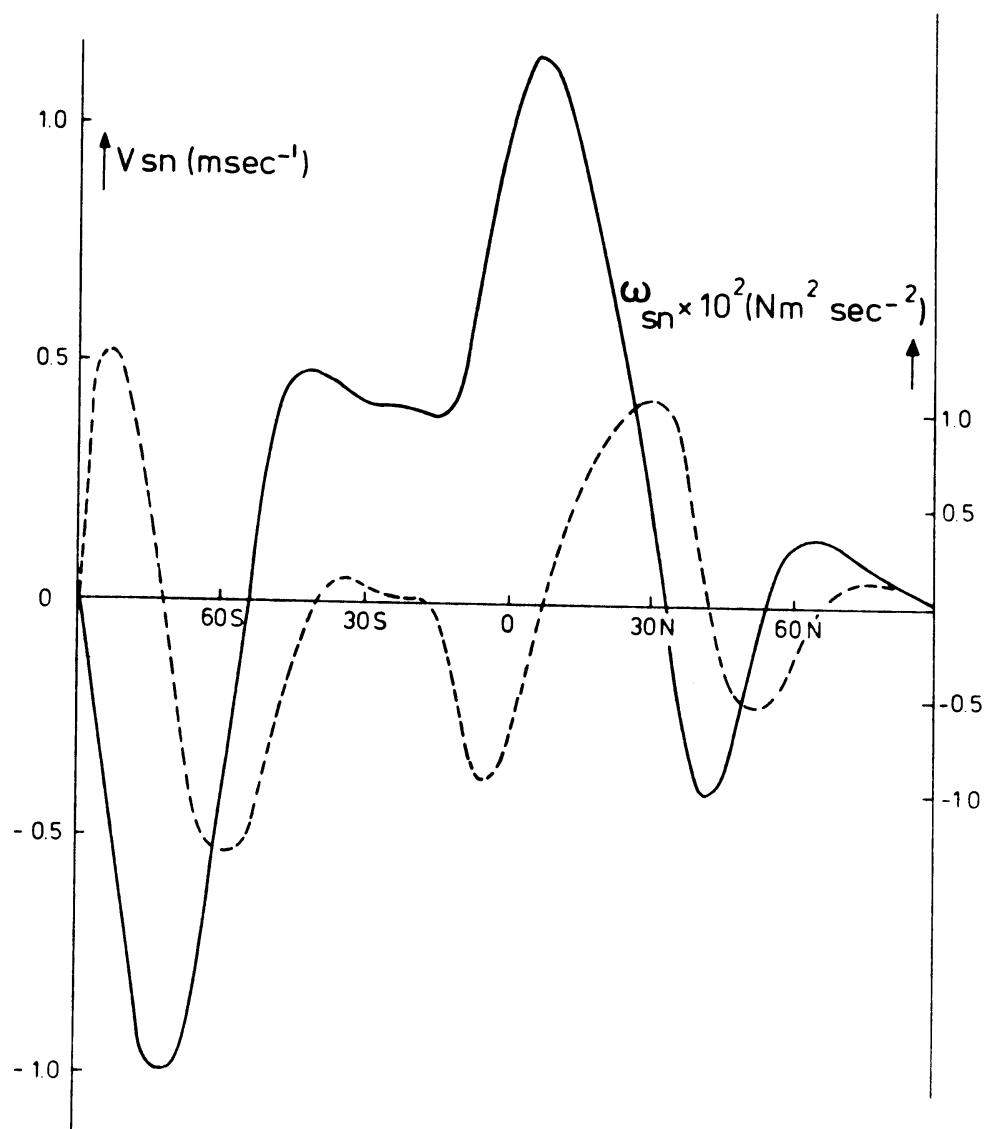


Fig. 2 : January mean zonally averaged meridional circulation. The solid line gives the meridional wind at 400 mb. The vertical circulation at 400 and 800 mb is given by the dashed line.

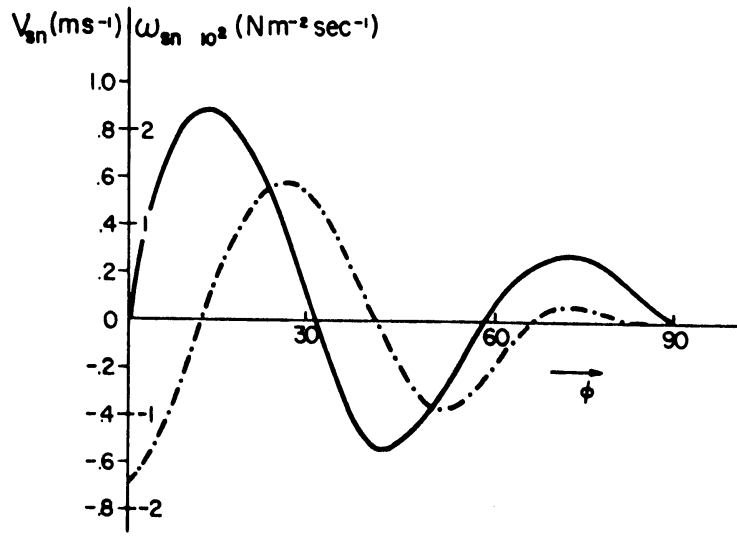


Fig. 3 : Idealized January mean zonally averaged meridional circulation used in the hemispheric model. The solid line gives the meridional wind at 400 mb. The vertical circulation at 400 and 800 mb is given by the dashed dotted line.

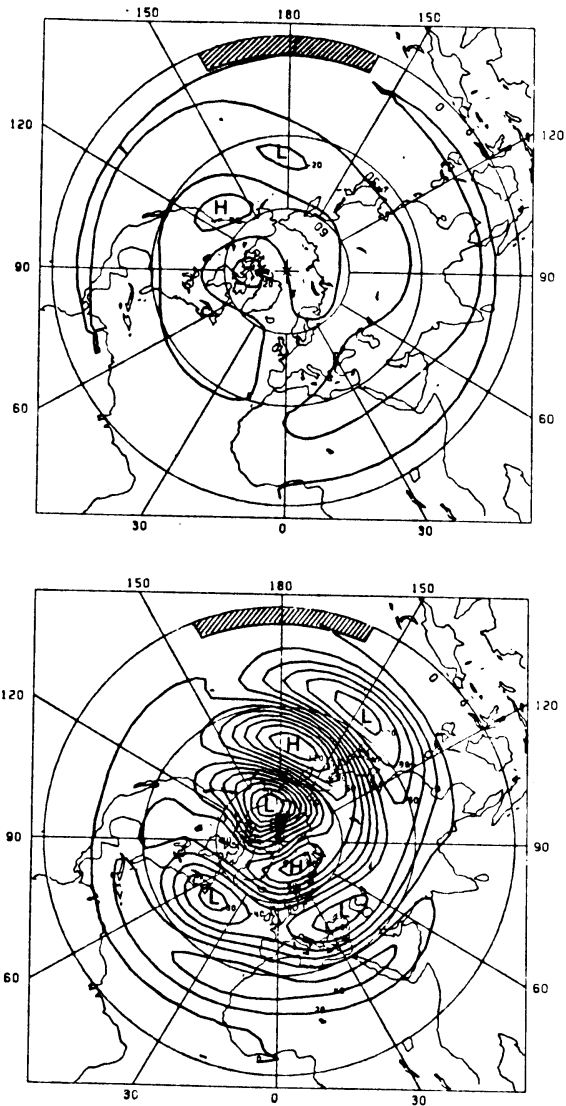


Fig. 4 : Geopotential height response, at 400 mb to a tropical heat source. The heat source extends from the equator to 5°N. The top figure gives the results without inclusion of the mean meridional circulation (MMC) in the basic state. The lower figure shows the response when the MMC is included. Contour interval is 20 m² sec⁻².

experiments with (sub)tropical heating in earlier papers (OD, Webster 1981, Hoskins and Karoly 1981) but the amplitudes are smaller and the phase is almost opposite.

The dependence of this response on the strength of the easterlies is investigated by adjusting the prescribed zonally-symmetric zonal winds. Fig. 5 shows the normal January zonal winds (solid line) and the adjusted profiles. The only change in the profiles is the strength of the easterlies. The solid line in fig. 6 shows the amplitude of the geopotential height response in zonal wavenumber 1, 2 and 3 as a function of latitude for the experiment with normal zonal winds. The response in wavenumber one dominates over higher wavenumbers. The dashed line shows the same amplitudes for the experiment with adjusted zonal wind profile. The response in all wavenumbers is smaller than in the experiment with normal zonal wind conditions and is strongly dominated by zonal wavenumber 1. The reduction in the amplitude of wavenumber 1 is less than 2. In wavenumbers 2 and 3 the reduction is 4 and 10 respectively.

I will next discuss the results of another experiment with a local tropical heat source. This heating has a latitudinal extent from the equator to the zero wind line at the upper level of the model (approximately 8N). In longitudinal direction the heat source covers the same area as in the previous tropical forcing experiment. The heating rate is also the same. Fig. 7 shows the geopotential height response at 400 mb for the experiments with and without MMC. In contrast with the previous tropical forcing experiment a mid-latitude wave pattern shows up in both cases. The amplitude of the various pressure systems is much weaker for the experiment with MMC and the phase is quite different.

The impact of the MMC on the zonal wind is shown in fig. 8. The figure shows the zonal wind at 400 mb with and without MMC. In both experiments the circulation is thermally direct over the heating, namely zonal inflow at 800 mb (not shown) and zonal outflow at 400 mb. The vertical circulation is upward over the heating area and downward at every other longitude. Inclusion of the MMC causes a weakening of this circulation. In the experiment without MMC we find a region of

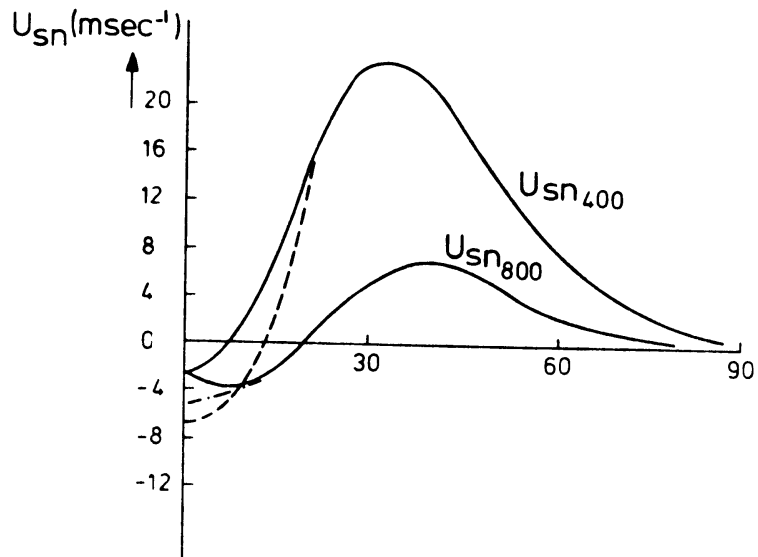


Fig. 5 : Normal (solid line) and adjusted (dashed and dashed-dotted line) zonal wind profiles at 400 and 800 mb.

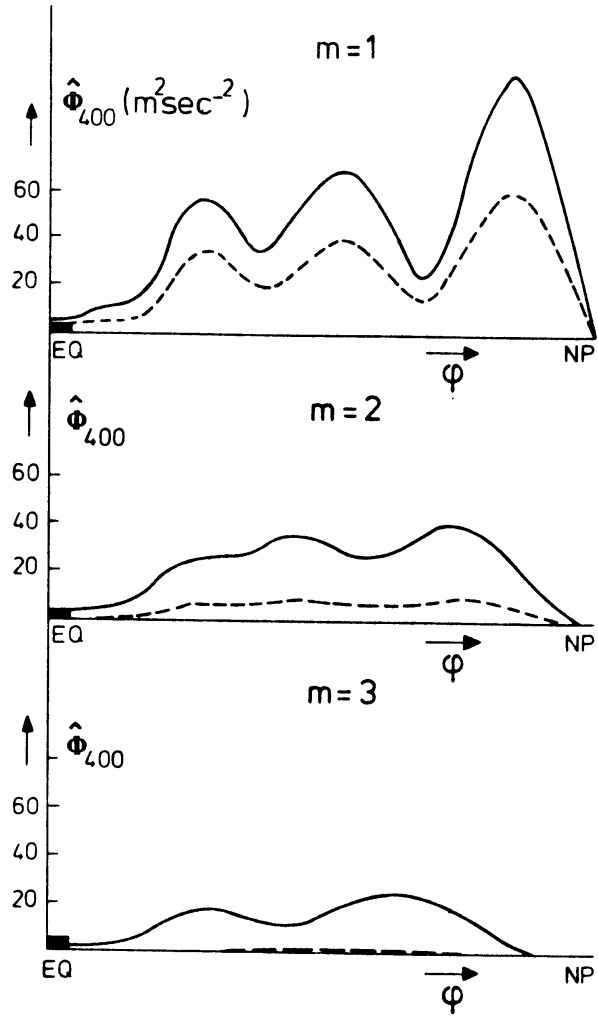


Fig. 6 : Amplitude of the response in geopotential height at 400 mb for wavenumber 1, 2 and 3 to tropical heating (0-5 N). The MMC is included in the mean state (solid line). The dashed line shows the same for the experiment with increased strength of the easterlies.

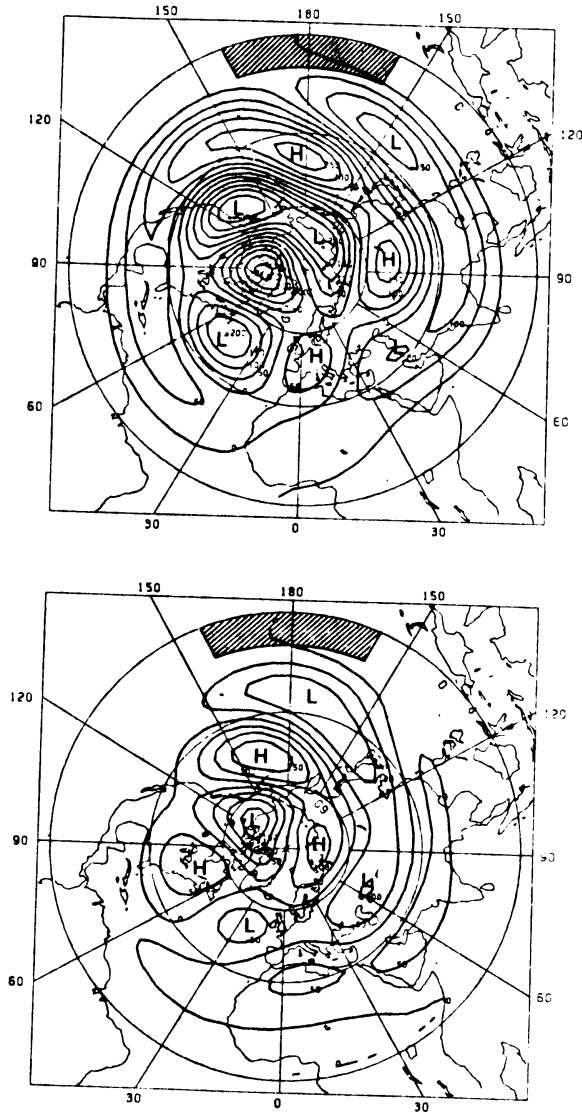


Fig. 7 : As fig. 4 for the geopotential height response to tropical forcing (0-8 N). Contour interval is $50 \text{ m}^2 \text{ sec}^{-2}$.

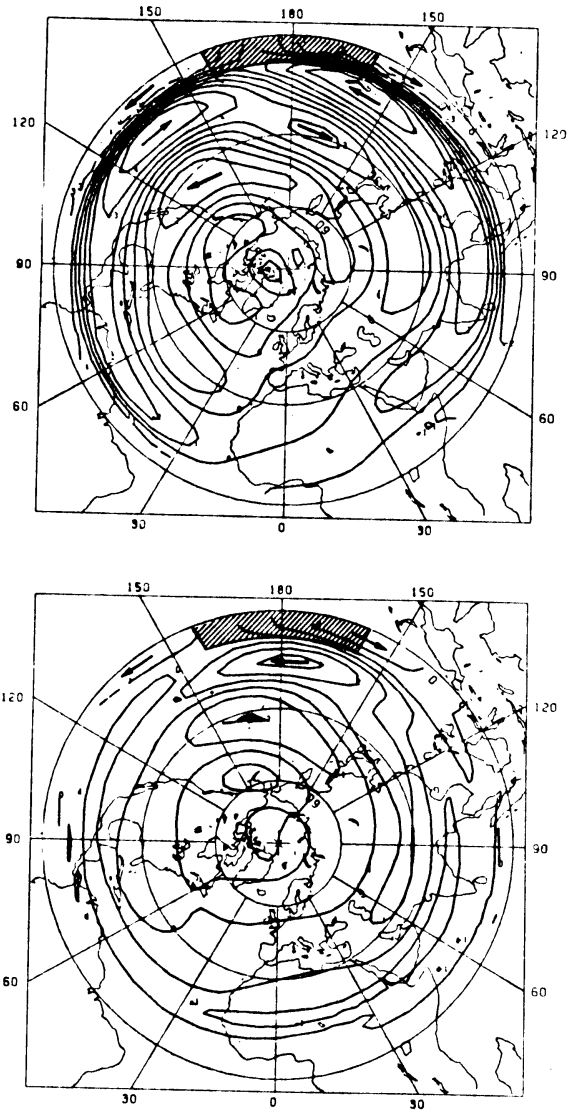


Fig. 8 : As fig. 4 for the zonal wind response to tropical forcing (0-8 N). Contour interval is 1 msec^{-1} .

westerlies north-west of the heating and easterlies north-east of the heating. With MMC the westerlies shift to the longitudes of the heating and weaken. The region of easterlies has almost disappeared.

The response of geopotential height at 400 mb for an experiment for which a substantial part of the heat source in the westerlies is shown in fig. 9. The heating area extends from the equator to almost 20 N. The longitudinal position and heating rate are again the same as in the previous experiments. In contrast with the first two experiments, inclusion of the MMC has only a marginal effect. The only significant difference is the weaker amplitude of the teleconnection pattern in the experiment with MMC. The phase of the waves does not change. Another contrast with the results of the first two experiments is that the results of the present experiment show good agreement with observed teleconnection patterns (Horel and Wallace 1981). It must be concluded that the response is dominated by the part of the heating which is located in the weak westerlies and that the influence of the MMC on that part of the total response is small.

A subtropical heat source is located between 16°N and 40°N. It has the same longitudinal position as the tropical heating. The heating rate is again 1 Kday^{-1} .

The zonal wind distribution at 400 mb of the experiment without MMC is shown in fig. 10. In contrast with the tropical experiment zonal inflow over the heating is observed at 400 mb together with strong upward motion. The compensating divergence comes from the meridional wind. South of the heat source a very strong easterly jet shows up, whereas at 60 degrees to the east of this jet strong westerly winds can be observed. These strong tropical winds are completely different from an overturning Walker circulation. The vertical circulation connected with these winds is small. The almost horizontal flow is geostrophically connected to the pressure pattern. The fact that it is so easy to excite a strong jet in the tropics with weak persistent subtropical forcing is an indication that diabatic processes in the subtropics are very important for the existence of tropical jets and the associated tropical wave phenomena. As this is not the subject of the present study I will not elaborate on this interesting part of the response.

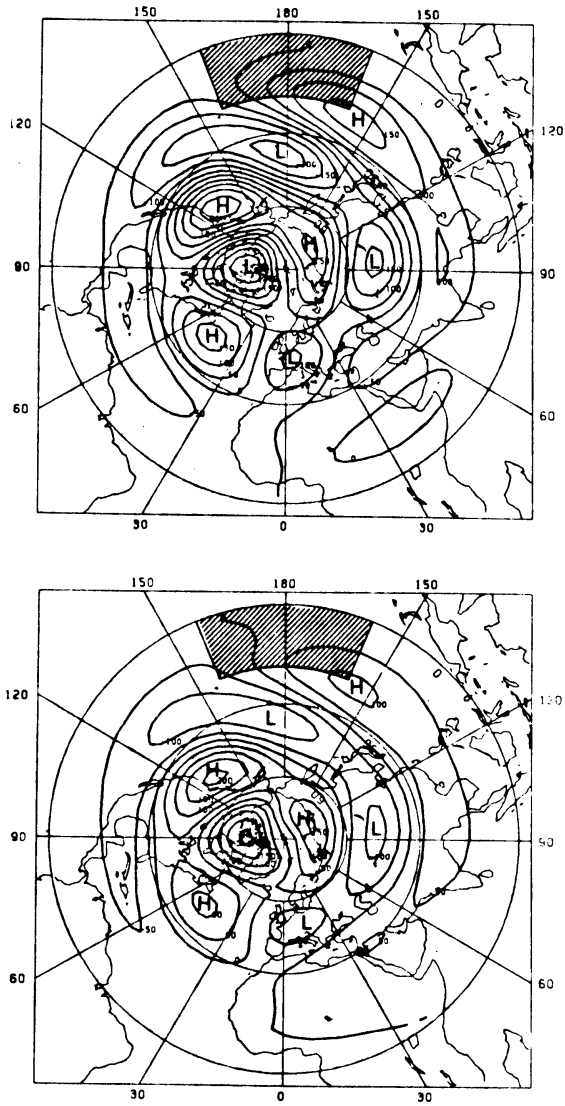


Fig. 9 : As fig. 4 for the geopotential height response to tropical forcing (0-20 N). Contour interval is $50 \text{ m}^2 \text{ sec}^{-2}$.

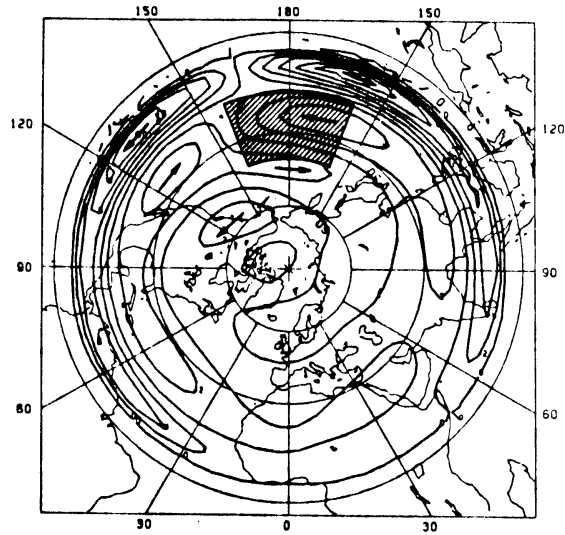


Fig. 10 : Zonal wind response at 400 mb to subtropical forcing without MMC in the basic state. Contour interval is 2 msec⁻¹.

Fig. 11 shows the geopotential height response at 400 mb for both experiments. The only significant differences away from the heat source is the reduction in amplitude when the MMC is included. This was also found in the experiment with tropical forcing in the weak westerlies.

The results of the hemispheric model show that the MMC is only of importance for the teleconnection patterns resulting from diabatic heat forcing in the tropical easterlies. If the forcing is in the westerlies the response is relatively insensitive to the MMC.

4.5. Cross equatorial propagation

The influence of the MMC on the ability of stationary Rossby waves to propagate through a region of easterlies is investigated with the global model. As was pointed out in section 3, the Hadley circulation in the global model version is much more in agreement with the observations as in the hemispheric model.

The amplitude of the response in geopotential height for wavenumbers 1 and 2 to a local heat source in the subtropics of the SH is shown in fig. 12. The solid line is with and the dashed line without inclusion of the MMC in the zonally-symmetric state. The latitudinal extent of the heat source is indicated in the figure. In longitudinal direction it covers 45 degrees. The exact position is unimportant. The heating rate is 1 K day^{-1} . When the MMC is neglected the response in both wave numbers is restricted to the SH, but with Hadley circulation a remote response in the NH shows up, especially in wavenumber 1. The high latitude response in the SH is much weaker when the MMC is included, both for wavenumbers 1 and 2. From these results we may conclude that the Hadley circulation has an important role to play in the spherical response to local heat sources, especially with regards to the exchange of wave energy between both hemispheres. This mechanism is only of importance for very long waves. A second mechanism for cross equatorial propagation of wave energy is the existence of local westerlies at the equator (Webster 1981, Simmons 1981). Simmons (1981) also showed the importance of transients with respect to cross equatorial propagation of stationary Rossby waves.

The main conclusion drawn from experiments with the hemispheric model is that the MMC is only important for the response to forcing in the easterlies. The response to forcing in the westerlies of the NH appears

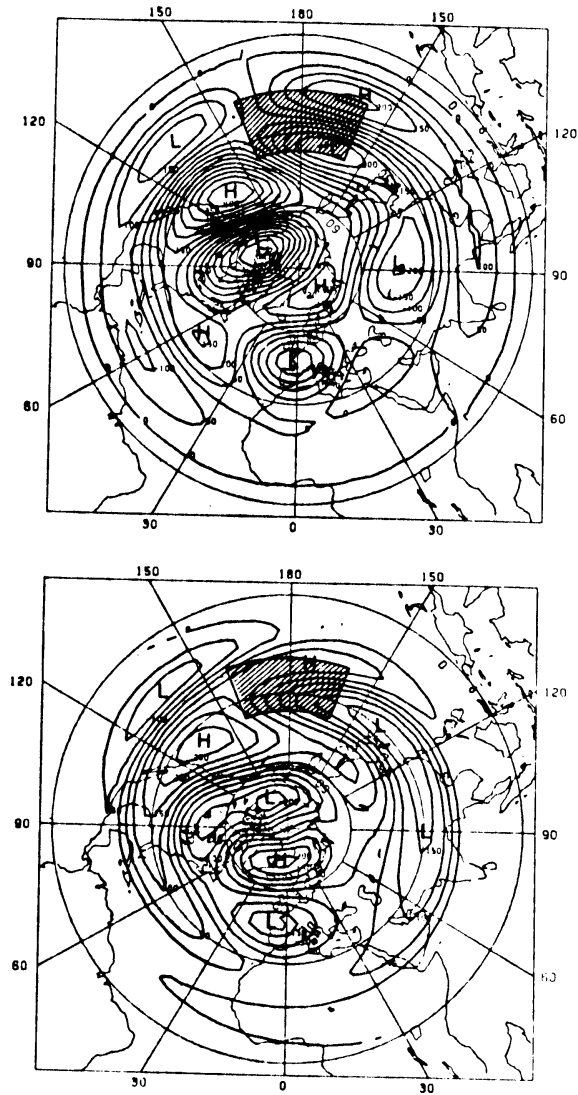


Fig. 11 : As fig. 4 for the geopotential height response to subtropical forcing (16 N-40 N). Contour interval is 50 m²sec⁻².

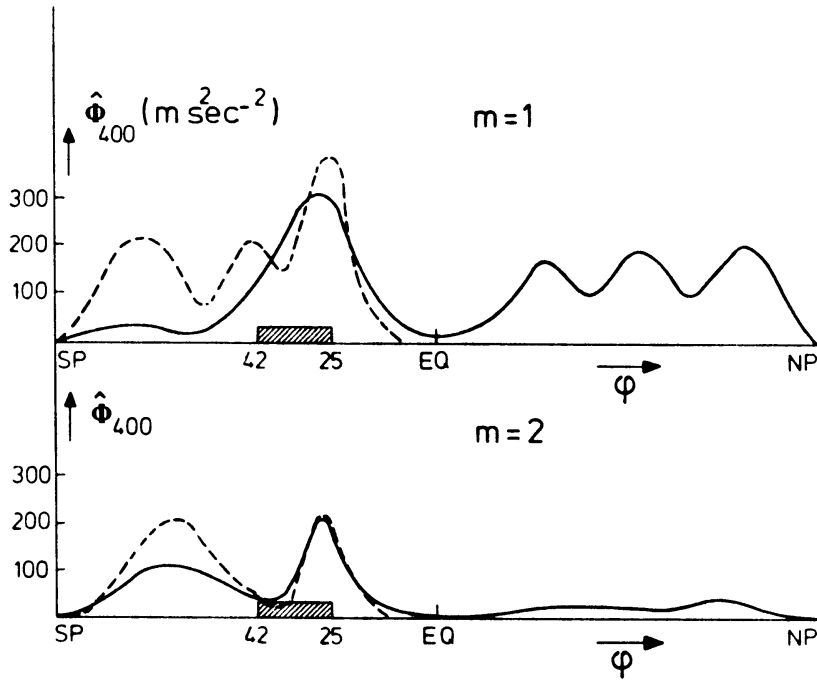


Fig. 12 : Amplitude of the geopotential height response in wavenumbers 1 and 2 at 400 mb to subtropical forcing in the southern hemisphere with (solid line) and without (dashed line) MMC.

to be insensitive for the MMC. Results with the global model indicate that subtropical forcing in the SH not only generates a wavepattern in the NH but also drastically reduces the response at high latitudes of the "forced" hemisphere.

In order to investigate the apparent discrepancy between the results of the hemispheric and the global model the experiment with the global model is repeated with the same subtropical forcing placed in the NH. Fig. 13 shows the amplitude as a function of latitude of the geopotential height response in wavenumber 1 and 2 at 400 mb. It is clear that the differences are much less dramatic. The cross equatorial propagation is small and the differences in the NH are also small, which is in agreement with the results of the hemispheric model.

For these experiments we have used the NH winter Hadley circulation. From the results we get the impression that the direction of the Hadley cell is somehow important for the transport of wave energy to another hemisphere and for the associated reduction in amplitude of the teleconnection pattern in the "forced" hemisphere.

We will elaborate on these results a little more in the next section.

4.6. Some simple arguments and concluding remarks

In order to get some understanding of the results of the numerical simulations, some simple arguments will be put forward on the properties of linear barotropic perturbations embedded in a mean flow which has a meridional component. The vorticity equation for this case is:

$$\frac{\partial \hat{\zeta}}{\partial t} + U_n \frac{\partial \hat{\zeta}}{\partial x} + V_n \frac{\partial \hat{\zeta}}{\partial y} + \beta \hat{v} = 0 \quad (7)$$

U_n and V_n are the zonal and meridional components of the basic flow. $\hat{\zeta}$ and \hat{v} are relative vorticity and meridional velocity associated with the perturbations. $\hat{\zeta}$ and \hat{v} can be expressed in a streamfunction $\hat{\Psi}$ as follows:

$$\begin{aligned} \hat{\zeta} &= \nabla^2 \hat{\Psi} \\ \hat{v} &= \frac{\partial \hat{\Psi}}{\partial x} \end{aligned}$$

Looking for wavelike solutions for $\hat{\Psi}$ of the form:

$$\hat{\Psi} = A e^{i(mx + ny - vt)} \quad (8)$$

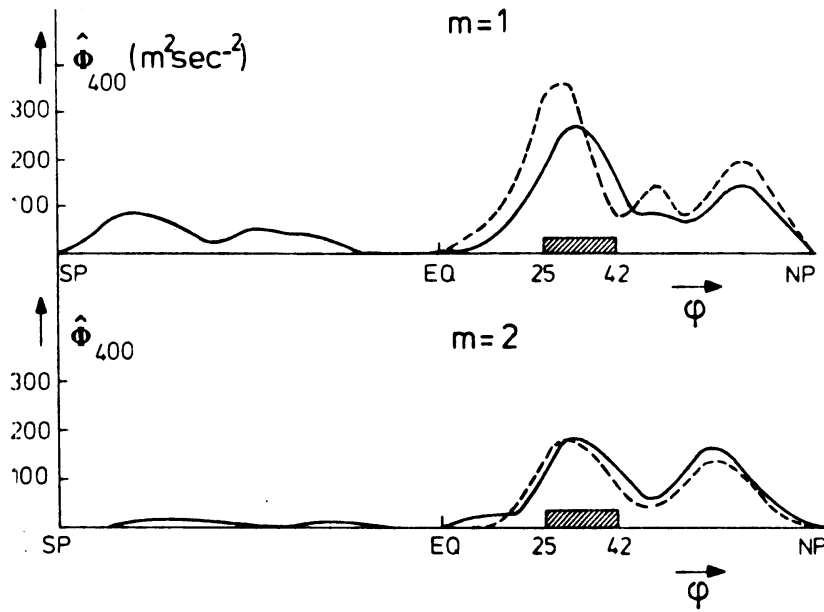


Fig. 13 : Amplitude of the geopotential height response in wavenumbers 1 and 2 at 400 mb to subtropical forcing in the northern hemisphere with (solid line) and without (dashed line) MMC.

leads to the following relation for the frequency ν :

$$\nu = U_n m + V_n n - \beta \frac{m}{K^2} \quad (9)$$

with

$$K^2 = m^2 + n^2.$$

For particular values of U_n the wave (m,n) becomes stationary. This value depends on V_n , m and n as follows:

$$U_{ns} = \frac{\beta}{K^2} - V_n \left(\frac{n}{m}\right) \quad (10)$$

It is easy to see from (9) that with zero meridional velocity U_{ns} must be positive for all waves. However, if V_n is nonzero Rossby wave solutions do exist which are stationary perturbations of an easterly mean flow. To illustrate this I have computed U_{ns} for various combinations of zonal and meridional wavenumbers. For V_n a value of 1 msec^{-1} is assumed, while for β a low latitude value (at 5 degrees) is used. m and n satisfy the following relations:

$$m = \frac{2\pi}{D} m^*$$

$$n = \frac{2\pi}{D} n^*$$

D is the scale of the motion. It's value is taken 10,000 km. The wavenumbers m and n run from 1 to 10. The results for U_{ns} are given in table 1. For small values of n^* U_{ns} is always positive independent of the value for m^* . For large values of n^* stationary Rossby wave solutions exist in the presence of a negative value for U_{ns} . For large values of m^* , U_{ns} is only marginally negative, but for small values of the zonal wavenumber U_{ns} has negative values which are approximately in agreement with the observed strength of the tropical easterlies.

The results of table 1 are in agreement with our findings that the ability of stationary Rossby waves to propagate wave energy through a region with easterlies is restricted to very low zonal wavenumbers and even more so when the strength of the easterlies increases (see fig. 6).

The direction of the energy flow is computed from the groupvelocity of the stationary wave.

Table 1: U_{ns} as a function of zonal wavenumber m^* and meridional wavenumber n^* . $V_{ns} = 1 \text{ m sec}^{-1}$. The value for β is computed at 5 N.

$m^* \backslash n^*$	1	2	3	4	5	6	7	8	9	10
1	27.8	9.5	2.8	-0.6	-2.8	-4.4	-5.8	-7.1	-8.3	-9.4
2	11.0	6.2	2.9	0.9	-0.5	-1.6	-2.4	-3.2	-3.8	-4.4
3	5.4	3.8	2.2	1.0	0.0	-0.7	-1.3	-1.9	-2.4	-2.8
4	3.1	2.4	1.6	0.8	0.2	-0.4	-0.9	-1.3	-1.7	-2.0
5	2.0	1.6	1.1	0.6	0.2	-0.3	-0.6	-1.0	-1.3	-1.5
6	1.4	1.1	0.8	0.4	0.1	-0.2	-0.5	-0.8	-1.0	-1.2
7	1.0	0.8	0.6	0.3	0.1	-0.2	-0.4	-0.6	-0.8	-1.0
8	0.8	0.6	0.4	0.2	0.0	-0.2	-0.4	-0.5	-0.7	-0.9
9	0.6	0.5	0.3	0.1	-0.0	-0.2	-0.3	-0.5	-0.6	-0.8
10	0.5	0.4	0.2	0.1	-0.0	-0.2	-0.3	-0.4	-0.6	-0.7

$$C_{gx} = \left(\frac{\partial v}{\partial x} \right)_{v=0} = -V_n \frac{n}{m} + \frac{2\beta m^2}{(K^2)^2} \quad (11)$$

$$C_{gy} = \left(\frac{\partial v}{\partial y} \right)_{v=0} = -V_n + \frac{2\beta mn}{(K^2)^2} .$$

with

$$K^2 = m^2 + n^2 = \frac{\beta m}{U_n m + V_n n}$$

In order for a stationary Rossby wave to exist, K^2 must be positive. If m is taken positive and U_n is negative then the product of V_n and n must be positive. So V_n and n must have equal sign. The direction of the energy flow in meridional direction is given by C_{gy} . From (11) it is clear now that C_{gy} and V_n must have equal sign.

The energy can thus only be transported in the direction of V_n . In the Hadley cell of the NH winter V_n is positive in the upper part of the troposphere and negative in the lower part. So wave energy is transported from SH to NH in the upper troposphere and from NH to SH in the lower part.

As the strength and width of the easterlies decreases with height it can be anticipated that in the NH winter it is much easier to transport wave energy from SH to NH than vice versa, which is in very good agreement with the results of the numerical experiments. This one way filtering activity of the Hadley cell may provide part of the explanation for the fact that tropically forced teleconnection patterns are so easily found in the NH winter, but less so in the NH summer (Arkin et al 1980, Horel and Wallace 1981).

Acknowledgement

I thank Huug van den Dool and Cor Schuurmans for their critical remarks and Marlie Collet for typing the manuscript.

4.7. References

- Arkin, P.A., W.Y. Chen, and E.M. Rasmusson, 1980: Fluctuations in mid and upper tropospheric flow associated with the Southern Oscillation. Proceedings of the Fifth Annual Climate Diagnostics Workshop, October 22-24, 1980, US Department of Commerce, Washington DC.
- Egger, J., 1977: On the linear theory of the atmospheric response to sea surface temperature anomalies. *J. Atmos. Sci.*, 34, 603-614.
- Grose, W.L., and B.J. Hoskins, 1979: On the influence of orography on large scale atmospheric flow. *J. Atmos. Sci.*, 36, 223-245.
- Horel, J.D. and J.M. Wallace, 1981: Planetary scale atmospheric phenomena associated with the interannual variability of sea surface temperature in the Equatorial Pacific. *Mon. Wea. Rev.*, 109, 813-829.
- Hoskins, B.J. and D.J. Karoly, 1981: The steady linear response of a spherical atmosphere to thermal and orographic forcing. *J. Atmos. Sci.*, 38, 1179-1196.
- Lau, N.C.L., 1979: The observed structure of tropospheric stationary waves and the local balances of vorticity and heat. *J. Atmos. Sci.*, 36, 996-1016.
- Opsteegh, J.D. and H.M. van den Dool, 1980: Seasonal differences in the stationary response of a linearized primitive equation model: Prospects for long range weather forecasts? *J. Atmos. Sci.*, 37, 2169-2185.
- Simmons, A.J., 1981: Tropical influences on stationary wave motion in middle and high latitudes. Technical Report of E.C.M.W.F. No. 26.
- Webster, P.J., 1981: Mechanisms determining the atmospheric response to sea surface temperature anomalies. *J. Atmos. Sci.*, 38, 554-571.

- V. A simulation of the January Standing Wave Pattern including the Effects of Transient Eddies.[†]

J.D. Opsteegh and A.D. Vernekar.

[†]Accepted for publication in J. Atmos. Sci., 1982.

Abstract

A steady-state linear, two-level primitive equation model is used to simulate the January standing wave pattern as a response to mountain, diabatic and transient eddy effects. The model equations are linearized around an observed zonal mean state which is a function of latitude and pressure. The mountain effect is the vertical velocity field resulting from zonal flow over the surface topography. The diabatic heating is calculated using parameterized forms of the heating processes. The transient eddy effects, that is the flux convergence of momentum and heat by transient eddies, are computed from observations. Separate responses of the model are computed for each of the three forcing functions.

The amplitude of the response to diabatic heating is small compared to observed values. The vertical structure is highly baroclinic. At the upper level, the phase of the waves is approximately in agreement with the observations. The amplitude of the response to mountain forcing is comparable with observations. The wavelength of the response in the Pacific sector is shorter than observed. The vertical structure is equivalent barotropic. The combined response to diabatic heating and mountain forcing is dominated by the contribution from the mountains. The phase shows agreement with the observations, but the Aleutian low is located too far to the west and an unrealistic high appears to the west of the dateline.

The amplitude of the response to transient eddy effects is comparable to the observations in middle and low latitudes. At high latitudes the amplitudes are much too large. The assumption of linearity is not valid for strong forcing at high latitudes where the zonal wind is very weak. The vertical structure of the response is almost equivalent barotropic.

A comparison of the responses to mountain and transient eddy effects show an interesting phase relationship. The troughs

produced by the transient forcing are found in the lee of the troughs produced by the mountains (very close to the ridge) indicating that transient forcing is organized by the mountain effects.

The combined model response to all three forcing functions shows a good agreement with observations except at very high latitudes.

5.1. Introduction

The quasi-stationary wave pattern on monthly or seasonal mean maps of the atmospheric circulation is often interpreted as an atmospheric response to forcing from the earth's surface. This forcing is mainly due to effects of surface terrain and diabatic heating resulting from the different thermal properties of continents and oceans. However, the equations for the stationary waves derived from the time-averaged equations for atmospheric flow, with a time averaging period of a month to a season, show the influence of transients on the quasi-stationary waves as an additional force in the momentum equations and as additional heating in the thermodynamic equation (see, e.g., Saltzman, 1968). Various observational studies dealing with the time averaged equations suggest that this forcing of quasi-stationary waves by transient eddies is an important process (Holopainen, 1973, Lau 1979, Opsteegh and van den Dool 1979).

Numerous studies have been made to simulate the quasi-stationary wave pattern as a response to mountain effects or diabatic heating effects or both (Charney and Eliassen 1949, Smagorinsky 1953, Döös 1962, Saltzman 1965, Sankar Rao and Saltzman 1969, Derome and Wiin-Nielsen 1971, to name a few). The earlier models used for these simulations had a very crude meridional structure. The earth's geometry was simplified to a β plane and the zonal mean state, around which the equations were linearized, was independent of latitude. Consequently only the mid-latitude standing wave pattern was simulated and the meridional structure of the waves was neglected. However, certain assumptions about the meridional scale of the waves had to be made. Saltzman (1965) and Derome and Wiin-Nielsen (1971) found that their solutions were very sensitive to the particular choice of the meridional scale parameter, which means that this parameter can be used to tune the solutions with the observations. Recent investigations used more complicated models, including a realistic zonal mean state and

earth geometry (Egger 1976b, Ashe 1979). The results with these models show some agreement with the observed standing eddy pattern, especially in the upper part of the troposphere. But large errors in the phase of the waves occur as well. Recently, Youngblut and Sasamori (1980) simulated the influence of internal forcing with a linear steady-state model. They computed this eddy forcing from observations. Their model results indicate that the role of internal forcing in generating the quasi-stationary waves is important. However, their results are inconclusive because they do not try to simulate the standing eddy pattern with independent estimates of the various forcing mechanisms involved.

The purpose of this study is to simulate the quasi-stationary waves as a response to mountain, diabatic heating and transient eddy effects. We use a linear steady-state two-layer primitive equation model. The mountain effects are the vertical velocities produced by the zonal flow over the surface topography. Diabatic heating processes are calculated using parameterized forms of the heat fluxes. The transient eddy effects are computed from observations based on a five year data set.

In the next two sections we briefly describe the model and computations of the forcing functions. Section 4 presents the results of the separate and combined responses of the model to all three forcing functions.

The response of the model to the mountain and transient eddy effects show an interesting relationship, suggesting a possibility of parameterizing the transient eddy effects in terms of mountain effects. The combined response of the model to all the forcing functions is in good agreement with the observations except at very high latitudes.

5.2. The model

The model used in this study is described in detail in Opteegh and van den Dool (1980). However, for the convenience

of the reader only the important features are presented here. The model equations are derived from the time averaged primitive equations on a sphere with an averaging time of one month. The tendency terms in these equations are neglected because they are small compared to the other terms in the equations (Opsteegh and van den Dool 1979). The time averaged variables are resolved into two components: zonal average and departures from zonal average (stationary waves). The equations are simplified by linearizing around the zonally averaged basic state. This basic state depends on latitude and pressure, and is prescribed from observations. The data were kindly supplied by Dr. A.H. Oort. It is the zonal mean state for the years 1969-1973. Fig. 1 shows the zonal mean state as a function of latitude. It is the zonal mean wind at 800 and 400 mb and the zonal mean temperature at 600 mb. The static stability at 600 mb is also a parameter of the mean state. It varies only slightly with latitude. It's hemispheric average value is approximately $5.5 \cdot 10^{-4} \text{ KPa}^{-2}$.

The linear system of equations for stationary waves as used in Opsteegh and van den Dool (1980) read as follows:

zonal momentum balance

$$\frac{U}{a \cos \phi} \frac{\partial \hat{u}}{\partial \lambda} + \frac{\partial U}{a \partial \phi} \hat{v} + \frac{\partial U}{\partial p} \hat{\omega} - f \hat{v} + \frac{1}{a \cos \phi} \frac{\partial \hat{\Phi}}{\partial \lambda} - \hat{F}_{Wx} = \hat{F}_{Ex} \quad (1)$$

meridional momentum balance

$$\frac{U}{a \cos \phi} \frac{\partial \hat{v}}{\partial \lambda} + f u + \frac{1}{a} \frac{\partial \hat{\Phi}}{\partial \phi} - \hat{F}_{Wy} = \hat{F}_{Ey} \quad (2)$$

first law of thermodynamics

$$\frac{U}{a \cos \phi} \frac{\partial \hat{T}}{\partial \lambda} + \frac{\partial T}{a \partial \phi} \hat{v} - \sigma_{sn} \hat{\omega} = \frac{\hat{Q}}{C_p} + \hat{Q}_E \quad (3)$$

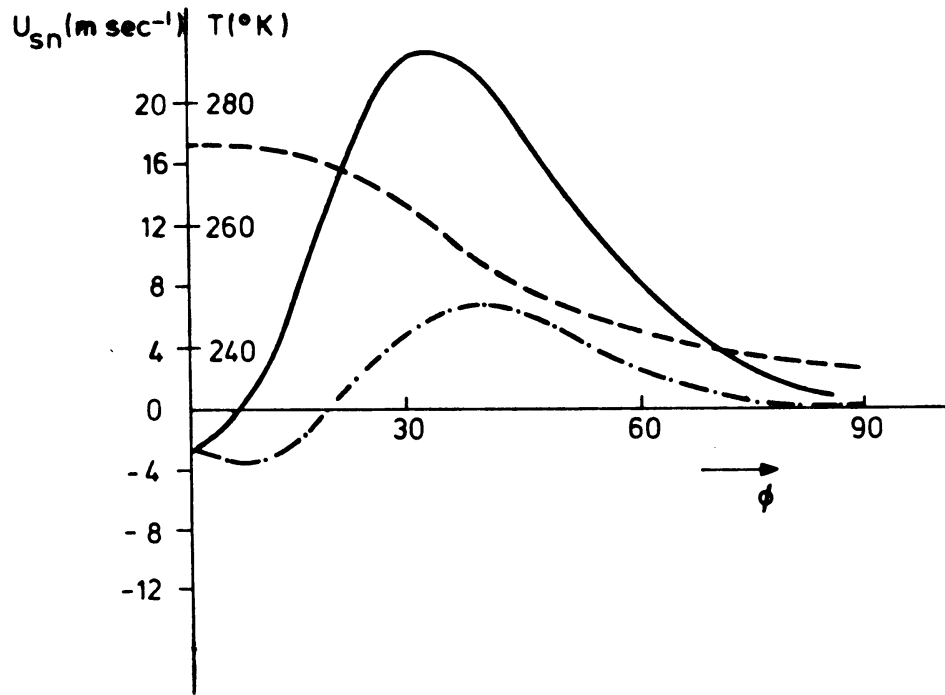


Fig. 1 : The January mean zonally averaged wind at 400 mb (solid line) and at 800 mb (dashed dotted line) and the zonal mean temperature at 600 mb (dashed line) as a function of latitude.

continuity equation

$$\frac{1}{a \cos \phi} \frac{\partial \hat{u}}{\partial \lambda} + \frac{1}{a \cos \phi} \frac{\partial}{\partial \phi} (\hat{v} \cos \phi) + \frac{\partial \hat{\omega}}{\partial p} = 0 \quad (4)$$

hydrostatic approximation

$$\frac{\partial \hat{\phi}}{\partial \phi} = - \hat{\alpha} \quad (5)$$

equation of state

$$p \hat{\alpha} = R \hat{T} \quad (6)$$

where U_{sn} , T_{sn} and σ_{sn} are the zonal mean wind, temperature and static stability respectively. The model variables for the stationary planetary waves are \hat{u} , \hat{v} , $\hat{\omega}$, $\hat{\phi}$, \hat{T} , $\hat{\alpha}$. These symbols have their conventional meaning. \hat{F}_{Wx} and \hat{F}_{Wy} are the dissipation terms. These terms are specified below. \hat{F}_{Ex} , \hat{F}_{Ey} and \hat{Q}_E are the internal sources of momentum and heat. \hat{Q} is the diabatic heating.

The vertical discretization of the model is shown in the upper part of Fig. 2. The momentum equations and the continuity equation are applied at 400 and 800 mb, while the thermodynamic equation is applied at 600 mb. The upper and lower boundaries are at 200 and 1000 mb, where we assume that the vertical velocity vanishes, except when mountain forcing is considered. In that case, the vertical velocity produced by the surface airflow over the mountains is taken as the lower boundary condition.

The variables as well as the forcing components are expanded in Fourier series along a latitude circle. This leads to sets of equations in terms of Fourier coefficients, which can be solved for each of the zonal waves independently. We arrive at the total model response by adding the response for the individual zonal wavenumbers. Only the first five zonal wavenumbers are retained. Higher wavenumbers give a negligible contribution to the total geopotential height response (Opsteegh and van den Dool 1980).

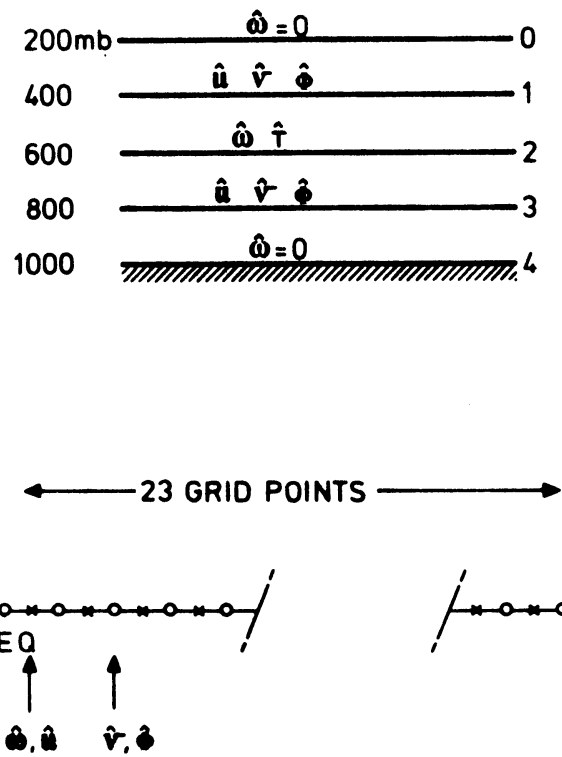


Fig. 2 : Discretization of the two-level model in the vertical (upper part) and in the meridional direction (lower part).

In meridional direction a gridpoint representation is used with 23 gridpoints between Equator and Northpole. The grid is shown in the lower part of Fig. 2. A staggered grid system is used. \hat{u} and \hat{v} are defined at the gridpoints, whereas $\hat{\phi}$ and \hat{v} are formulated at intermediate points, indicated with open circles. The boundary conditions are:

$$\begin{aligned} \hat{v} \cos \phi &= 0 \quad \text{at } \phi = \pi/2 \\ \frac{\partial \hat{\phi}}{\partial \phi} &= 0 \quad \text{at } \phi = 0 \end{aligned} \tag{7}$$

$\hat{v} \cos \phi$ is a variable which is used in the model instead of \hat{v} .

At the lower level of the model we have friction terms that are linear functions of the perturbation velocities. Following Egger (1976a), we also incorporate the vertical exchange of momentum. The resulting equations for \hat{F}_{Wx} in the zonal momentum equations are:

$$\hat{F}_{Wx3} = K_D(\hat{u}_1 - \hat{u}_3) - K_W\hat{u}_3 \tag{8}$$

$$\hat{F}_{Wx1} = -K_D(\hat{u}_1 - \hat{u}_3) \tag{9}$$

where the subscript 1 refers to 400 and 3 to 800 mb. K_D and K_W are vertical diffusion and surface friction coefficients respectively. They are constants in the model. The numerical value used for the friction coefficient is $2 \cdot 10^{-6} \text{ sec}^{-1}$. The value for the vertical diffusion coefficient is $1 \cdot 10^{-7} \text{ sec}^{-1}$. The friction terms in the meridional momentum equation (2) are obtained by replacing \hat{u}_1 and \hat{u}_3 by \hat{v}_1 and \hat{v}_3 in (8) and (9).

5.3. The forcing functions

The diabatic heating resulting from inhomogeneities in the earth's surface is accounted for by using parameterizations for the various physical processes involved. These processes

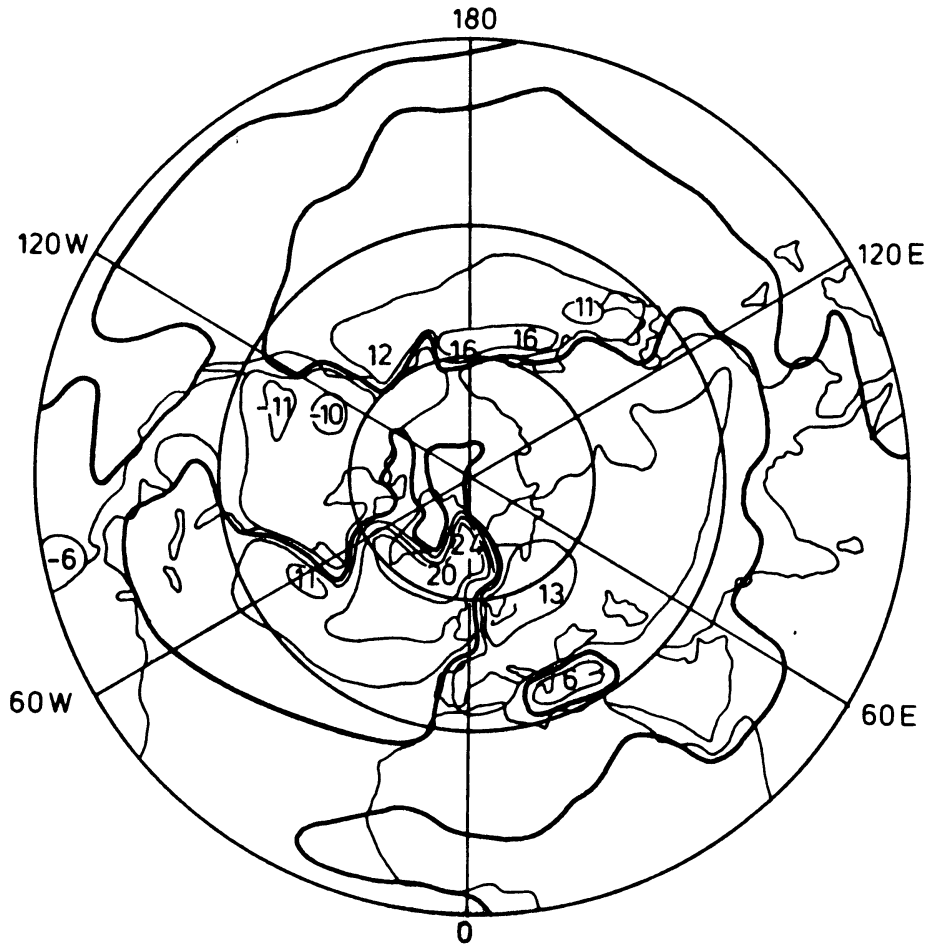


Fig. 3 : Computed asymmetric component of the January mean heating at 600 mb in Kday^{-1} . Contour interval is 0.5 Kday^{-1} .

are shortwave radiation, long wave radiation, small scale convection, evaporation and condensation and subsurface conduction and convection. We adopted the parameterizations of these processes from Vernekar and Chang (1978). The validity of the parameterizations is discussed in various papers (Smagorinsky 1963, Saltzman 1967, Vernekar 1975). The heating is dependent on surface temperature and albedo, atmospheric temperature and albedo, radiation-convection parameters and subsurface temperature. The heating scheme treats the surface and atmospheric temperatures as dependent variables of the model and other quantities are derived from observations. We take atmospheric temperature at 600 mb which is the dependent variable of the model. To determine the surface temperature we use the heat balance condition at the earth's surface. The heating in the atmospheric column \hat{Q}_2 can be expressed as:

$$\hat{Q}_2 = A(\phi)\hat{T}_2 + B(\phi,\lambda) \quad (10)$$

The first part of the right hand side of (10) is a Newtonian cooling term and is dependent on the solution. The second part is fixed. For details on the derivation of (10) the reader is referred to Vernekar and Chang (1978). As the Newtonian cooling term also acts on the temperature perturbations created by mountain forcing and internal transient forcing, the resulting diabatic heat forcing is not the same when these processes are neglected. Nevertheless the diabatic heating is very much dominated by the fixed part of (10) so that this dependence of \hat{Q}_2 on the other forcing processes is not large. Fig. 3 shows the diabatic heating rate when the forcing due to mountains and transient eddies is neglected. The figure shows cooling over the continents and warming over the oceans, with maximum warming close to the east coasts of the continents. The distribution of the heating is in good agreement with estimates of this quantity

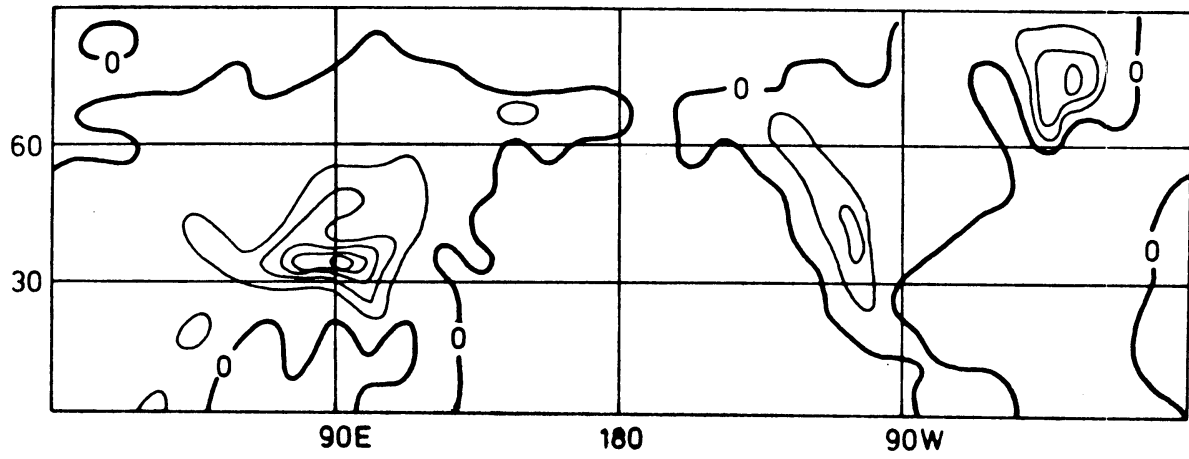


Fig. 4 : Large scale features of the topography of the northern hemisphere. Contour interval is 1000 M.

by Lau.(1979). The heating rate is of the order of 1 K day^{-1} , which is smaller than the values given by Lau. This is because Lau's estimates are for the total heating whereas Fig. 3 shows only the departures from the zonal average.

The effects of mountains on the standing eddies is introduced via a vertical velocity at the lower boundary. We use

$$\hat{\omega}_4 = \frac{-\bar{\rho}_4 \cdot U_{sn} \frac{\partial gH}{\partial \lambda}}{a \cos \phi} \quad (12)$$

to determine the vertical velocity at the lower boundary. U_{sn} is the zonal mean wind at a representative level, which is taken to be the 900 mb level. H is the topographic height. It is shown in Fig. 4.

The transient forcing is computed from observational data. The data came from the same data set that was used for the computation of the zonal symmetric state. So it is the mean January internal forcing for the years 1969-1973. The forcing can be written in terms of the convergence of eddy fluxes of momentum and heat as follows:

$$\hat{F}_{Ex} = - \left(\frac{1}{a \cos \phi} \frac{\partial \overline{u'^2}}{\partial \lambda} + \frac{1}{a} \frac{\partial \overline{u'v'}}{\partial \phi} + \frac{\partial \overline{u'\omega'}}{\partial p} - \frac{2 \tan \phi}{a} \overline{u'v'} \right) \quad (12)$$

$$\hat{F}_{Ey} = - \left(\frac{1}{a \cos \phi} \frac{\partial \overline{u'v'}}{\partial \lambda} + \frac{1}{a} \frac{\partial \overline{v'^2}}{\partial \phi} + \frac{\partial \overline{v'\omega'}}{\partial p} + \frac{\tan \phi}{a} (\overline{u'^2} - \overline{v'^2}) \right) \quad (13)$$

$$\hat{Q}_E = - \left(\frac{1}{a \cos \phi} \frac{\partial \overline{u'T'}}{\partial \lambda} + \frac{1}{a} \frac{\partial \overline{v'T'}}{\partial \phi} + \frac{\partial \overline{\omega'T'}}{\partial p} - \frac{R}{pC_p} \overline{\omega'T'} \right) \quad (14)$$

The data set contained five year averages of $\overline{u'^2}$, $\overline{u'v'}$, $\overline{v'^2}$, $\overline{u'T'}$ and $\overline{v'T'}$. The data on vertical fluxes were not available. We therefore omitted the vertical fluxes in computing \hat{F}_{Ex} , \hat{F}_{Ey} and \hat{Q}_E . Before computing the gradients in (12) and (14) the data were smoothed twice in ϕ direction with a three point smoother. Because of the very large uncertainty in the eddy fluxes at high latitudes we interpolated \hat{F}_{Ex} , \hat{F}_{Ey} and \hat{Q}_E between 70 N and the

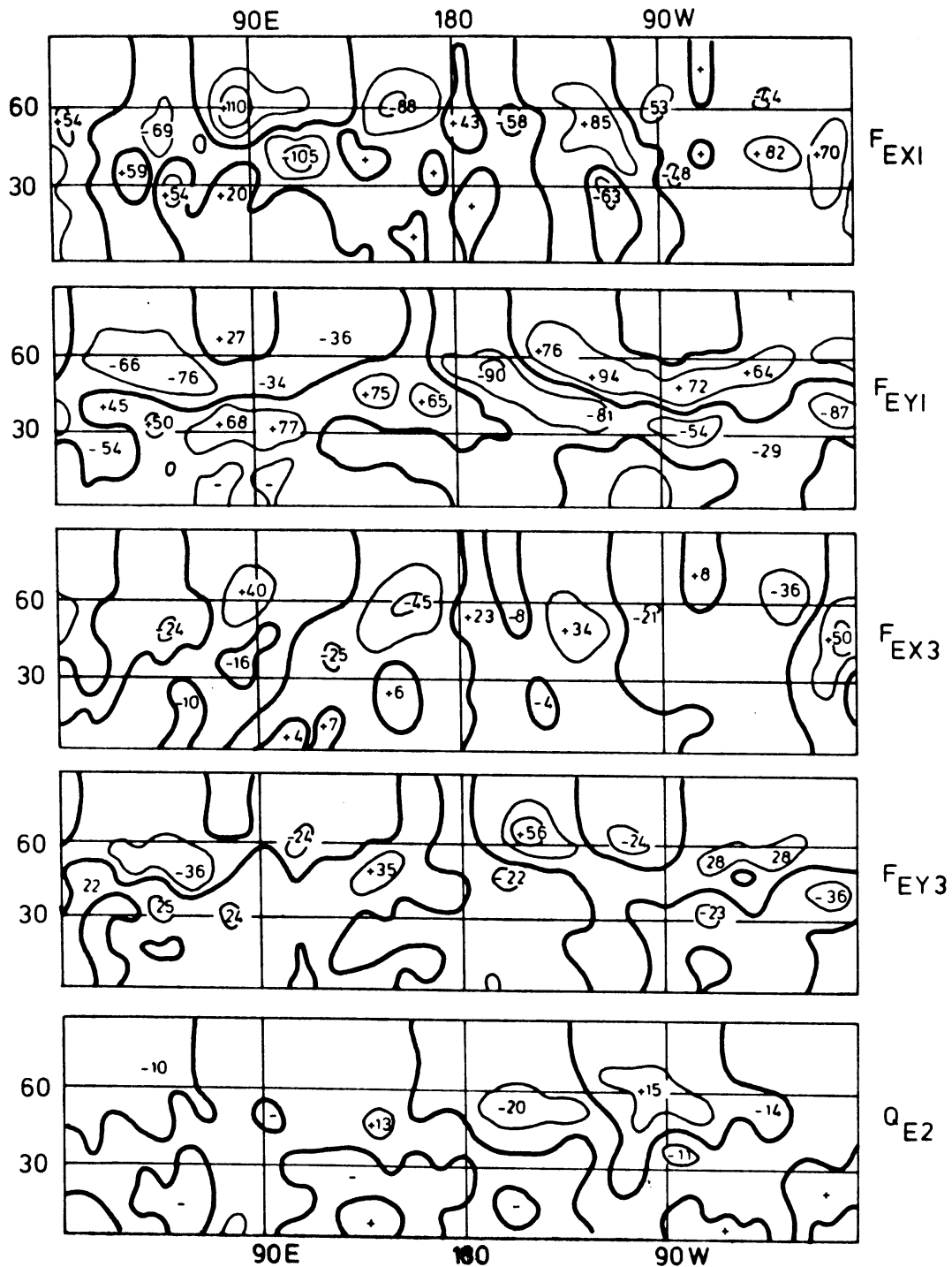


Fig. 5 : Hemispheric distribution of the internal forcing by transient eddies. The upper two figures show the forcing in the zonal and meridional momentum equations at 400 mb respectively. The next two figures show the same forcing fields at 800 mb. The lower figure shows the forcing in the thermodynamic equations at 600 mb. Units are 10^{-5} Msec⁻² for the upper four figures and 10^{-5} Ksec⁻¹ for the bottom figure.

pole such that the internal forcing components decrease linearly from 70N to zero at the pole. Fig. 5 shows the distribution of the internal forcing components in the five model equations. In spite of the general noisy character of these transient forcing fields they show some large preferred regions of convergence and divergence of momentum and heat. As the model response to high zonal wavenumbers is always very small compared to that for low zonal wavenumbers the response to these noisy forcing fields will be very much dominated by the large scale pattern in these fields.

5.4. Results

Fig. 6 shows the mean observed January standing eddy pattern at 400 and 800 mb. The data are from Crutcher and Meserve (1970)². In zonal direction the pattern is very much dominated by wavenumbers up to three. In meridional direction the amplitude shows maxima in the subtropics, middle latitudes and high latitudes. The mid-latitude maxima have the largest amplitude. The phase changes near 30N are very large, so that the lows and highs at middle latitudes are always accompanied by pressure systems of opposite sign in the subtropics. We shall see to what extent the model is able to reproduce these observed characteristics of the standing eddy pattern.

In order to determine the relative importance of the various forcing components involved in the generation of the standing eddies we shall discuss the separate contribution of the forcing components.

Diabatic heating and mountain forcing

Fig. 7 shows the geopotential height response at 400 mb to the diabatic heating field. Apart from a rather large response at high latitudes which is probably an artifact of the linear

²Crutcher, H.L., and J.M. Meserve, 1970: Selected level heights, temperature and dew points for the Northern Hemisphere, NAVAIR-50-1C-52 (Available from Naval Weather Service Command, Washington Navy Yard, Washington, D.C.).

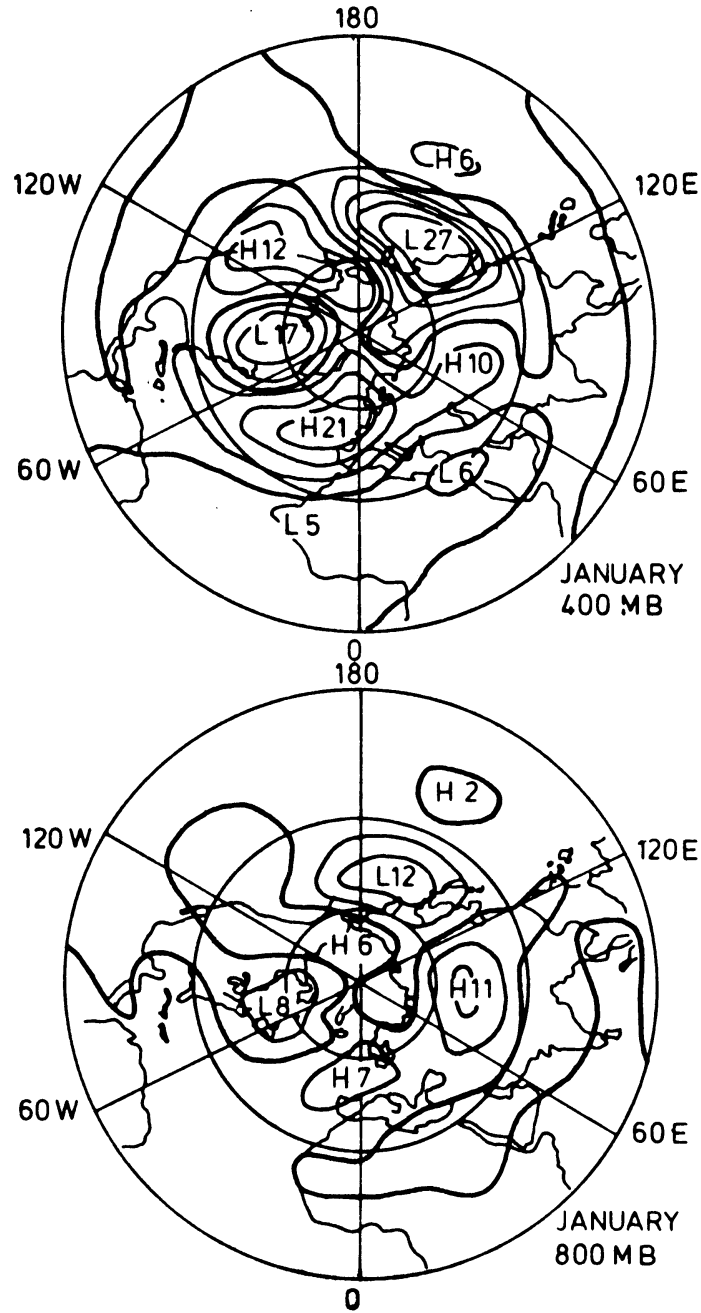


Fig. 6 : Observed January standing eddy pattern at 400 and 800 mb. Units are in gpdam. The same units will be used in all the remaining figures. The zero line is indicated with a thick line. Contour interval is 5 gpdam.

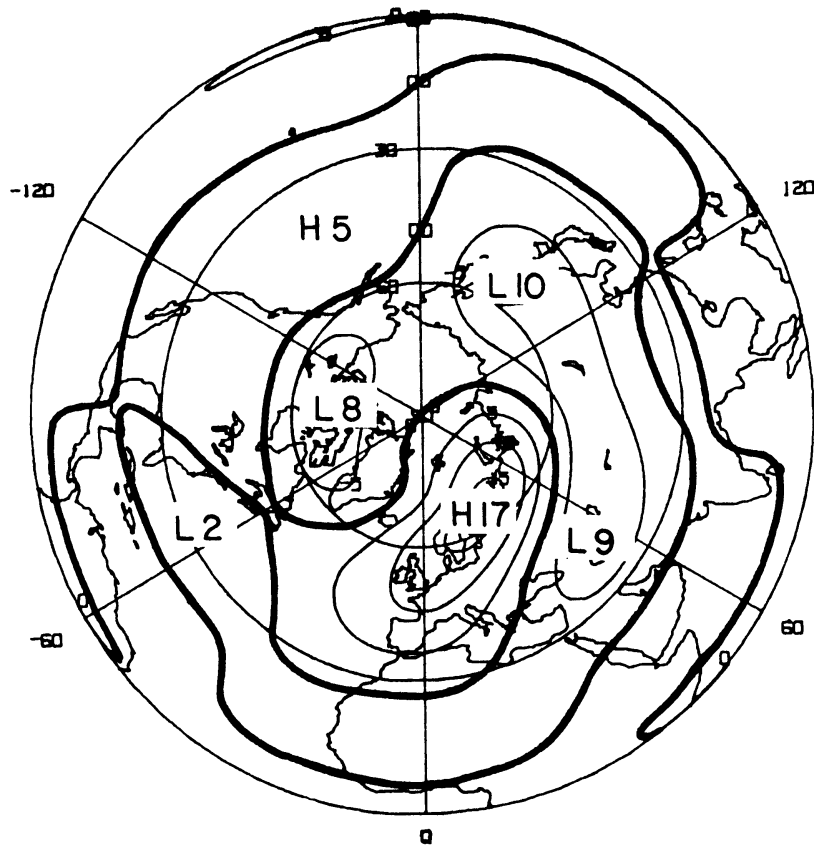


Fig. 7 : Geopotential height response at 400 mb to diabatic heating.

model, the amplitude of the pressure systems at middle latitudes is of the order of 5 to 10 gpdam. So the contribution of the heating to the observed mid-latitude maxima of the standing eddy pattern is not very large. However, the phase of the waves is in good agreement with the observed highs along the west coasts and to the observed lows along the east coasts of the American and European continents.

Vernekar and Chang (1978) used the same heating parameterizations to simulate January quasi-stationary waves. The response of their model had approximately the same phase as in these results but the magnitudes were larger by a factor of two. Their model was based on quasi-geostrophic approximations and the zonally averaged state was uniform with latitude. We made several experiments on both the models to determine the reason of the differences between these responses. It appears that the different quasi-resonant properties of the two models were responsible for the different results. In the quasi-geostrophic model the quasi-resonant mode was wavenumber 3. This mode had the highest amplitude, whereas in the PE model the quasi-resonant wavenumber 4 played only a minor role. In order to determine the sensitivity of the results in both models to the dissipative processes, we made the same experiment by increasing the friction coefficient by an order of magnitude. In the quasi-geostrophic model the amplitude of wavenumber 3 was reduced by a factor of two. As a result the cumulative response of all the waves was also reduced by a factor of two. In the PE model the amplitude of wavenumber 4 was also reduced, but the cumulative response of all the waves was not significantly affected.

The geopotential height perturbations in the tropics are very small. In Opsteegh and van den Dool (1980) it was shown that the balancing processes in the stationary waves are different for middle latitudes and tropics. In middle latitudes the perturbations are almost geostrophic and the balancing process is the horizontal advection. In the tropical easterlies the flow has the character

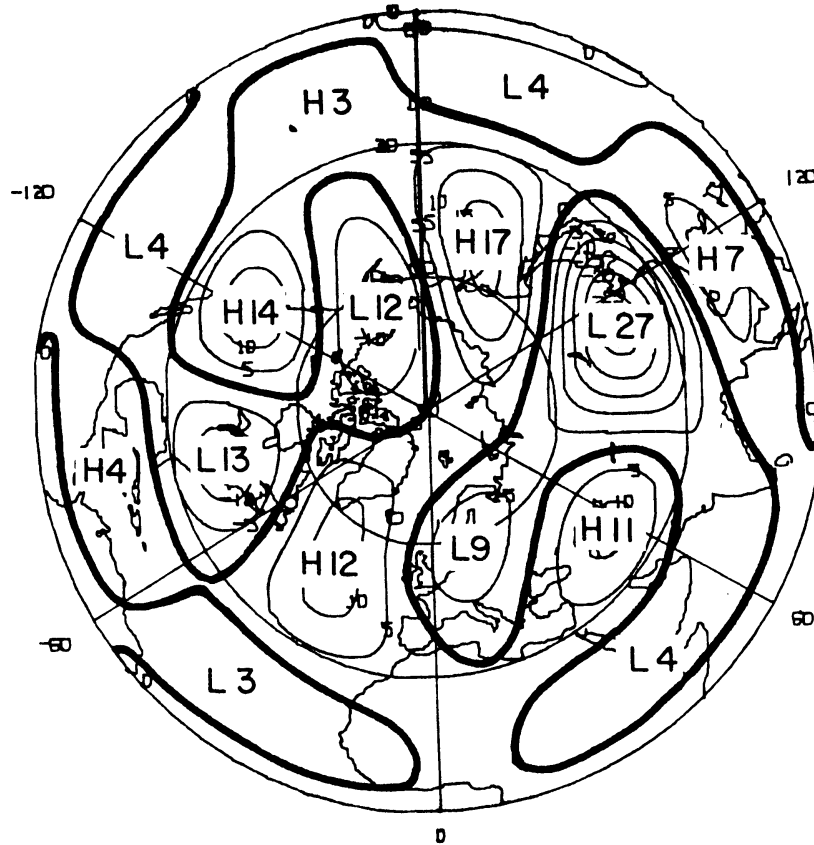


Fig. 8 : Geopotential height response at 400 mb to topographic forcing.

of a direct thermal circulation, which is highly ageostrophic (Walker type circulations). Here the balancing process is cooling (warming) in upward (downward) motions.

Fig. 8 shows 400 mb height field simulated using orographic forcing. The amplitudes of these results are much closer to the observations as compared to those forced by the heat sources and sinks. This is in agreement with the results of several other studies, which suggest that the effect of orographic forcing is dominant at middle and higher tropospheric levels. (Charney and Eliassen 1949, Derome and Wiin-Nielsen 1977, Manabe and Terpstra 1974). The diabatic heating may be important for the observed surface lows and highs. It was shown by Smagorinski (1953) and recently by Hoskins and Karoly (1981) that the pressure distribution near the surface is extremely sensitive to diabatic heat sources and sinks at low altitudes, whereas the response at upper levels is probably more determined by the vertically averaged heating. These shallow heating effects cannot be dealt with in the present two level model and therefore we cannot expect to simulate more than the mid and upper tropospheric standing wave pattern.

Comparison between Fig. 8 and the observed standing eddy pattern (Fig. 6) shows that the simulated mountain effect has a shorter wavelength than observed, especially in the Pacific sector. This was also found by Hoskins and Karoly (1981). In fact these results show a very close agreement with their results for mountain forcing, which were obtained with a five-level steady-state primitive equation model, suggesting that the results are not very sensitive to the vertical resolution of the model. Fig. 8 shows a fair agreement with the observations for the low and high associated with the Rockies. However, the low over Western Europe and the high west of the date line are not observed. The Aleutian low is located too far to the west.

Fig. 9 shows the combined effects of heat and orographic forcing at 400 mb. Because of the relative importance of orographic forcing, the results are not much different from Fig. 8.

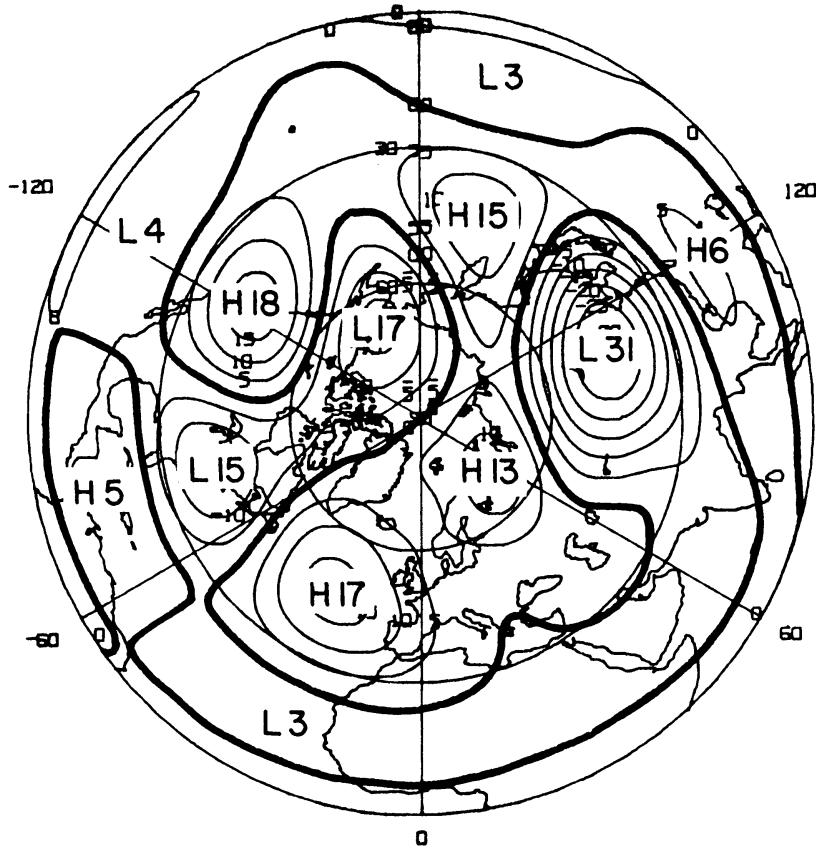


Fig. 9 : Geopotential height response at 400 mb to both diabatic heating and topographic forcing.

However, the unrealistic low over Western Europe, produced by the effects of mountains is counteracted by the heating and has disappeared in the combined results.

Internal forcing by transient eddies

The effect of internal forcing by transient eddies is shown in Fig. 10. In middle latitudes and subtropics the pressure systems have amplitudes that are comparable with the observed values. However, the amplitude of the wave pattern at high latitudes is unrealistically large. Here we see a serious drawback of the assumption of linear behavior of stationary planetary waves. In spite of the fact that we modified the transient forcing by decreasing it linearly to zero from 70N to the Northpole, the forcing has still considerable strength at high latitudes. This forcing is balanced mainly by zonal advection. However, due to very small values of the zonal mean wind at high latitudes the resulting asymmetrical perturbation has to be large in order to balance the forcing fields. The tendency of creating large amplitudes at high latitudes could also be seen in the computation of the effect of diabatic heating. In his simulation of January standing waves, Ashe (1979) computed the effects of heating and mountain forcing with a linear and a nonlinear model. The differences between the results of both models were among others that the linear model created large amplitudes at high latitudes but the nonlinear model did not.

Because of the unrealistic response of the linear model to forcing at high latitudes we cannot expect to be able to simulate the high latitude structure of the standing eddies with any degree of accuracy. It is interesting however to investigate to what extent the response at middle and low levels is determined by the high latitude behavior of the wave pattern. We investigated this for small changes in the zonal mean wind at high latitudes. The amplitude of the response at high latitudes appeared to be very sensitive for these small changes. It could change by a factor of almost two.

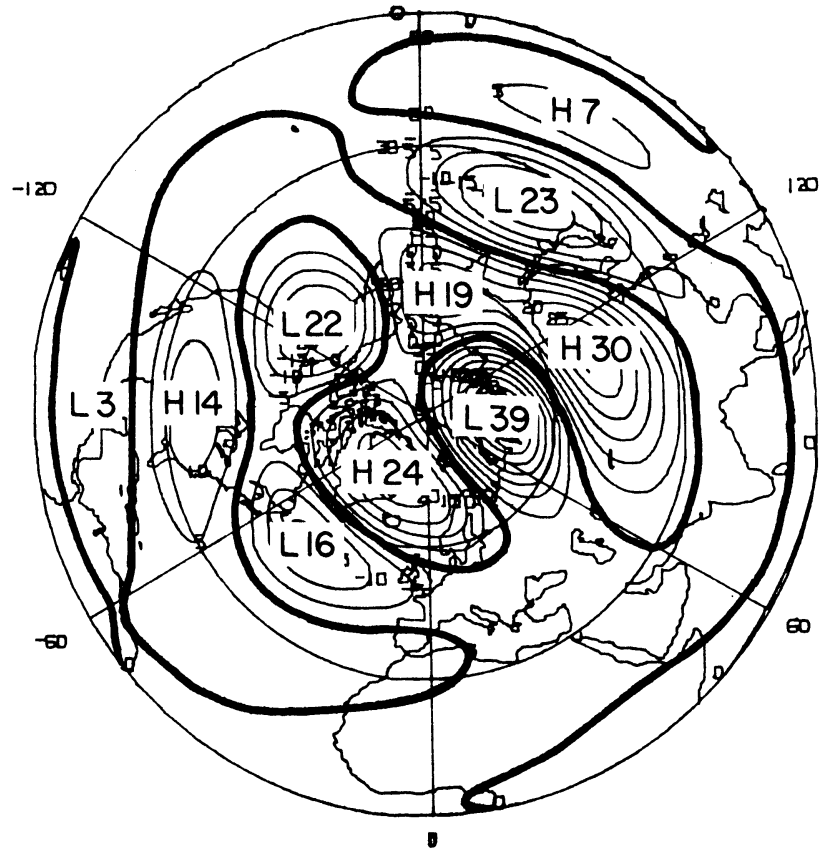


Fig. 10 : Geopotential height response at 400 mb to internal forcing by transient eddies.

However, the amplitude of the wavepattern at mid and low latitudes changed only slightly. Here the changes amounted to a maximum of 20%. More importantly the phases of the waves were not at all affected. Although unrealistic behavior of the linear model due to strong forcing at high latitudes creates some uncertainty in amplitude, we still have confidence in its ability to simulate the mid and low latitude effects of internal forcing.

Analysis of mid-latitude response

Fig. 11 shows the geopotential height response at both levels along 45N for the three forcing components separately and combined. The vertical structure of the mid-latitude response to diabatic heating is highly baroclinic, whereas the response to orographic forcing has an equivalent barotropic structure. This is also true for the vertical structure of the perturbations due to internal forcing by transient eddies. Since the transient forcing consists partly of heating in the thermodynamic equation this result is a little surprising. Therefore we did two additional experiments with transient forcing. In one experiment we retain the forcing only in the momentum equations and in the second we retain only heat forcing. The results are shown in Fig. 12. The eddy flux convergence of momentum is much more important for the standing eddies than the convergence of eddy heat flux, which explains the equivalent barotropic vertical structure of the total response. The small tilt that can be seen in the combined results is of course due to the effects of diabatic heating.

An interesting feature shows up in Fig. 11. Comparing the results for mountain and transient forcing it can easily be seen that there seems to exist a phase relationship between both wave patterns. The troughs produced by transient forcing are found without exception in the lee of the mountain produced troughs, very close to the ridge. As it is well known that cyclogenesis generally occurs in the lee of the troughs of planetary waves, we

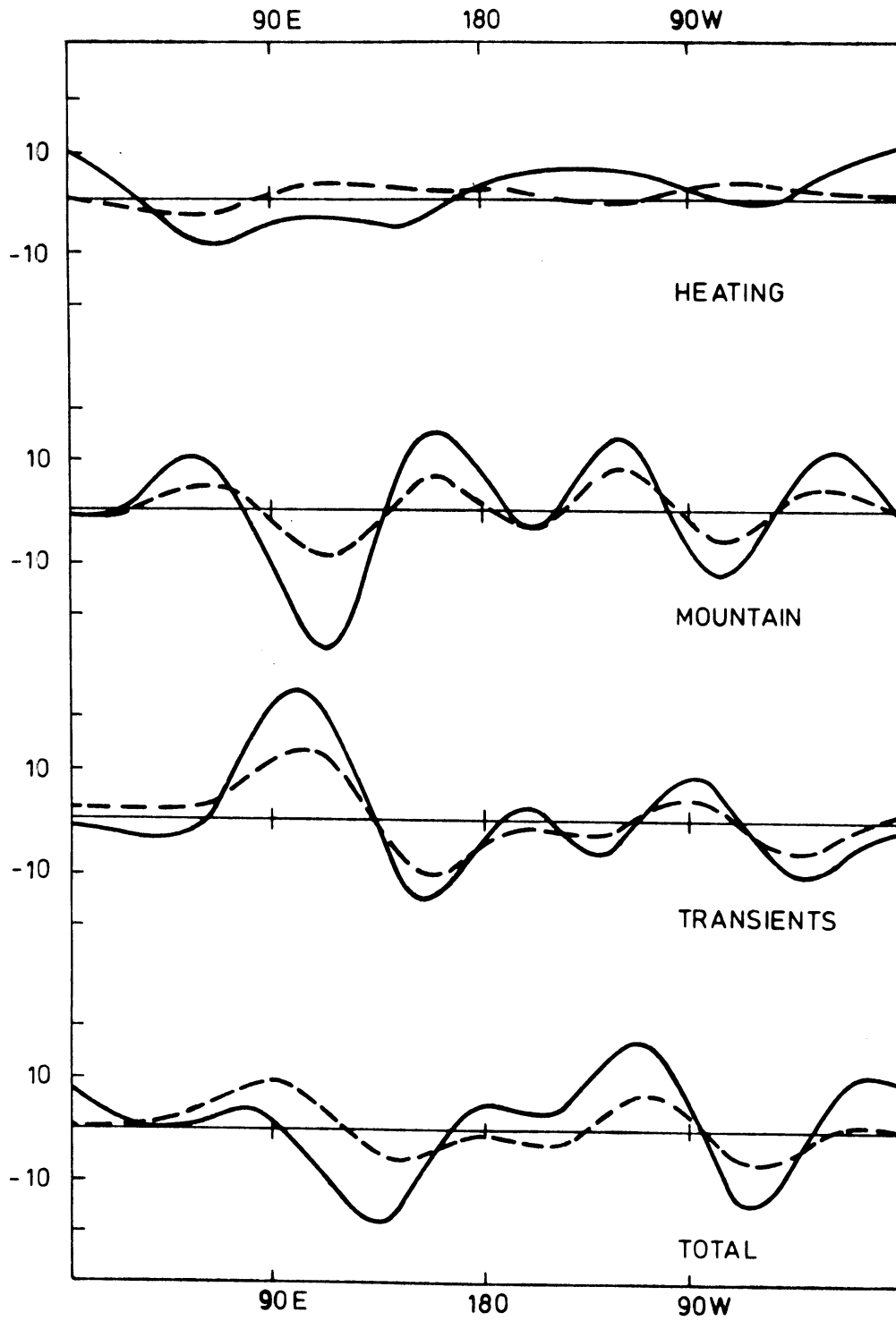


Fig. 11 : Geopotential height response at 400 (solid line) and 800 mb (dashed line) along 45N to the three forcing components separately and combined.

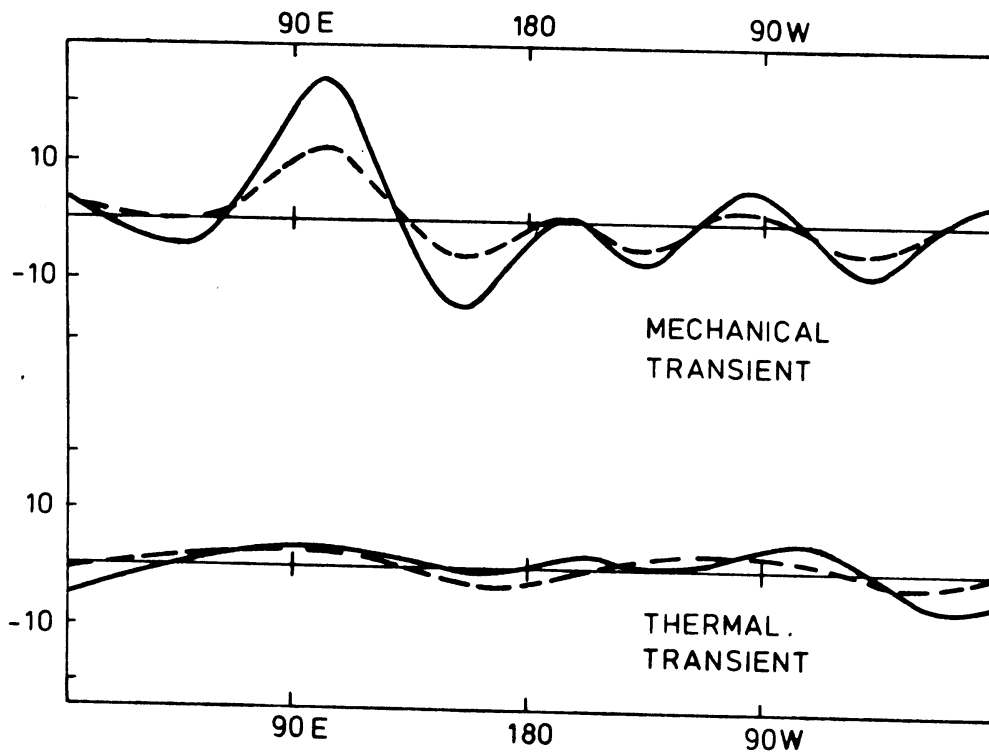


Fig. 12 : Geopotential height response at 400 (solid line) and 800 mb (dashed line) along 45N to the separate effects of transient forcing in the momentum equations and transient forcing in the thermodynamic equation.

may simply interpret these results as the statistical effect of deepening cyclones on the monthly mean pattern. Apparently the internal forcing is organized by the externally forced planetary waves. Lau and Wallace (1979) showed that the convergence of eddy flux of vorticity is connected to the mean winter surface lows and highs in such a way that the eddies simply act to maintain the surface pressure systems against friction. Surface heating processes may have a large impact on the location and depth of the surface lows and highs, however it seems likely that the location of the surface pressure systems is also partly determined by cyclogenetic processes aloft. The total picture of how the statistical effects of transient eddies are related to external heat and mountain forcing is not yet clear. Nevertheless we believe that there is some indication that such a relation exists and that this might provide a way of parameterizing the effect of transient eddies on the mean flow in terms of the conditions at the earth's surface.

Comparison with observations

First, we shall compare the results with the observed standing eddy pattern at middle latitudes. Fig. 13 shows the geopotential height at 45N as a function of longitude. The upper part of the figure is the response to diabatic heat forcing. In the next curve the effect of mountains is added and finally the effect of the three forcing components is shown. The lower curve shows the observed wave pattern along 45N. Again it can be seen that the heating contributes to the observed lows along the east coasts and to the observed highs along the west coasts of the American and Eurasian continents. Adding the effects of orographic forcing gives an amplitude that is comparable with the observed wave pattern. The main deficiencies are the unrealistic high to the west of the date line and the Aleutian low which is located too far to the west. Adding the effects of transient forcing eliminates the unrealistic high and causes the Aleutian low to shift to the east. The simulation

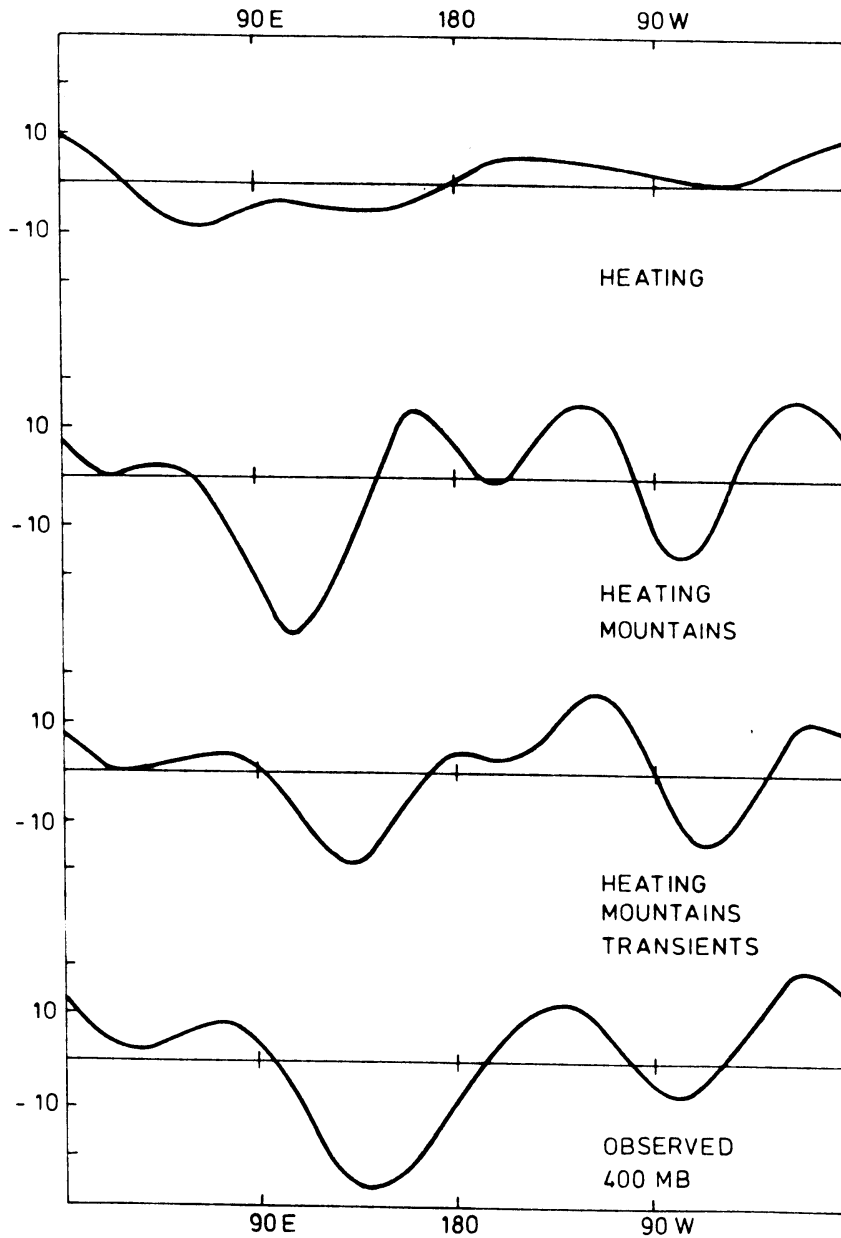


Fig. 13 : Geopotential height response at 400 mb along 45N. The upper curve gives the results for diabatic heating. The second curve gives the response to diabatic heating and mountain forcing. The third curve gives the response when all three forcing components are included. The lower curve gives the corresponding observed geopotential height at 400 mb.

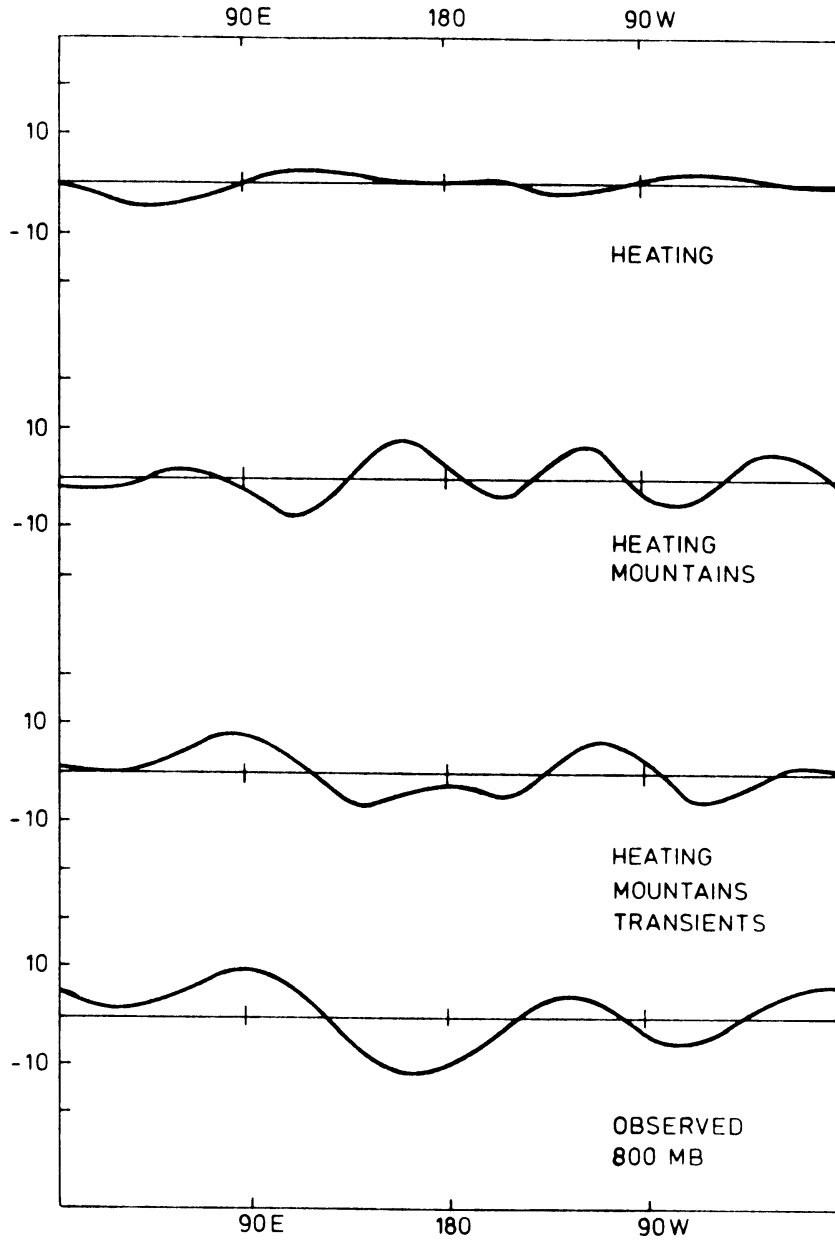


Fig. 14 : The same as Fig. 13 except for 800 mb.

is in very good agreement with the observed pattern shown by the bottom curve.

In Fig. 14 the results are presented for the lower level of the model (800 mb). The same arguments apply for the simulation at this level. Adding the effects of internal forcing eliminates the unrealistic high west of the date line and shifts the Aleutian low to the west. It is clear that also on the 800 mb level the transient forcing contributes much to the observed wave pattern. It seems to be especially important for the simulation of the Siberian high and the Aleutian low.

Figs. 15 and 16 show the simulated hemispheric wave pattern at 400 and 800 mb respectively for the experiment in which all three forcing components are included. The response is dominated by the high latitude wave pattern which shows a strong wave number 2. As a consequence of the dominance of the high latitude response the center of the mid-latitude pressure systems have been pushed 5 to 8 degrees south of the observed location. The correspondence between the middle latitudes and the subtropics is in good agreement with the observations. The results show large phase changes at approximately 25N so that the mid-latitude lows and highs are always accompanied by a subtropical pressure system of opposite sign. The amplitude of the sub-tropical lows and highs is close to the observed values.

5.5. Conclusions and discussion

We have shown that the transient eddies have a large impact on the January standing wave pattern. In spite of the fact that forcing by inhomogeneities in the surface of the earth is strong enough to explain the observed amplitude of the standing eddies, the effect of internal forcing was needed to simulate the proper phase of the waves. This is especially true for the Siberian high and the Aleutian low.

Our results suggest that the statistical effect of transient eddies on the monthly mean flow is organized by the externally

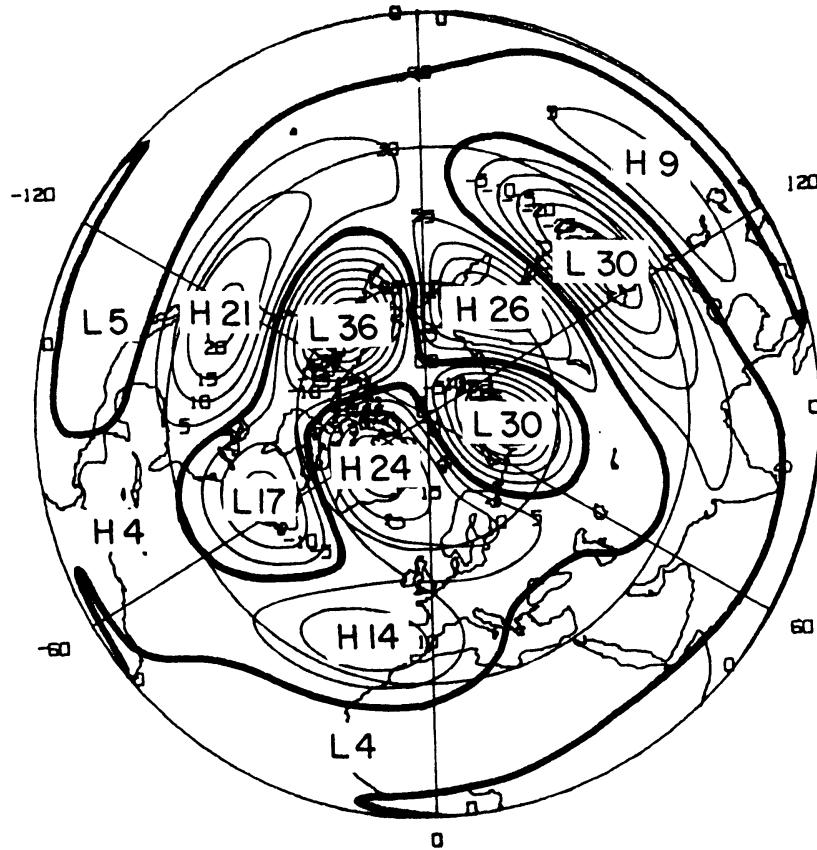


Fig. 15 : Geopotential height response at 400 mb to diabatic heating, topographic forcing and internal forcing by transient eddies.

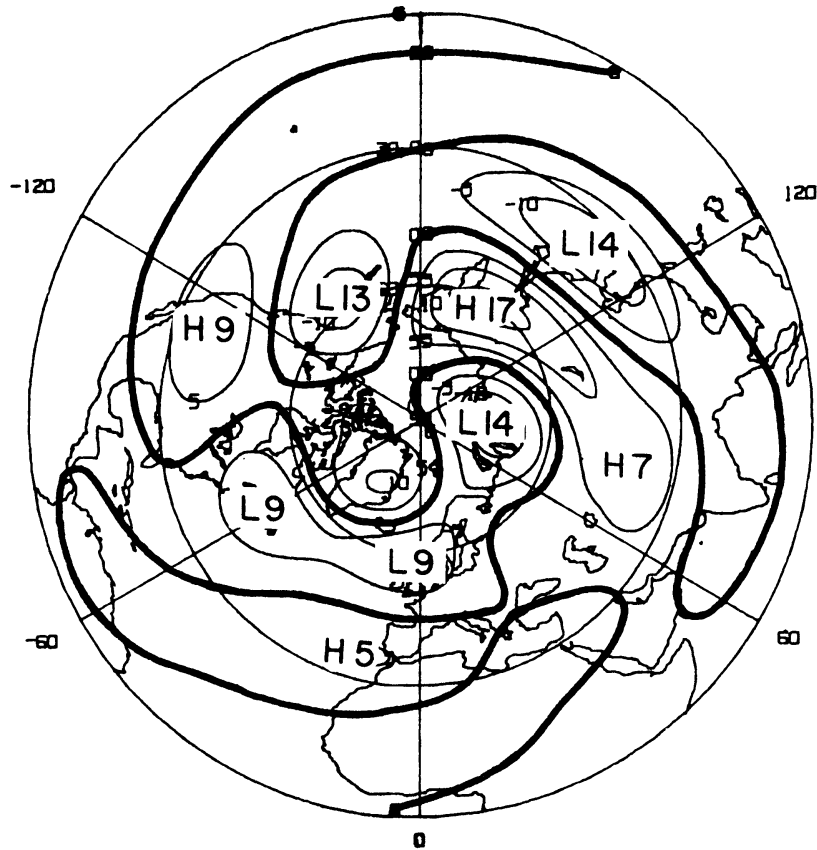


Fig. 16 : The same as Fig. 15 except for 800 mb.

forced waves. There is a phase relation between the mountain induced stationary wave and the internally forced wave. The troughs produced by the transients occurred downstream of the mountain troughs, close to the ridge. It is well known that the phase of planetary waves determines the areas that are favoured for cyclogenetic processes to take place. It is believed that the simulation of the effect of transient eddies is a reflection of this organization of cyclogenetic activity. Lau and Wallace (1979) show from observations that the transient eddies act to maintain the winter mean surface lows and highs against the effect of friction. Therefore the location of these pressure systems is possibly partly determined by cyclogenetic activity aloft.

The upper tropospheric effect of asymmetric diabatic heating from ocean-continent contrast is probably somewhat smaller than the effects of mountains and transient eddies. However, it seems likely from the results of simulations with models that have a larger resolution in the vertical that heating may be very important for the mean surface pressure systems.

The simulated wave pattern at middle and low latitudes shows a good agreement with observations, indicating that the assumption of linear behavior of stationary planetary waves is realistic. This was also shown by Lau (1979) from observations. The linearity assumption breaks down for strong forcing at high latitudes where the zonal mean wind is very small. In order to obtain a good simulation of the standing eddies at all latitudes nonlinear effects should be included. In spite of the unrealistic behavior of the model at high latitudes, this study clearly demonstrates the role of internal forcing by transient eddies as compared to the external forcing by mountain and diabatic heating effects.

Acknowledgements. This research has been supported by the Climate Dynamics Section of the National Science Foundation under Grant ATM-80-24881. We are grateful to Caren Klarman for typing the manuscript and Clare Villanti for preparing the figures.

5.6. References

- Ashe, S., 1979: A nonlinear model of the time-average axially asymmetric flow induced by topography and diabatic heating. J. Atm. Sci., 36, 109-126.
- Charney, J.G., and A. Eliassen, 1949: A numerical method for predicting the perturbations of the middle latitude westerlies, Tellus, 1, 38-55.
- Derome, J., and A. Wiin-Nielsen, 1971: Response of a middle latitude model atmosphere to forcing by topography and stationary heat sources. Mon. Wea. Rev., 99, 564-576.
- Döös, B.R., 1962: The influence of exchange of sensible heat with the earth's surface on the planetary flow. Tellus, 14, 133-147.
- Egger, J., 1976a: The linear response of a hemispheric two-level primitive equation model to forcing by topography. Mon. Wea. Rev., 104, 351-363.
- Egger, J., 1976b: On the theory of steady perturbations in the troposphere. Tellus, 28, 381-389.
- Holopainen, E.O., 1973: An attempt to determine the effects of turbulent friction in the upper troposphere from the balance requirements of the large scale flow: A frustrating experiment. Geophysika, 12, 151-176.
- Hoskins, B.J., and D. Karoly, 1981: The steady linear response of a spherical atmosphere to thermal and orographic forcing. J. Atm. Sci., 38, 1179-1196.
- Lau, N.C.L., 1979: The observed structure of tropospheric stationary waves and the local balances of vorticity and heat. J. Atm. Sci., 36, 996-1016.

- Lau, N.C.L., and J.M. Wallace, 1979: On the distribution of horizontal transports by transient eddies in the northern hemisphere wintertime circulation. J. Atm. Sci., 36, 1844-1861.
- Manabe, S., and T.B. Terpstra, 1974: The effects of mountains on the general circulation of the atmosphere as identified by numerical experiments. J. Atm. Sci., 31, 3-42.
- Opsteegh, J.D., and H.M. van den Dool, 1979: A diagnostic study of the time-mean atmosphere over Northwestern Europe during winter. J. Atm. Sci., 36, 1862-1879.
- Opsteegh, J.D., and H.M. van den Dool, 1980: Seasonal differences in the stationary response of a linearized primitive equation model: prospects for long-range forecasting? J. Atm. Sci., 99, 2169-2185.
- Saltzman, B., 1965: On the theory of the winter average perturbations in the troposphere and stratosphere. Mon Wea. Rev., 93, 195-211.
- Saltzman, B., 1967: On the theory of the mean temperature of the earth's surface. Tellus, 19, 219-259.
- Saltzman, B., 1968: Surface boundary effects on the general circulation and macroclimate: A review of the theory of the quasi-stationary perturbations in the atmosphere. The causes of climate change, Meteor. Monogr., no. 30, Amer. Meteor. Soc., 4-19.
- Sankar Rao, M., and B. Saltzman, 1969: On a steady-state theory of global monsoons. Tellus, 21, 308-330.
- Smagorinsky, J., 1953: The dynamical influence of large-scale heat sources and sinks on the quasi-stationary mean motions in the atmosphere. Quart. J. R. Met. Soc., 100, 342-366.

- Smagorinsky, J., 1963: General circulation experiments with the primitive equations: I, The basic experiment. Mon. Wea. Rev., 91, 99-164.
- Vernekar, A.D., 1975: A calculation of normal temperature at the earth's surface. J. Atm. Sci., 32, 2067-2081.
- Vernekar, A.D., and H.D. Chang, 1978: A statistical-dynamical model for stationary perturbations in the atmosphere. J. Atm. Sci., 35, 433-444.
- Youngblut, C., and T. Sasamori, 1980: The nonlinear effects of transient and stationary eddies on the winter mean circulation. Part 1: Diagnostic analysis. J. Atm. Sci., 37, 1944-1957.

VI. Appendix:

A Note on the Boundary Conditions

APPENDIX

6.1. A note on the boundary conditions

In Opsteegh and van den Dool (1980) and Opsteegh and Verneker (1982) we use a boundary condition for $\hat{\phi}$ at the equator, which is meant to be a symmetry condition, namely:

$$\frac{\partial \hat{\phi}}{\partial \phi} = 0 \quad \text{at } \phi = 0 \quad (1)$$

Application of this boundary condition gives mid-latitude solutions of geopotential height that are in good agreement with the results of similar experiments with other models (Hoskins and Karoly 1981, Webster 1981). However, a closer look at the solutions for \hat{u} and \hat{v} at the equator shows strange results. For waves that are symmetric around the equator with respect to geopotential height both $\hat{\phi}$ and \hat{u} should be symmetric and \hat{v} must be anti-symmetric. Therefore the application of (1) should lead to solutions with nonzero zonal velocities and zero meridional velocities at the equator. It appears that forcing in the tropics leads to solutions with zero zonal velocities and small nonzero meridional velocities. The change of sign of the coriolis parameter of course is the reason for symmetry in \hat{u} and anti-symmetry in \hat{v} . We must conclude that (1) does not contain the information on the change of sign of the coriolis parameter.

I have investigated the influence of boundary condition (1) at the equator on the solutions of the model for a tropical heat source. Such forcing can be expected to give the most erroneous results. The forcing extends from the equator to 20 N and has a width of 45 degrees in longitudinal direction. The exact position of the heating is unimportant. The heating rate is 1 K day⁻¹. In experiment A I have retained the original erroneous boundary conditions ($\frac{\partial \hat{\phi}}{\partial \phi} = 0$ at the equator, $\hat{v} = 0$ at the pole) and in experiment B I have used correct conditions $\hat{v} = 0$ at the equator and $\hat{\phi} = 0$ at the pole (Egger 1976). The results for both experiments are given in fig. 1. Fig. 1 shows the amplitude and phase of \hat{v} and \hat{u} at 400 mb as a function of latitude for the response in zonal wavenumber 1. The results are approximately the same except for the first gridpoint (at 2N). In this point $\hat{u} \approx 0$ in A and $\hat{v} \approx 0$ in B. The figure gives only the results for the first zonal wavenumber but the response in the other wavenumbers shows identical differences.

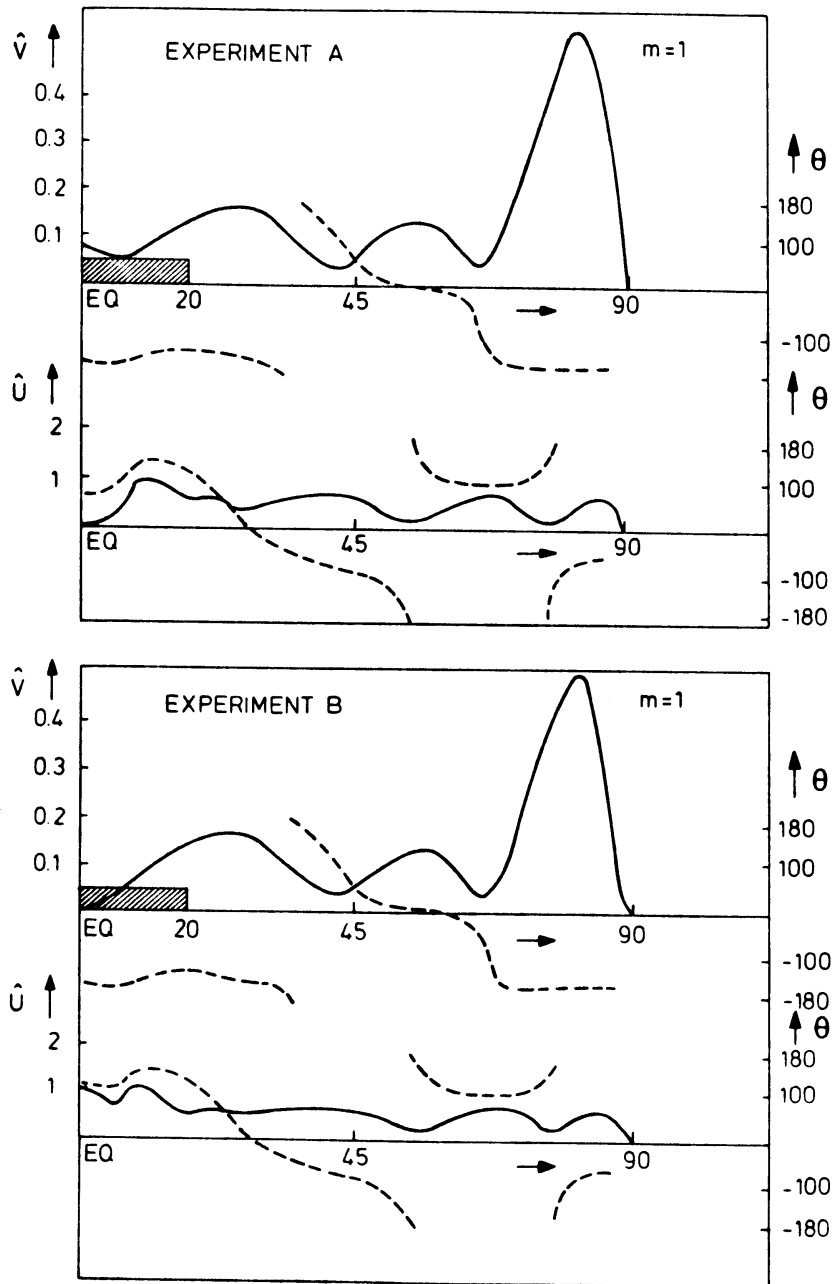


Fig 1: Response of the amplitude (solid line) and phase (dashed line) of wave-number 1 as a function of latitude to a local heat source in the tropics. The top two figures give the response in \hat{v} and \hat{u} for experiment A. The lower two figures give the same for experiment B.

Fortunately the error due to the application of boundary condition (1) is restricted to the first gridpoint and does not influence at all the solution at higher latitudes. So the application of correct boundary conditions will not change any of the results shown in Opsteegh and van den Dool (1980) and Opsteegh and Vernekar (1982). In those papers we only show solutions for $\hat{\phi}$, but $\hat{\phi}$ in the first gridpoint is so small that the changes will not be visible in the figures. Mid-latitude values of $\hat{\phi}$ will not change when correct boundary conditions are applied.

6.2. REFERENCES

- Egger, J., 1976: The linear response of a hemispheric two-level primitive equation model to forcing by topography. *Mon. Wea. Rev.*, 104, 351-363.
- Hoskins, B.J., and D. Karoly, 1981: The steady linear response of a spherical atmosphere to thermal and orographic forcing. *J. Atmos. Sci.*, 38, 1179-1196.
- Opsteegh, J.D., and H.M. van den Dool, 1980: Seasonal differences in the stationary response of a linearized primitive equation model: prospects for long range weather forecasting? *J. Atm. Sci.*, 37, 2169-2185.
- Opsteegh, J.D. and A.D. Vernekar, 1982: A simulation of the January standing wave pattern including the effects of transient eddies. Accepted for publication in *J. Atm. Sci.*
- Webster, P.J., 1981: Mechanisms determining the atmospheric response to sea surface temperature anomalies. *J. Atm. Sci.*, 38, 554-571.

Curriculum Vitae

Jacobus Dorotheus Opsteegh werd op 1 september 1946 in Dubbeldam geboren. Na de lagere school doorlopen te hebben, bezocht hij het Titus Brandsma College te Dordrecht. Het diploma HBS B werd behaald in 1964. Hierna werd begonnen met de studie voor werktuigkundig ingenieur aan de Technische Hogeschool in Delft. Het kandidaats-examen werd behaald in 1968. Hierna werd het accent gelegd op de theoretische aspecten van de werktuigbouwkunde. Als hoofdvak werd wiskunde gekozen. In het laatste jaar van de studie werd een onderzoek verricht bij het Shell "Exploratie en Produktie" Laboratorium te Rijswijk. Het doktoraal examen werd afgelegd in 1971. In dat jaar kwam hij in dienst van het KNMI. Tot 1977 werkte hij aan de ontwikkeling van voorspelmodellen voor korte termijnverwachtingen, vanaf 1977 aan problemen van de algemene circulatie. Van september 1980 tot september 1981 werkte hij bij het "Department of Meteorology" van de universiteit van Maryland (USA).